HERSCHEL / PLANCK

Planck PLM design Report

H-P-3-ASP-RP-0313

Product Code : 22000

Rédigé par/*Written by*	Responsabilité-Service-Société *Responsibility-Office -Company*	Date	Signature
PPLM Team		09/04/04	
Vérifié par/*Verified by*			
J.B. Riti	Planck PLM Technical manager	09/04/04	[signature]
T. Banos	Planck PLM manager	09/04/04	[signature]
E. Pourrier	Product Assurance	09/04/04	[signature]
Approbation/*Approved*			
J.J Juillet	Project Manager	09/04/04	[signature]

Data management : Christiane GIACOMETTI

Entité Emettrice : Alcatel Space - Cannes
(détentrice de l'original) :

DISTRIBUTION / *DISTRIBUTION RECORD*

EXTERNAL DISTRIBUTION	For Information For Application For Approbation For Action For Acceptation	INTERNAL DISTRIBUTION	
ESA	For Acceptation	**HP team** T. Banos E. Gavila Ph Martin D. Dubruel M. Nadarassin B. Spiel K.Hibberd C. Masse E. Pourrier P.Rideau Y.Roche I.Bénilan Ph.Clavel B.Marchand B. Demolders B.Collaudin J. Ph Chambelland D.Montet P. Armand **Clt Documentation**	Ori g.

ENREGISTREMENT DES EVOLUTIONS / *CHANGE RECORD*

Issue. Revision	DATE	§ : CHANGE RECORD	AUTHOR
1.0	01 July 2002	PDR issue	
2.0	09 April 2004	CDR issue	

TABLE OF CONTENTS

LIST OF FIGURES AND TABLES

1. INTRODUCTION

1.1 Scope

This document the presents the Planck PLM design and associated main performances at the PPLM CDR :

– The chapter 2 defines the subsystems which are included in the PPLM and the so-called extended PPLM. The development status is also briefly described.

– The chapter 3 is dedicated to the review of the main requirements and the description of their breakdown into subsystem specifications. No evolution has been implemented in this chapter excepted concerning the update of the interface and applicability specification.

– The chapter 4 lists the main design evolutions which have been implemented since the PDR

– The chapter 5 is a detailed description of the PPLM baseline design. The general mechanical and thermal architecture is presented as well as the telescope and cryo-structure sub-systems and the thermal control design. A special care is paid to the description of the instrument interfaces implementation since their are one of the major contributors to the PPLM complexity. A presentation of the assumption taken into account for the design of the interfaces is done and a clear status is established in RD 16. To conclude this chapter, the updated integration sequence is shown. The major evolution of this sequence compared to the SRR one is that now, the integration of the telescope is performed after the mating onto the SVM.

– The brief summary of performance analyses presented in the chapter 6 of the PDR design report have been removed. The detailed description of the optical, RF, thermal and mechanical analyses performed for the PPLM CDR are presented respectively in [RD1], [RD2], [RD3] and [RD4].

– At the end, the performance budgets are summarised in chapter 7.

1.2 Applicable and reference documents

1.2.1 Applicable documents

AD 1 : SCI-PT-RS-05991_last issue, H/P System requirement specifications

AD 2 : H-P-3-ASPI-SP-0274_last issue, Planck telescope Optical and RF system specifications

AD 3 : H-P-3-ASPI-IS-070_last issue, Planck PLM Interface and Applicability specification

AD 4 : IIDB-PT-IIDB/LFI04142_last issue, LFI Instrument Interface Document

AD 5 : IIDB-PT-IIDB/HFI04141_last issue, HFI Instrument Interface Document

AD 6 : /

AD 7 : SCI-PT-RS-07422_last issue, Primary/secondary reflector specification

1.2.2 Reference documents

[RD1] H-P-3-ASPI-MX-0331_2_0, PPLM optical analyses
[RD2] H-P-3-ASPI-AN-323_2_0, PPLM RF performance analyses
[RD3] H-P-3-ASPI-AN-330_2_0, Planck PLM Thermal analysis
[RD4] H-P-3-ASPI-AN-329_2_0, Planck PLM Mechanical and thermoelastic analysis
[RD5] H-P-3-ASPI-BT-275_2_0, Planck PLM MCI budget
[RD6] H-P-3-ASPI-ID-320_2_0, Planck PLM Instrument interface drawings
[RD7] H-P-3-ASPI-ID-325_2_0, PPLM S/C Interface Control Drawings
[RD8] H-P-3-ASPI-PL-078_2_0, Planck Alignment Plan
[RD9] H-P-3-ASPI-SP-004_2_0, Planck telescope specification
[RD10] H-P-3-ASPI-SP-021_2_0, Cryo-structure and telescope baffle specification
[RD11] /
[RD12] SCI-PT-RS-07024, Planck telescope design specification
[RD13] SCI-PT-IIDA-04624, Instrument Interface Document – Part A
[RD14] /
[RD15] /
[RD16] H-P-3-ASPI-MX-0352_2_0, IPPLM nstrument IDR/ICD compliance matrix
[RD17] H-P-3-CSAG-DD-0001_2_0, Telescope and cryo-structure - Design definition report
[RD18] H-P-3-ASPI-ID-550_2_0, PPLM electrical interfaces
[RD19] H-P-3-ASPI-TN-521_2_0, Planck assembly plan

1.2.3 Acronyms

AD	Applicable Document
CFRP	Carbon Fiber Reinforced Plastic
CTE	Coefficient of thermal expansion
BOL	Begin of Life
EOL	End of Life
EP	Entrance Pupil
FPA	Focal Plane Assembly
FOV	Field-of-view
PPLM	Planck Payload Module
HFI	High Frequency Instrument
LFI	Low Frequency Instrument
LOS	Line Of Sight
MOS	Margin of Safety
N/A	Not applicable
PA	Product Assurance
PLM	Payload Module
PR	Primary Reflector
PtV	Pic to valley
RD	Reference Document
RH	Relative Humidity
RMS	Root Mean Square
S/C	Spacecraft
SR	Secondary Reflector
TA	Telescope Assembly
TBC	To be confirmed
TBD	To be determined
WFE	Wave Front Error
wrt	With Regards To

2. GENERAL DESCRIPTION

The Planck PayLoad Module (PPLM) is the current name used to define a subsystem including:

- the Planck telescope including Primary and Secondary reflectors both supplied by ESA/DSRI
- the cryo-structure which interfaces the telescope onto the SVM
- the main baffle
- the Planck instrument units, supplied by the principal investigators which have to be accommodated on the PPLM.

The instruments are composed of :

- a Focal Plane Unit (FPU) and the associated electronic units (HFI JFET, LFI BEU, HFI PAU) that shall be located respectively on the telescope and PPLM structure at a specific position from the FPU.
- the active cryogenic cooling systems routing from the SVM to the FPU
- warm electronics mounted on the SVM panels.

The “extended PPLM” is composed of the PPLM plus 6 of the 8 SVM lateral panels (the ones used for Instrument units implementation).

At the stage of the PPLM CDR, the current status of the main development phases is the following :

- The manufacturing of the cryo structure QM is completed. Acoustic test has been performed. Sine test is in progress
- The manufacturing of the telescope QM is completed. Cryo test at 100K has been performed and thermoelastic behaviour of the structure has been measured with videogrametry,
- Mechanical test have to be done
- The manufacturing of the cryo structure and telescope FM is in progress.

The next major step of the development will be the beginning of the integration phase of the PPLM which will lead to the CQM. The first test (acoustic) is planned July 2004.

3. MAIN REQUIREMENTS AND SUBSYSTEM REQUIREMENTS

3.1 Introduction

The Planck PLM requirements are specified in the following applicable documents:

- The Planck telescope optical and RF system specification (AD 2). This specification replaced the ESA Planck telescope design specification [RD12]. It has been issued by ASP at the PDR and updated at the CDR.
- The Planck PLM interface and applicability specification (AD 3)
- The HFI and LFI Instrument Interface documents (AD 1and AD 5).

The main requirements issued from these documents and the derived specification applicable to the PPLM subsystem or instruments are described here after.

3.2 Planck telescope and RF system specification

This document is an update of the Planck telescope design specification done at the PDR. Few corrections (mainly tipo error) have been implemented for the CDR issue.

This document clearly identifies the RF and optical specifications, which are applicable to the whole telescope assembly -i.e. the telescope and the FPU- assuming defined performances for the reflectors, (described in AD 7) and for the FPU, (as specified in the Plank alignment plan [RD8]which is attached to the IIDA).

In the PDR issue, only the following specifications have been maintained:

- The performance requirements :
  - Maximum WFE degradation for each frequency
  - Maximum gain degradation of the main lobe
  - Maximum Ellipticity degradation of the LFI horn pattern
  - Total emissivity of the telescope surfaces

Note 1 : The emissivity performance of the telescope optical surfaces is given by the EOL emissivity performance of the reflectors and by the contamination induced by the on ground operation and launch between the delivery of the reflectors and EOL. Since the EOL reflectivity requirement of both reflectors is 5%, the total emissivity requirement of the telescope surface has been increased from 5% to 6 % to cover contamination.

Note 2 : In order to be consistent with the telescope specification, an emissivity requirement should be placed on the reflectors.

- The interface temperature of the reflector
- The test requirements

On the other hand, the physical and environment specifications have been removed from this document. They have been directly specified in the Planck telescope specification [RD9] on the basis of the system requirements defined in AD 1, and of mechanical and contamination analysis performed at satellite level.

The maximum telescope assembly WFE degradation specification is breakdown into the following major contributors :

– At telescope level :
  - A maximum WFE telescope degradation
  - Stability and of the telescope focal surface position
  - stability of the FPU/telescope interface plane

These requirements are specified in the Planck telescope specification (RD 9).

– At FPU level :
  - Horn geometry accuracy
  - Horn tilt and decenter

These requirements are specified in the Planck alignment plan [RD8]. They are addressing the whole FPU and shall be breakdown into LFI and HFI sub-systems

– For the FPU/telescope integration
  - knowledge of the telescope focal surface position along Zordp axis
  - knowledge of the FPU focal surface position along Zordp axis
  - Shimming accuracy

These requirements are specified in the Planck alignment plan [RD8]

All these contributors are presented on the following figures

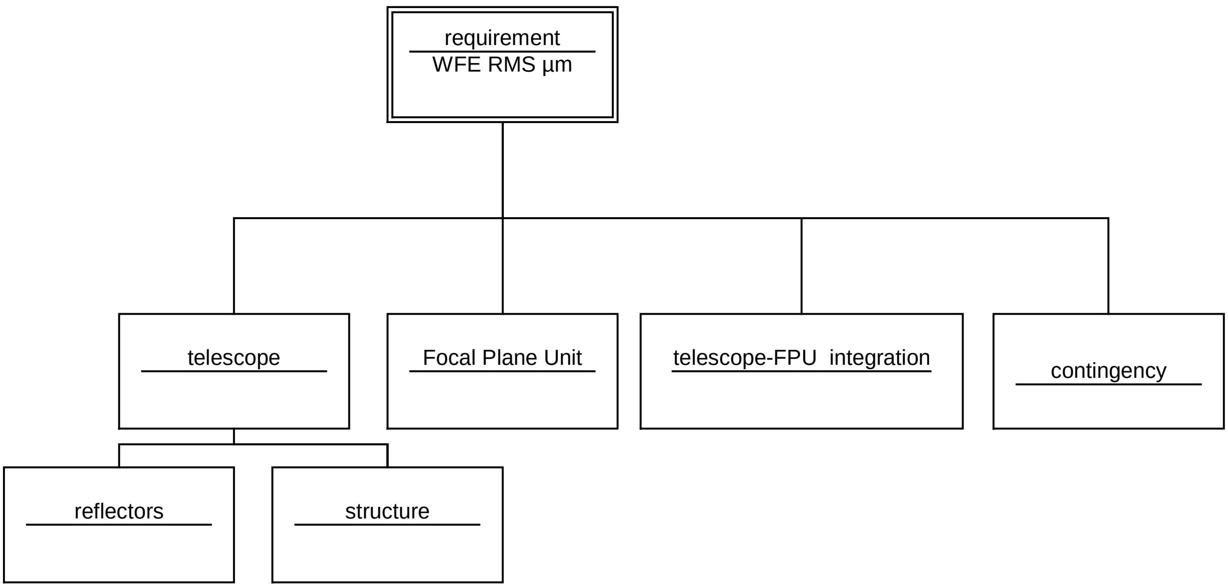

Figure 3.2-1 : WFE performance contributors

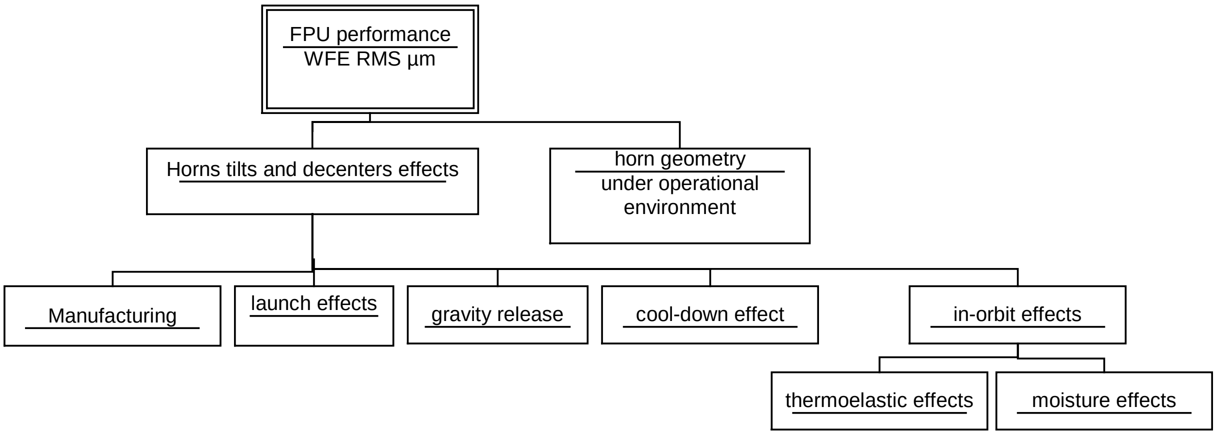

Figure 3.2-2 : FPU performance main contributors

3.3 PPLM interface and applicability specification

The Planck PLM interface and applicability specification (AD 3)defines the main following requirements:

- Mass, centring
- The SVM interface requirements and allocated volume to be compatible with the launcher
- The system requirements (AD 1) which are applicable to the PPLM, in particular :
  - The rejection toward the sun, earth and moon directions (SPER 060)
  - The ASD at the bolometer of any signal due to the fluctuation of the thermal emission from S/C elements (SPER 065) which is derived into temperature stability on PPLM and SVM elements
- EOL and LOS stability and knowledge
- short term (between 2 calibrations) LOS stability
- EOL around LOS stability and knowledge
- Thermal sensors interface definition

3.4 Instrument Interface documents

The major requirements issued from the IIDB are the temperature level requirements which are summarised here after:

PPLM interface temperature requirements		Required max temperature (K)	Location at which the required temperature must be guaranteed
LFI WG	VG1	170	on interface shield side
	VG2	120	
	VG3	60	
Sorption Cooler	VG1	170	at exchangers and on exchangers side
	VG2	120	
	VG3	60	
JFET box		60	on PR panel side
FPU		65	on PR panel side
Primary Reflector		50	average PR temperature
Secondary Reflector		50	average SR temperature

Table 3.4-1 : PPLM maximum interface temperature requirements

PPLM interface temperature requirements		Required min temperature (K)	Location at which the required temperature must be guaranteed
LFI WG	VG1	/	on interface shield side
	VG2	/	
	VG3	/	
Sorption Cooler	VG1	150	at exchangers and on exchangers side
	VG2	100	
	VG3	45	
JFET box		40	on PR panel side
FPU		40	on PR panel side
Primary Reflector		30	average PR temperature
Secondary Reflector		30	average SR temperature

Table 3.4-2 : PPLM minimum interface temperature requirements

These requirement are derived into the main following thermal design requirements which are defined in the cryo-structure [RD10]and telescope specifications [RD9]:

- Thermal conductivity of the grooves, baffle and at the various interfaces
- Low thermal conductivity of the cryo-structure struts
- high emissivity coating for the groove 3 and baffle external surface
- low emissivity and high specular reflectivity for the faces of the grooves 1 and 2 and the lower face of the groove 3.

4. MAIN DESIGN EVOLUTION/OPTIMISATION SINCE THE PDR

Since the PDR, the main evolutions of the PPLM mechanical and thermal architecture and design are the followings :

- Increase of the groove 1 size in order to improve the margin wrt the shadowing constrain for the grooves 2 and 3, the baffle and the telescope.
- Implementation of brace struts to minimise the dynamic displacements of the grooves close to the instrument interfaces
- Optimisation of the baffle edge geometry on the basis of the Ticra RF analyses results, to decrease manufacturing constrain
- Increase of the telescope SR struts stiffness to optimise the dynamic behaviour of the PPLM and in particular to decrease the mechanical loads on to the SR
- Optimisation of the telescope lower beam design to improve the thermoelastic stability of the FPU interfaces
- Reinforcement of the corner of the telescope frame
- Detailed definition of the shields to close the optical cavity :
  - between the FPU structure and the telescope PR panel
  - between the baffle and the groove 3
  - between the telescope and the groove 3
- Detailed definition of the thermal shields to close the grooves
  - between the cryo-struts and the grooves
  - between the Wave guide and the grooves
  - between 20K pipes and the grooves
  - between the Bellow 50K and the grooves
- Instruments interfaces and accommodation
  - removing of the LFI 100 GHz Wave Guides (
  - modification of the BEU in 3 units
  - modification of the WG Upper Support Structure truss
  - modification of the WG Lower Support Structure interface with the SVM and the Tel. Frame
  - reconnection of the HFI pipes at the 18K plate level
  - modification of the 0.1K pipe routing at Cryo-Structure level
  - modification of the Bellow 50K routing at Cryo-Structure level
  - creation of a volume for the cryo-harness routing of the 20K Cooler at Cryo-Structure level

These evolutions are described in the following chapters, dedicated to each sub-system.

5. BASELINE DESIGN

5.1 Introduction

The 2 following figures show the overall view of the PPLM with the part of the Instruments which is on PPLM side (consequently without the SVM Instruments part).

This configuration is the one used to compute the MCI of the PPLM "except units inside the SVM" in §8.1. That means, for the 3 coolers pipes :

- Sorption (20K) : from the SCCE (on the FPU) to the CSC interface (Compressors in the SVM).
- 4K Cooler : from the FPU (18K plate) to the 4K disconnection box on the Sub-platform (at 300K).
- Dilution Cooler : from the FPU (18K plate) to the Dilution disconnection box on the Sub-platform (at 300K).

Nota :for the mass budget, the Sorption Cooler pipes have been considered in the PPLM side up to the Compressors (in the internal part of the SVM) because of the non disconnectability aspect of the Sorption pipes.

The BEU and its ''internal'' harness (the one between the lateral trays and the central box) and PAU which are located on the Subplatform are also included in the PPLM.

The BEU external harness going to the DAE and routed on the subplatform is not considered on PPLM side.

The PAU harness going to the REU and routed on the subplatform is not considered on PPLM side.

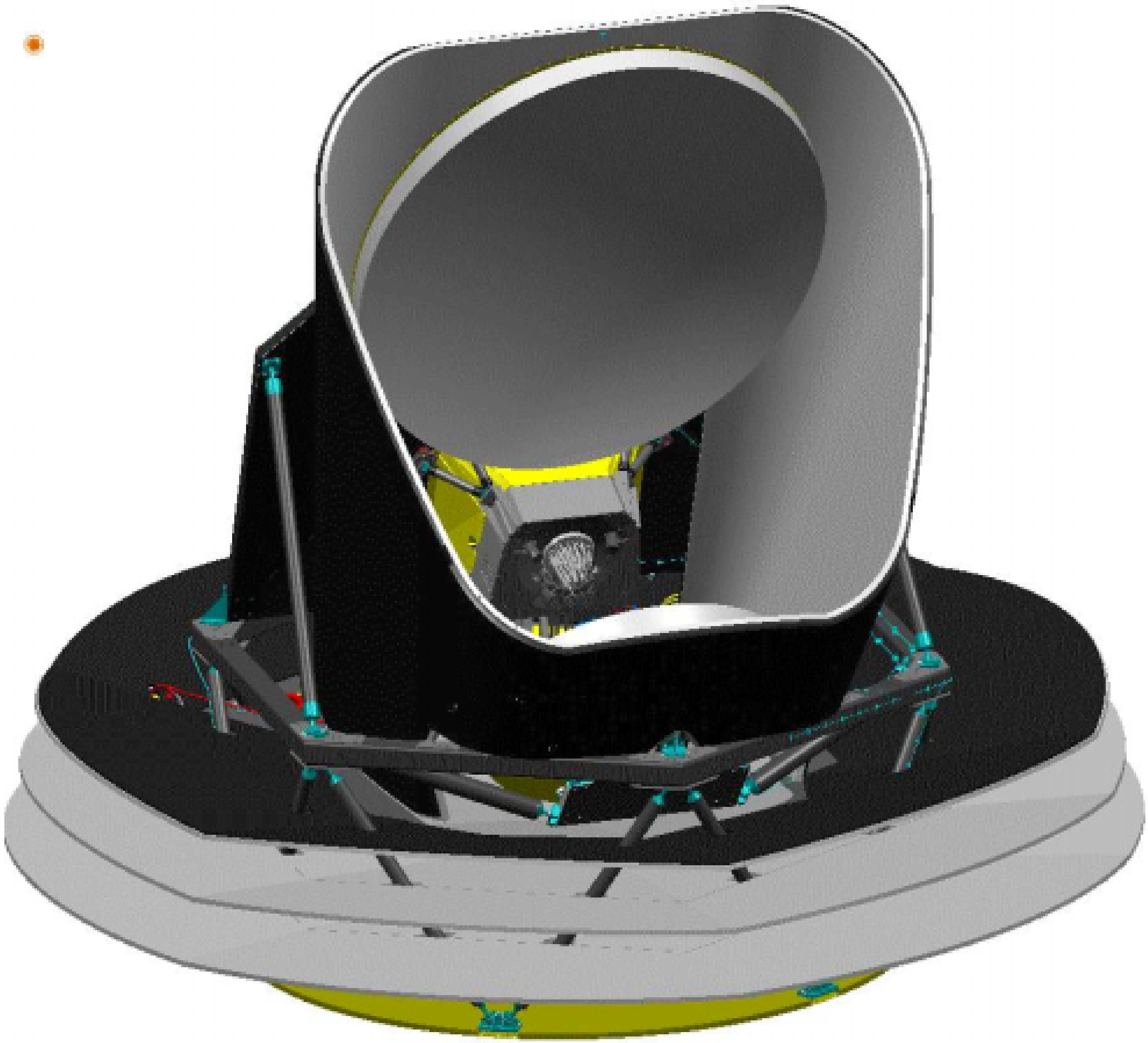

Figure 5.1-1 : Planck PLM General overview (front side, +Z)

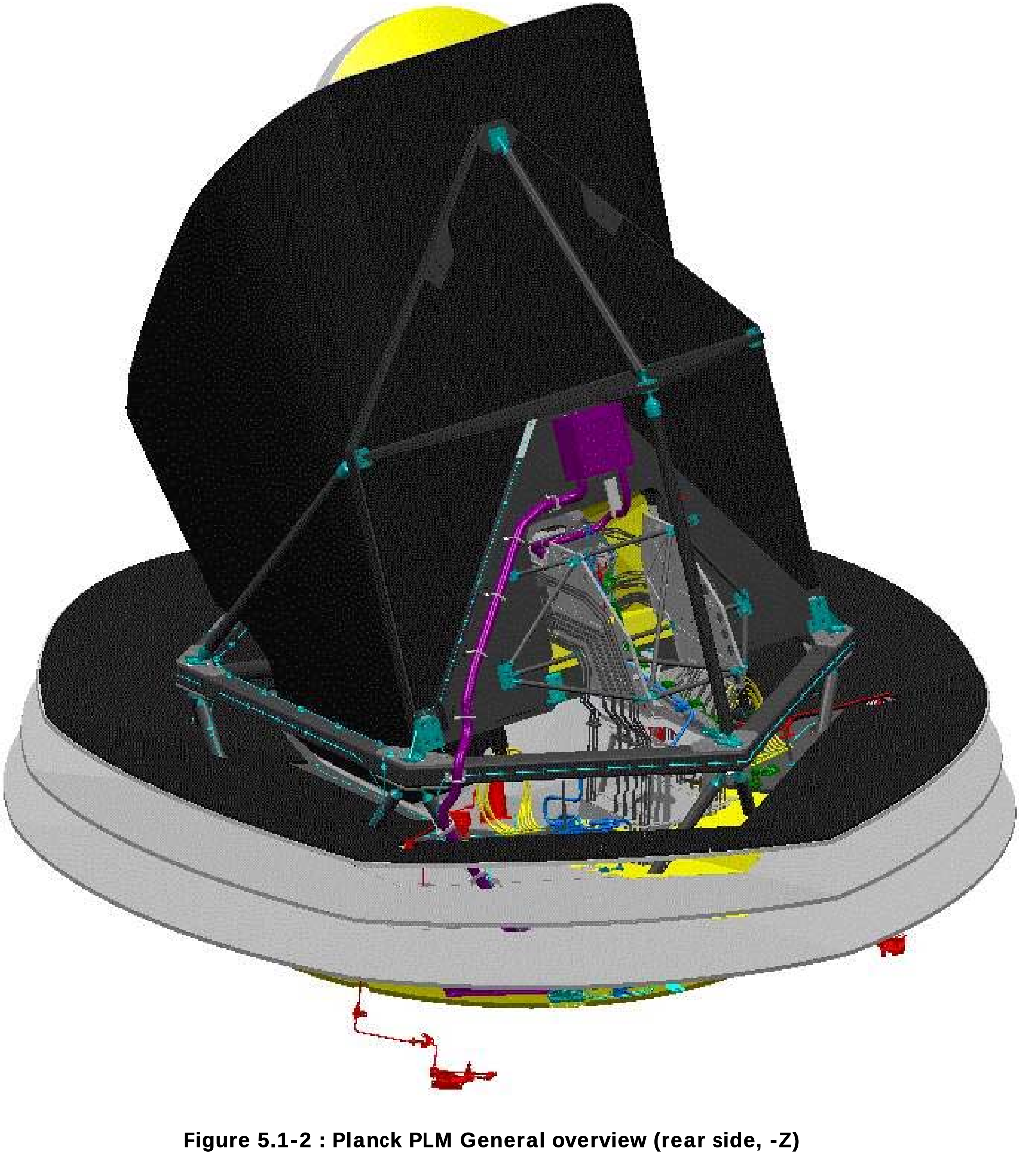

Figure 5.1-2 : Planck PLM General overview (rear side, -Z)

The axis system of the PPLM is derived from the Planck satellite coordinate system. The origin of the frame OPPLM is at the intersection of the spin axis and the interface plane made by the cryo-structure : Upper side of the PPLM Subplatform located at X+966.5 mm from the S/C origin point.

5.2 Mechanical and thermal architecture

5.2.1 Main geometrical design constrain

The overall design of the PPLM is mainly driven by the implementation of the large groove cryo-structure which is the basis of the Planck passive thermal control, the telescope and the instruments.

The main baffle and the groove 3 have direct view factor to the cold space : a maximum emissive area is needed to reach the very severe goal of temperature on Groove3 at the Coolers pipe heat exchangers interfaces.

For that purpose Baffle and Groove 3 provide the radiative surface of the radiator cold stage with a high emissivity required for maximum thermal coupling with space. A specific volume of 10 mm thick on these parts is allowed to implement a thermal black honeycomb (on the outer face of the baffle and on the upper side of Groove 3).

A deviation to this allowed volume has been agreed in order to have to best efficient open honeycomb geometry regarding emissivity, that means for the cells to have a ratio height/diameter=1.5, consequently with 3/8'' cells : height of 14.2 mm.

The baffle global size is driven by the allowed volume during launch (at integration temperature) and by the 12° shadowed cone of the SA and the optical beam for the lateral dimensions (at operational temperature).

The groove 3 global size is driven by the 12° shadowed cone of the SA (at operational temperature).

The grooves 2 and 1 external diameters (at operational temperature) are also limited toward the outside (maximal size) by the shadowed cone but also to the inside (minimal size) for efficient radiative discoupling :

- Groove 3 shall only has view factor with Groove 2 (about 100°K parts)
- Groove 2 shall only has view factor with Groove 1 (about 150°K parts)

Only Groove 1 is allowed to have a view factor with 300°K parts.

The Baffle is designed in such a way that it only has view factor with the Groove 3 shield.

The 12° shadowed cone is based on the solar array diameter at the spacecraft basis. It is a results from the maximum angle deviation of the spin axis w.r.t. the satellite sun axis (±10°) increased by a margin of 2°.

The high emissive area is equal to 15.6 m² (Groove 3 : 7.2m² + Baffle : 6.8m² + PR Panel : 1.6m²)

It has to be note that the use of a thermal honeycomb leads to a total emissive surface of 86.5 m² (with cells 3/8'' -9.5mm- diameter and a height of 14.2 mm).

5.2.2 PPLM overall dimensions

5.2.2.1 Main dimensions at operational temperature

PPLM main dimensions at operational temperature are presented her after. Note that the tolerance includes the main shimming capabilities and structure tolerances on shapes :

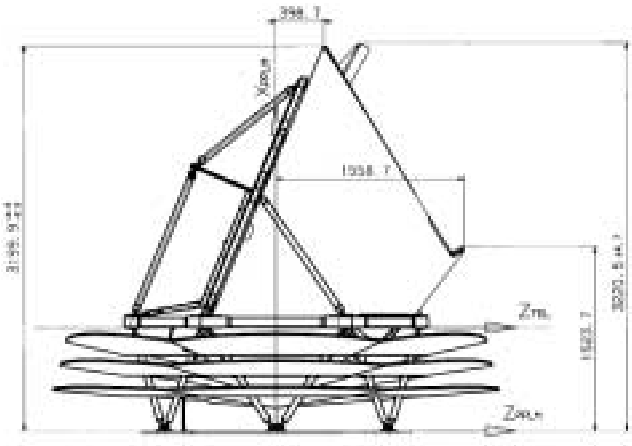

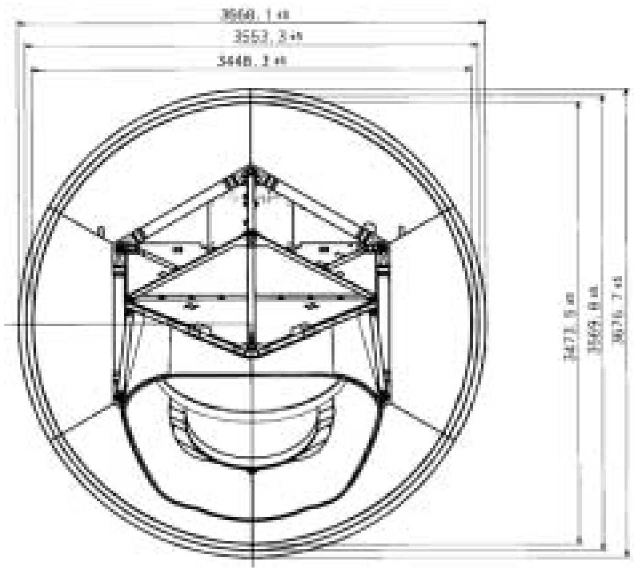

(from ICD drawing : PLAPLM0S9200A sheet 2)

Figure 5.2-1: PPLM main dimensions at Operational Temperature

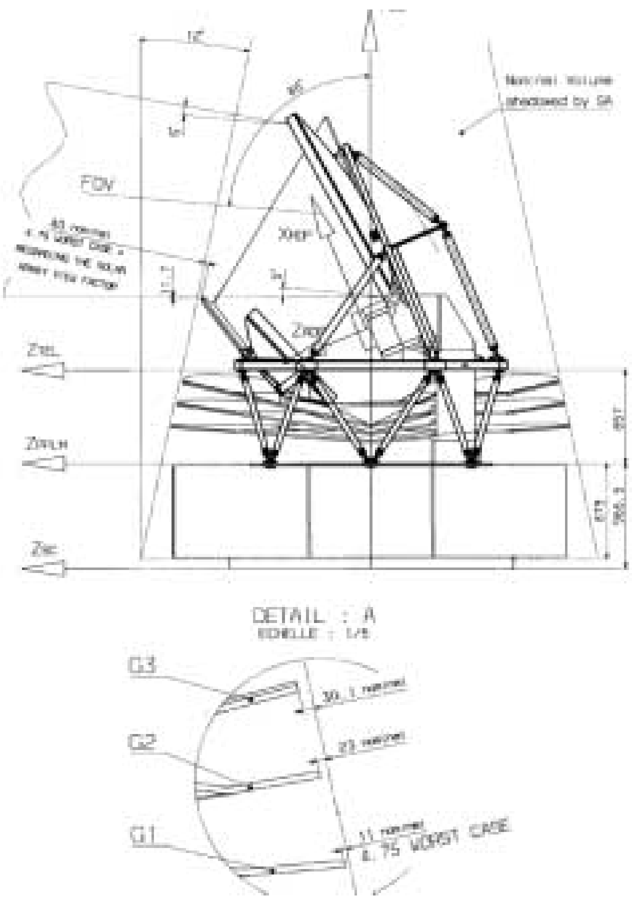

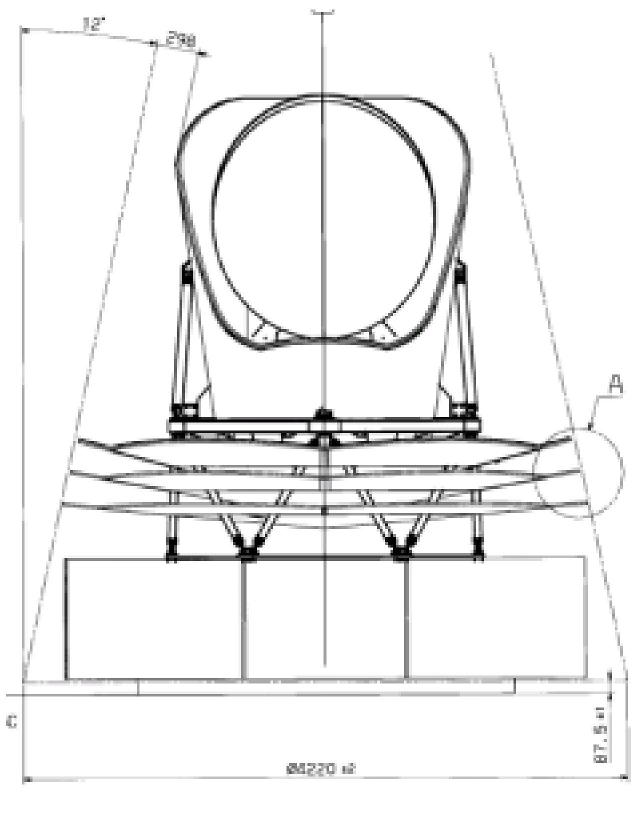

(from ICD drawing : PLAPLM0S4001A)

Figure 5.2-2 : PPLM main dimensions at Operational Temperature with the 12° shadowed cone and the optical beam

5.2.2.2 Main dimensions at ambient temperature

The current maximal dimensions are shown here after, they take into account :

- the max values for manufacturing and integration tolerances at Room Temperature (for example t: 3 mm for the shim plates between Telescope and Cryo-structure, adjustment of +5 mm along Xrdp for the PR, max height for the Baffle : nom +1.5 mm).
- thermoelastic compensations for the shrinking at ambient temperature for the aluminium parts (important CTE effect) in order to have at operational temperature the required dimension : for baffle height about +3 mm and for the Grooves ''diameters'' up to +14 mm (on Groove 3)

This leads for the PPLM to the overall maximal dimensions at ambiante temperature :

- **PPLM max. static height : 3 225.2 mm**
- **PPLM max. static diameter : ϕ 3 697 mm** (for Groove 1 shield measured along Z axis)

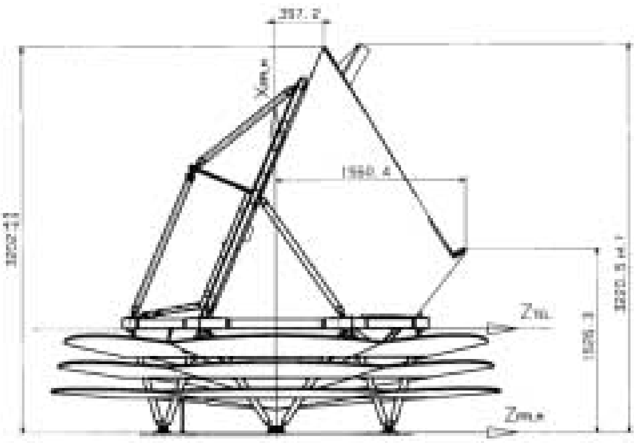

(from ICD drawing : PLAPLM0S9200A sheet 1)

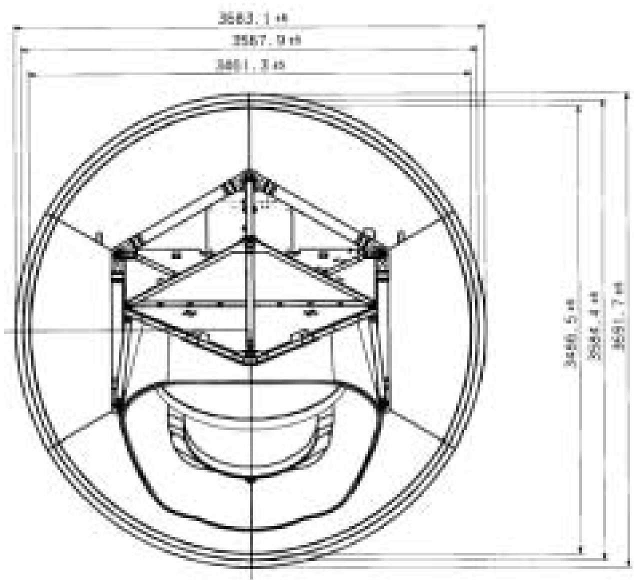

Figure 5.2-3 : PPLM main dimensions at ambient temperature

The following drawing shows the maximum PPLM overall maximal volume including max static tolerances and max dynamic displacements :

- **PPLM max. dynamic height : 3 230.2 mm**
- **PPLM max. dynamic diameter : ϕ 3 708.7 mm** (for Groove 1 shield measured along Z axis)

Here after the dynamic displacements of the structure taken into account for the definition of the max overall dynamic volume :

PPLM dynamic displacements	envelope value (mm)
Grooves - YZ plane	±6 mm
Grooves - X direction	±50 mm
Baffle - YZ plane	±27 mm
Telescope & Baffle - X direction	±5 mm

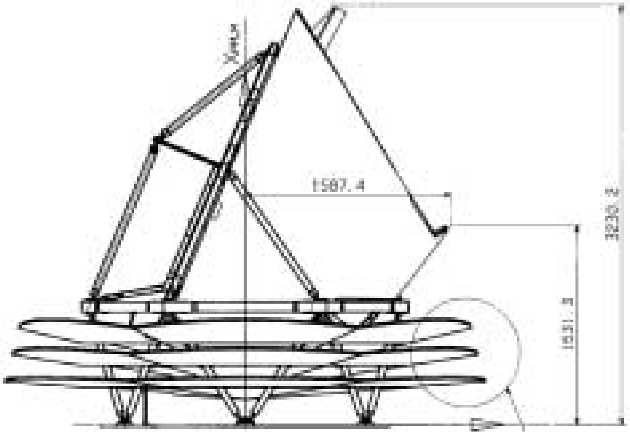

(from ICD drawing : PLAPLM0S9300A sheet 2)

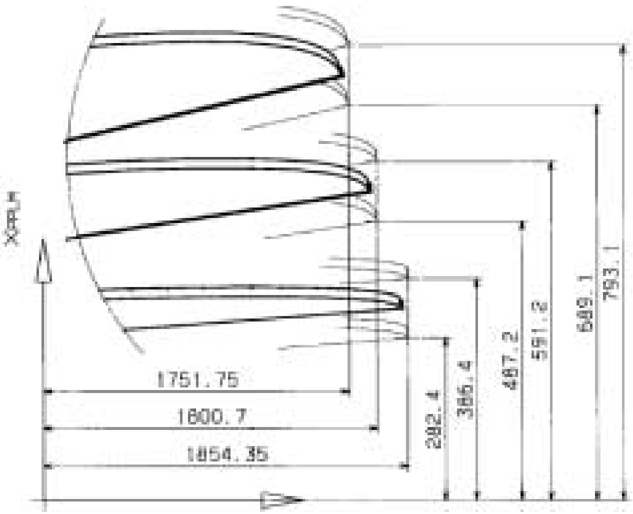

Figure 5.2-4 : PPLM max overall dynamic volume

5.3 Telescope design

5.3.1 Optical design

No evolution has been implemented on telescope optical design. Nevertheless, the definition of its lay out is described in Figure 5.3-1. It is consistent with the definition of the telescope specification which is issued from an optimization study carried out by ALCATEL in the frame of the PPLM Architect ESA contract.

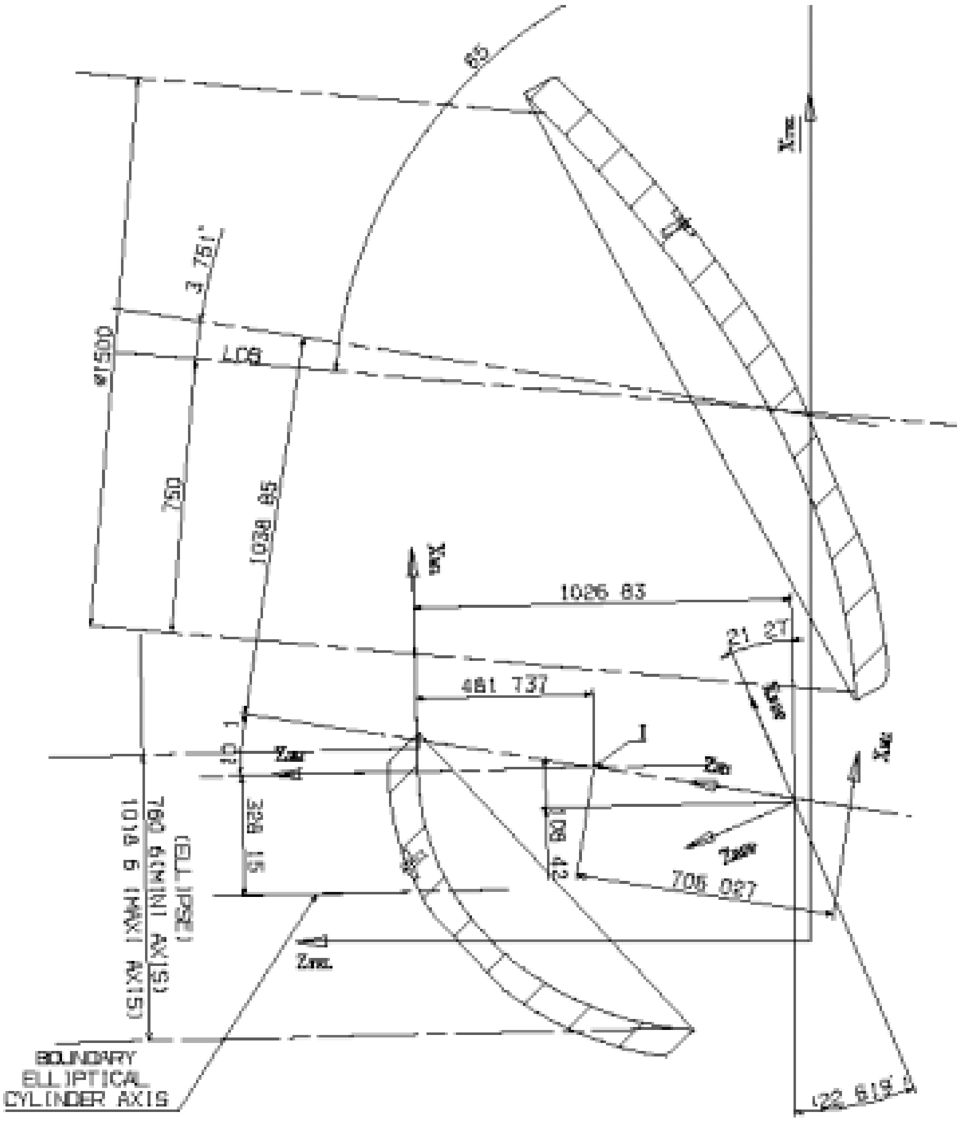

Figure 5.3-1: Telescope optical layout

5.3.2 Telescope overall design and dimensions

The Telescope is mounted on the Cryo-Structure and is mainly composed of :

- the Primary Reflector (PR) supported by the PR Support Structure ②
- the Secondary Reflector (SR) supported by the PR Support Structure ③
- the Frame ① which links the PR and SR Support Structures onto the Cryo-Structure

An overview of its design and of the main dimensions are given here after :

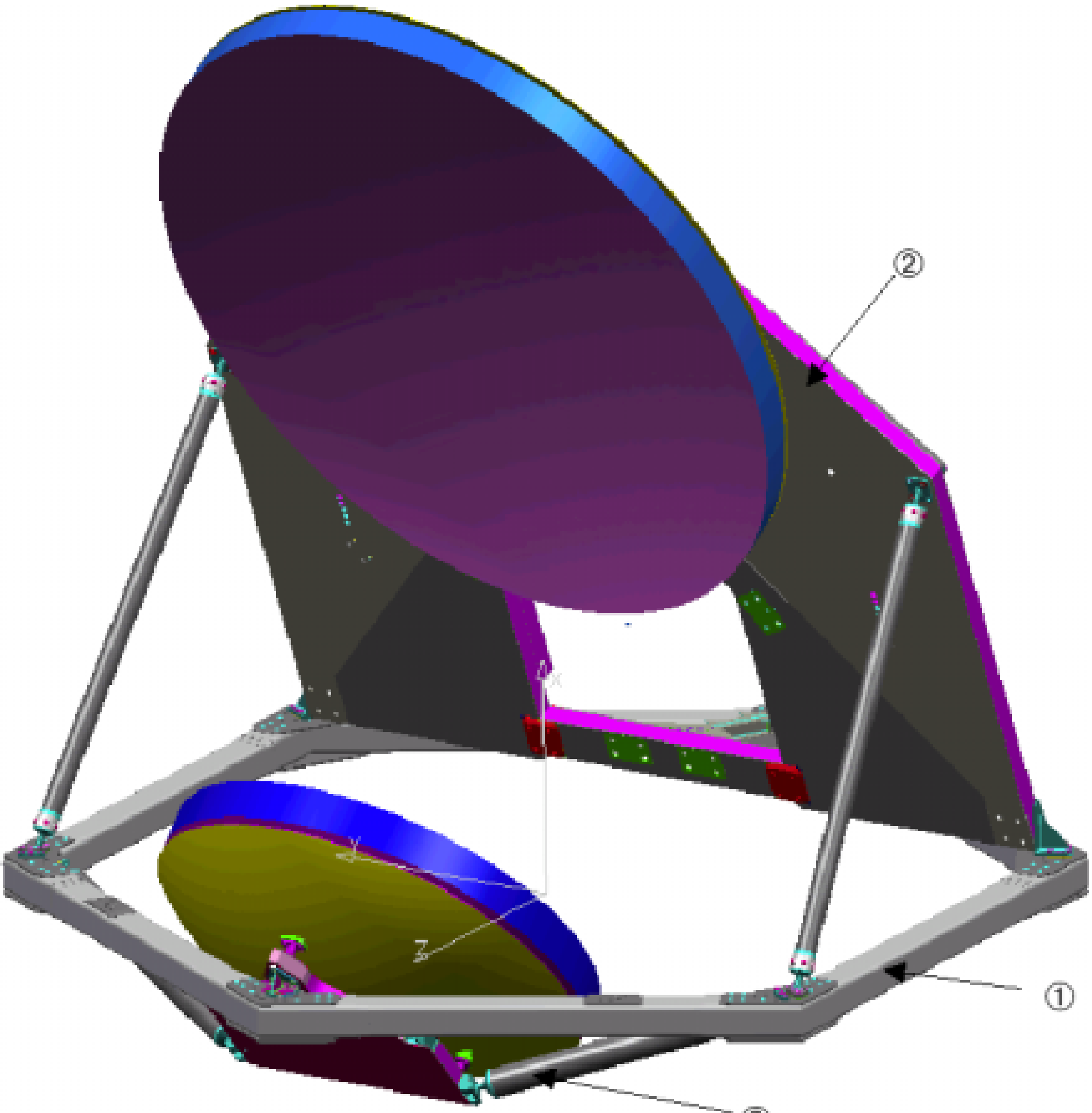

Figure 5.3-2 : Telescope structure with reflectors

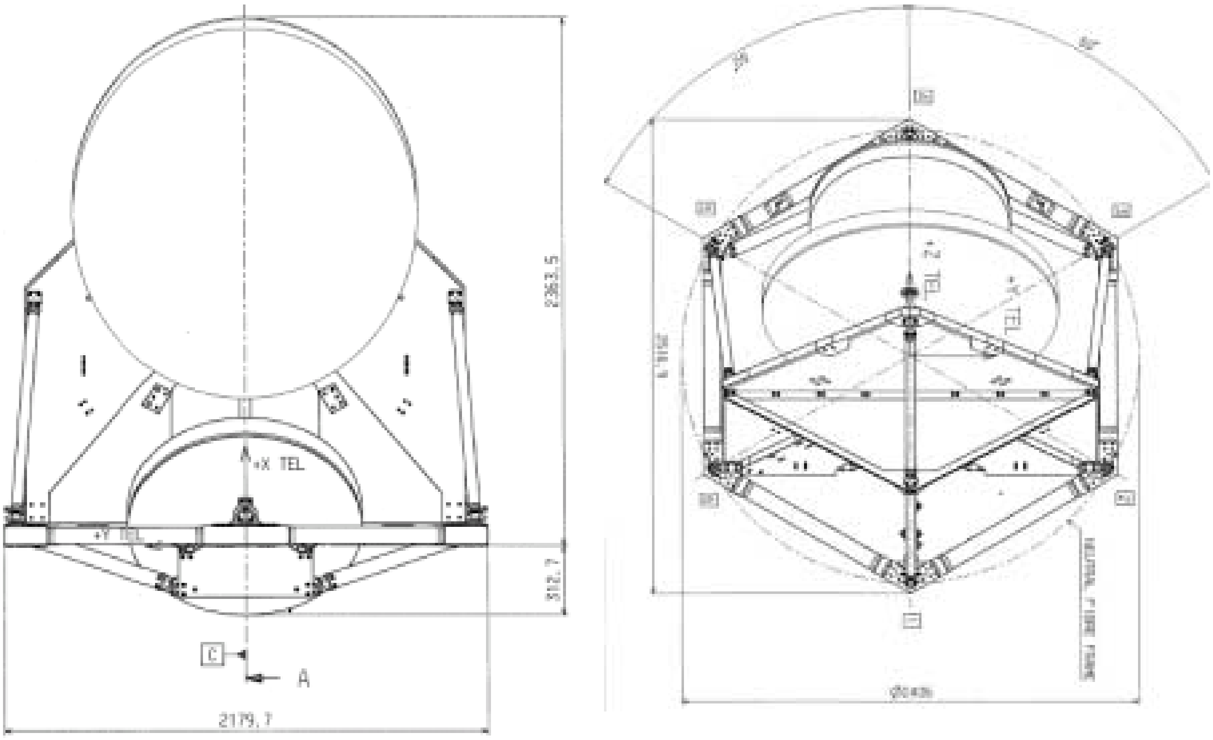

Figure 5.3-3 : Telescope main dimensions

5.3.3 Reflector interfaces

PR and SR : No shape modification but an more accurate repartition between the tolerance of the interface points :

– pin on the ISM foot localized at ± 2 mm (in-plane) w.r.t. M1 (or M2) coord. system (system attached to the optical surface at the vertex point).

Moreover, the pins location shall be known with an accuracy of 5µm after measurement w.r.t. the M1 (or M2) coord. system.

This measurement accuracy is needed for CSAG to manufacture the ISM adaptors. Those ones are attached to the PR Panel with H7g6 adjusted bushes on one side and on the ISM with H7g6 adjusted pins on the other side. This hyper-static configuration with positives contact (shearing parts) is required to withstand the mechanical loads coming from the sine environment.

5.3.4 Telescope structure design

The detailed description of the telescope structure is performed in [RD17]. The main evolutions of its design are described here after. Some pictures of the Qualification Model are presented at the end of the paragraph.

5.3.4.1 Main evolution of the telescope structure

– Telescope - PR Lower Beam with compensation system :

- This stiffener has evolved from a simple strut to a more complexe structural part with a CFRP double C profile connected back to back (to avoid tube end fittings and their positive CTE and also for the possibility to implement the compensation mechanism).
- a pair a triangular stiffeners connected to the ''FPU beam'' (for the dynamic behavior)
- a length compensation mechanism on the frame side end (for the FPU interface thermoelastic stability). This mechanism consists in a pair of aluminium blades (green in the figure bellow) connected to the end fitting using a set of CFRP blades.

Note that the maximum loads that could be withstood by the insert of the lower beam are low and currently not compatible with the interface loads introduced by the instruments. An action is pending on CSAG side to verify these values. In parallel, analyses on instrument side are performed to confirm the IF loads. If both are confirmed, local reinforcement will be needed.

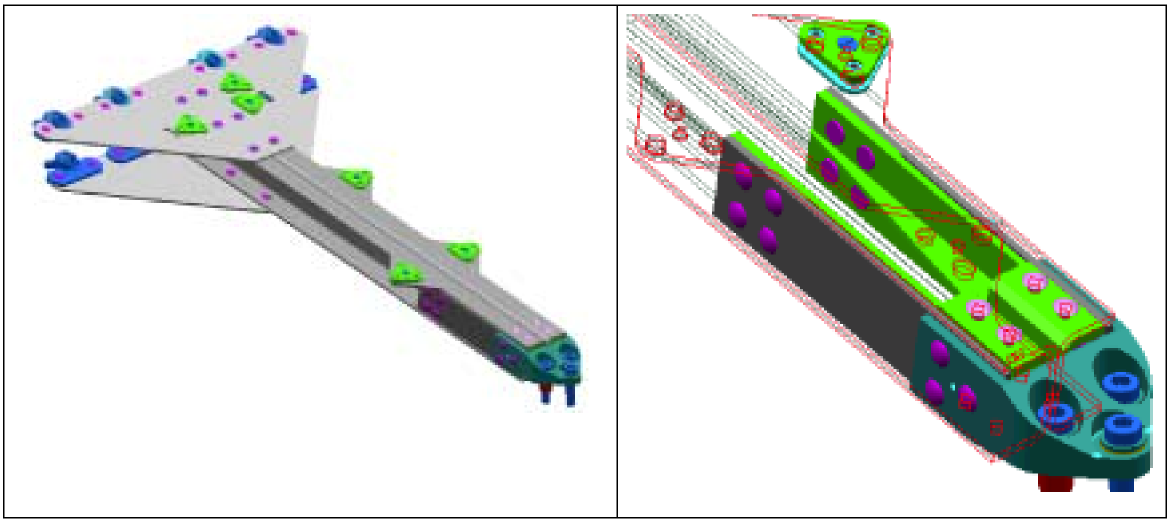

Figure 5.3-4 : Telescope lower beam & compensation system

– SR Support Structure struts - diameter increase :

  In order to limit the dynamic response of the SR and consequently to decrease the induced mechanical loads on it, the 2 struts of the SR Structure (connecting the SR Panel to the Frame corners) have been stiffened by increasing the diameter up to 64 mm (inner diameter) with a wall thickness of 2.8 mm.

– Main frame corner reinforcement :

  Node assemblies with CFRP tubes and threaded titanium anchor plates have been added at each of the frame corner in order to provide a stiff and strong out-of-plane load path between the Cryo-Structure struts and the Telescope struts. The figure here after shows a cross section of one of the reinforced corner.

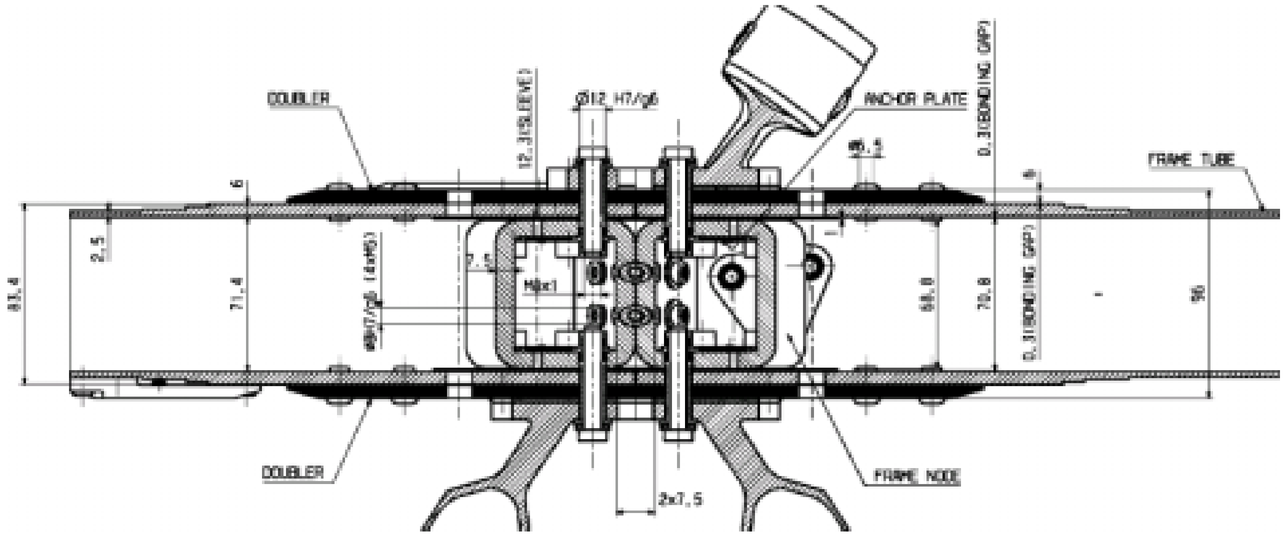

Figure 5.3-5 : Telescope Frame corners reinforcement

– Reflector adapters :

Interface parts at ISM interface (included in CSAG design) : these parts have an important stiffness compared to the ISM ones (no drop in frequency) and ease the integration. The main purpose is to fit the PR Panel interface with the Astrium ISM interface.

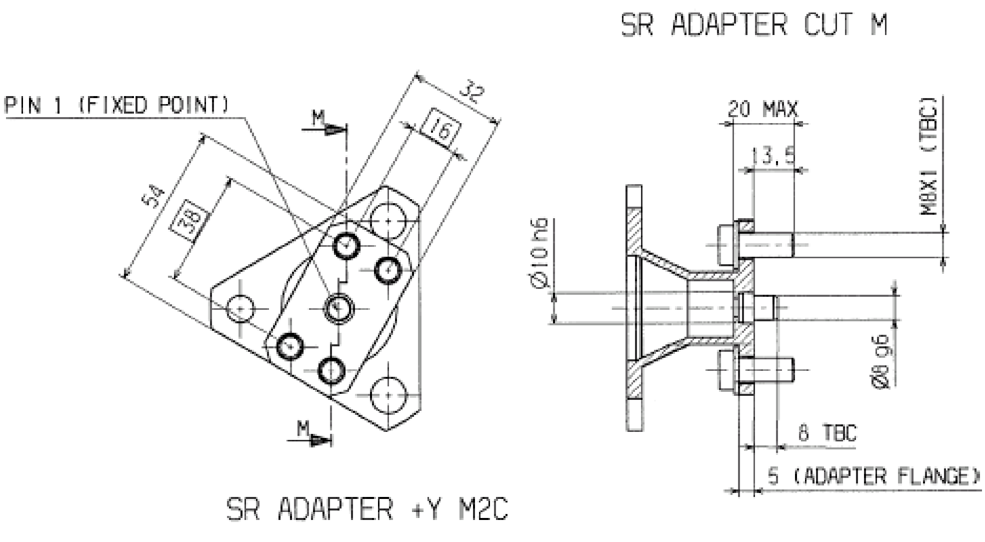

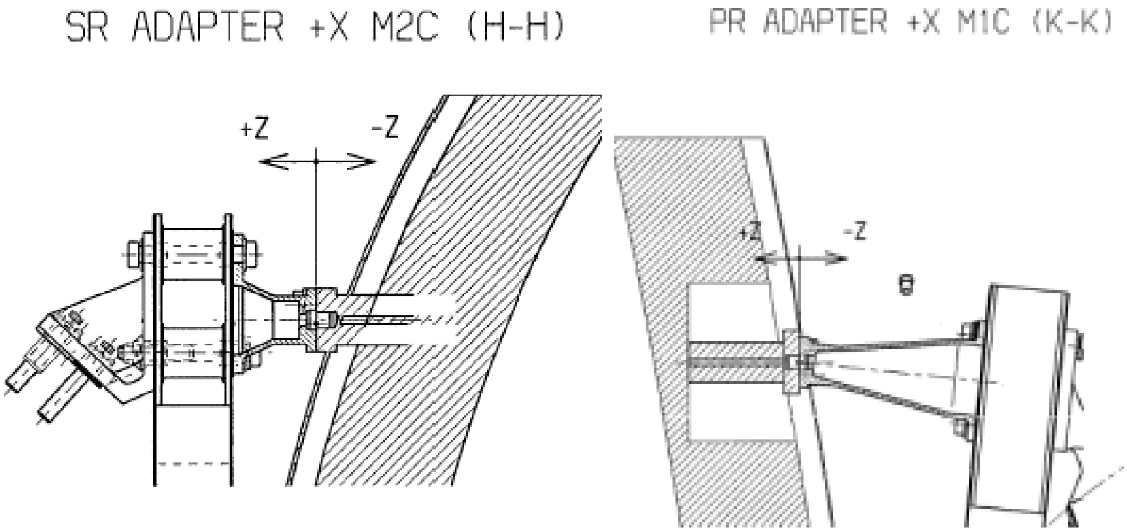

Figure 5.3-6 : Telescope adaptors for reflectors

5.3.4.2 Telescope adjustment range

The adjustment capability of this parts is as follow :

Reflectors adjustment capability	**PR**	**SR**
In-plane (X, Y)	ϕ 10 mm	ϕ 10 mm
Out-of-plane (Z)	+5 mm / -2 mm*	± 5 mm

** the limitation is given by the PR Panel proximity*

This capability cover the need described here after :

Reflectors adjustment budget	**PR**	**SR**
In-plane (X)	-4.32 / + 4.43	-4.38 / +4.95
In-plane (Y)	± 2	± 2
Out-of-plane (Z)	-0.13 / +2	-0.14 / +1.55

Due to the very small room between the reflectors and their supporting panels, there is no real potential solution to increase their adjustment capability if required to compensate reflector curvature unstability :

- Decreasing the thickness of the panel will modify strongly the mechanical behaviour of the telescope and of the PPLM
- Decreasing the thickness of the telescope frame will also modify the mechanical behaviour of the telescope

– Increasing the mean diameter of the hexagonal frame will completely modify the interface between the groove and the struts (diameter of the internal part) and cannot be envisaged at the stage of the development without an important planning impact.

5.3.4.3 Picture of the telescope QM

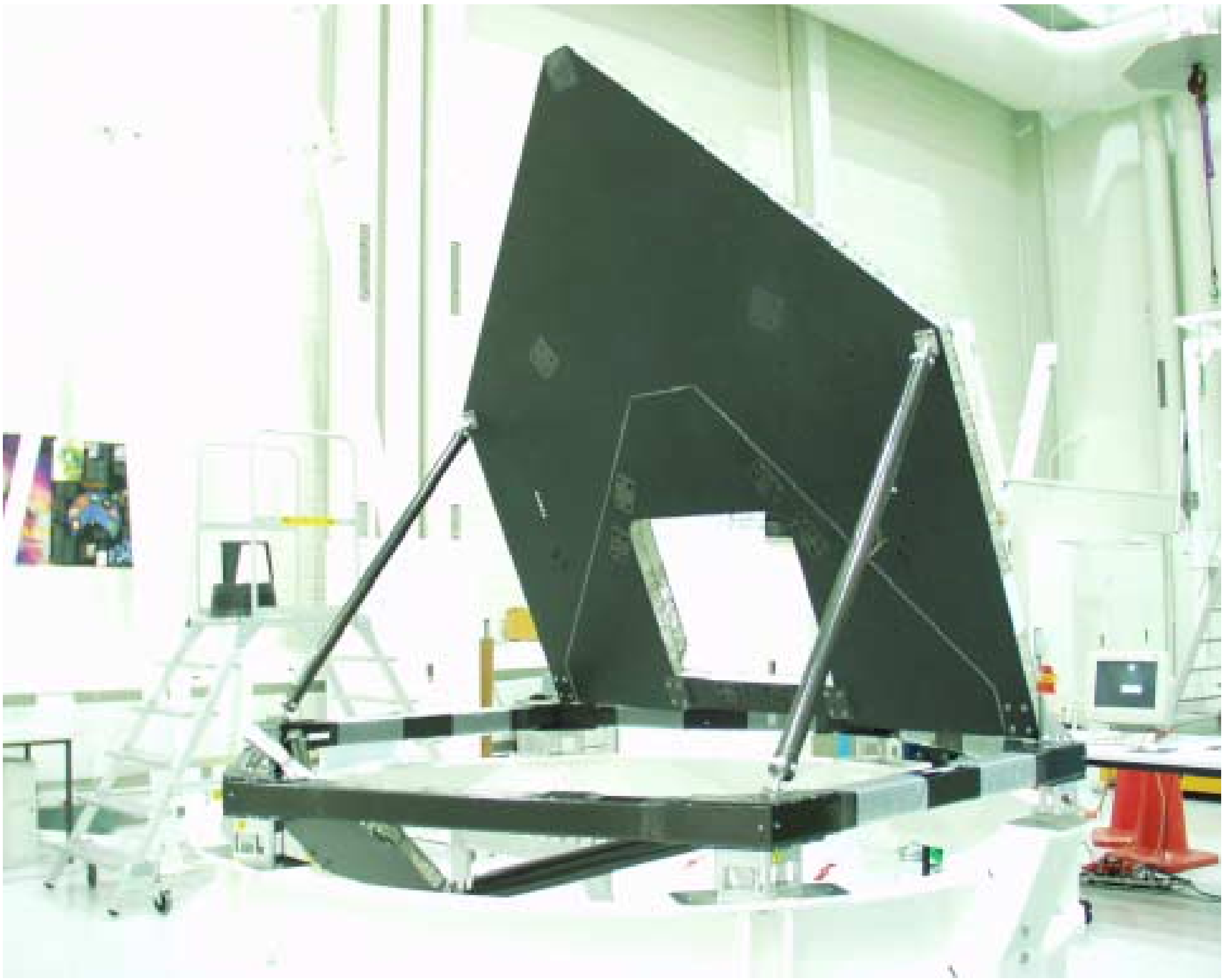

Figure 5.3-7 : Telescope qualification model

5.4 Shield of the optical cavity

RF rejection specification toward planets imposes to have a closed optical cavity with an aluminium shield of 10 µm minimum thickness layer. This means that the 10 µm of the Al layer for the closure skirts or other couple of material/thickness could be envisaged to respected this requirement.

5.4.1 FPU - PR panel shield

The goal of this shield is to close the optical cavity around the FPU; in particular the PR panel hole which allows the implementation of the wave guide. The design of this shield is critical since :

- it has a large surface which will be sensitive to acoustic environment
- it connects the FPU to the PR panel which shall be thermally discoupled. Consequently, the design of this shield will be driven by thermal constraints.

Two potential solutions have been trade off :

- an aluminum foil of about 5 µm max
- an TA6V foil with a possible thickness from 25 to 75 µm

In both cases a Kapton foil with VDA (t<0.1 µm) on cavity side is needed for the emissivity.

Investigation on metalic foil manufacturers has shown that the only material/thickness answering to the need is TA6V foil with thickness 43 µm. The complete shield is constituted of the following foils :

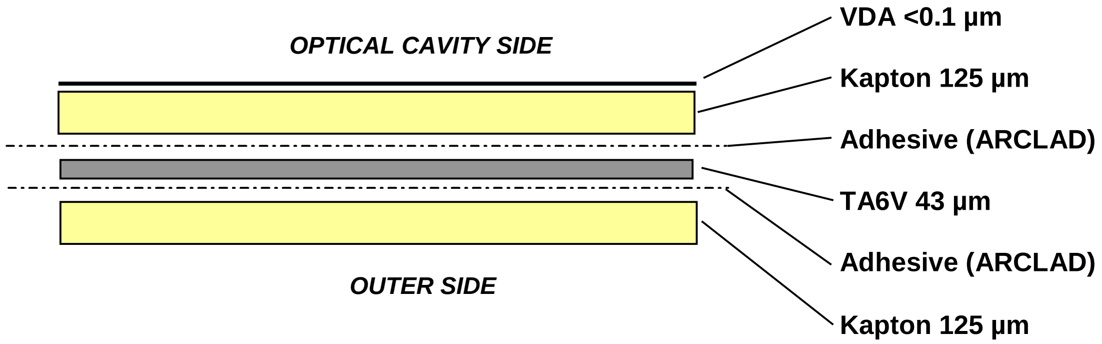

Figure 5.4-1 : FPU RF shield design

With this design we have the following performance :

- RF blanking performance (9 skin thicknesses) 1.8 times higher than the minimal required, taking into account material property at ambient (worst case)
- thermal load introduced on the FPU : ~ 40 mW assuming a perfect coupling between the shield and the FPU main frame which is a conservative assumption (in the current design the MLI is attached to the main frame with velcro which will introduce a thermal discoupling)

The implementation of such a design is presented in the following figures :

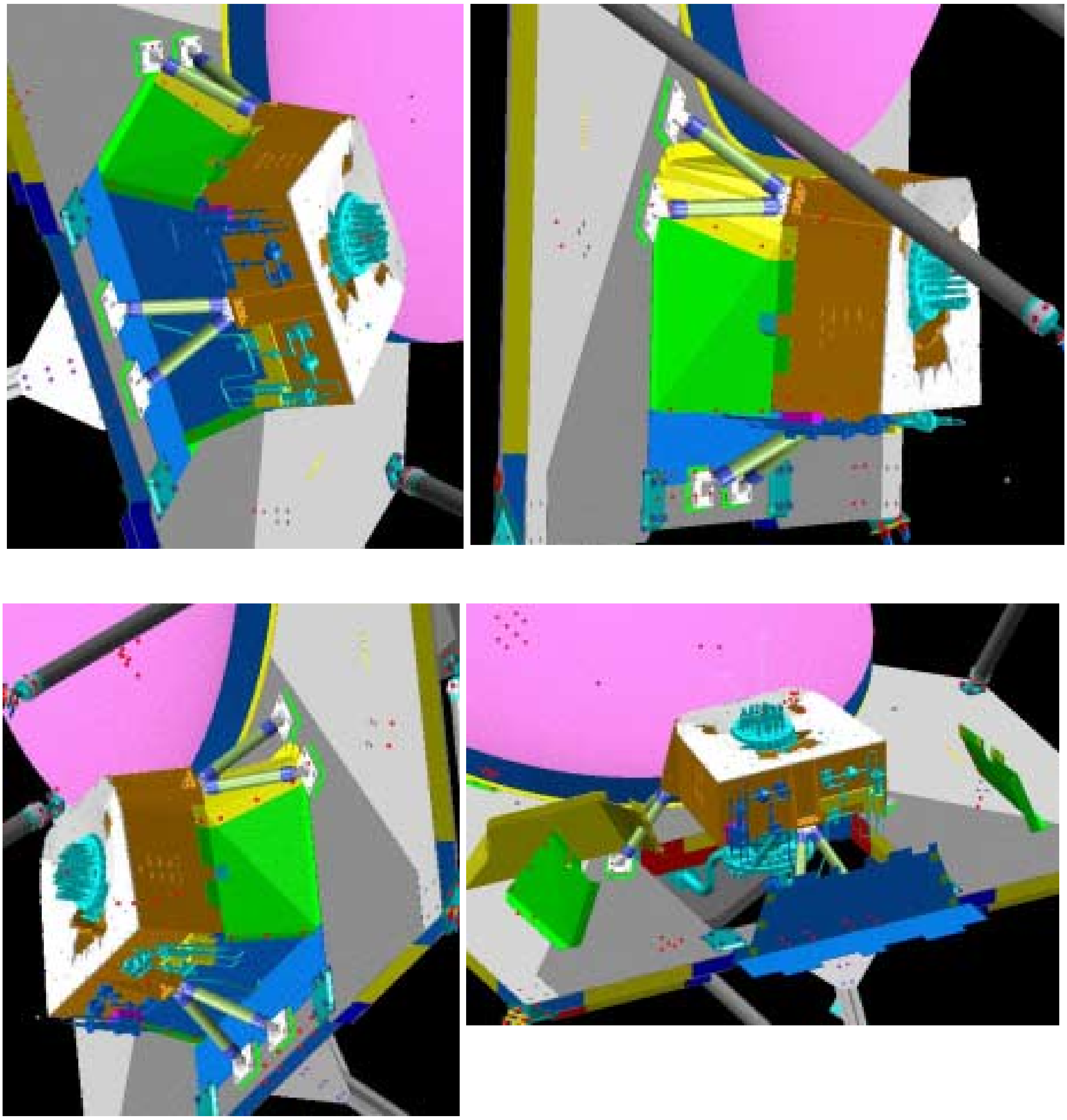

Figure 5.4-2 : FPU RF shield design and integration

The next step of the development of this shield are the followings :

- Refinement of the RF need to confirm if the shield in this area is mandatory (rejection budget displayed confortable margin in for this directions)
- To verify with the LFI instrument that the additional heat loads are compatible with FPU budget
- To verify the shield behaviour wrt acoustic loads

5.4.2 Baffle - Grooves 3 shield

The general drivers for the design of this large skirt are :

- The closure shape which follows as best as possible the baffle inner-side wall projection onto the Groove 3 surface (max deviation +/-20 mm)
- The acceptability of large dynamic displacements : up to ±45 mm laterally on the Baffle side walls.
- The attachment to the Baffle and Groove with Velcro (where it is not sliding) for mounting/dismounting capability
- The optical cavity emissivity need : parts inside the optical cavity : E < 0.05 (including parts of SR struts and frame concerned). Note that parts completely behind the SR (masked by the reflector) remain with bare material (the SR Panel for example).
- The RF shield need : 10 µm Al.

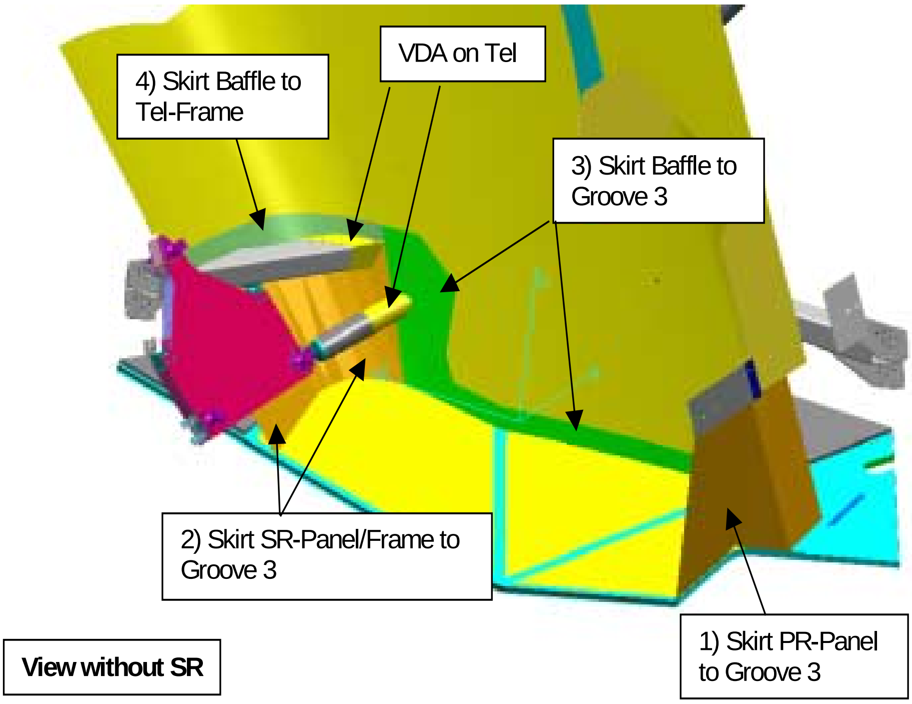

Figure 5.4-3 : overview of Baffle/Groove 3 skirt

The layup for the Baffle Skirts Blankets is :

"VDA-Kapton" + "10 µm Al-foil" + "Kapton-VDA"

Thickness of the Kapton-foils (Polyamide) = 25 or 125 µm depending of the Baffe zone.

VDA : aluminum coating on the Kapton foil, thickness < 0.1 µm

The 3 foils are bonded together with Scotchweld points : ϕ<10 mm in a pattern of about 100x100mm (bonding dimensions driven by the flexibility need for this multilayer).

Type of design depending of the Baffle zone :

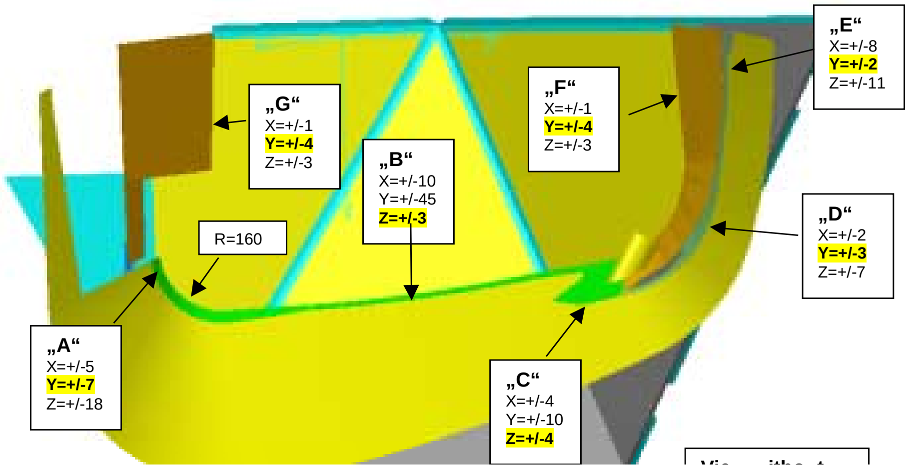

Slinding skirt	Attached (Vecro) skirt
Zone A and B (lateral sides & rear rounded corners)	**Zone G** (back side, directly on the PR Panel)
VDA-PI 125 µm / Al 10 µm / PI-VDA 125 µm	VDA-PI 25 µm / Al 10 µm / PI-VDA 25 µm

Exact definition for zones D, E & F (front side) are in progress

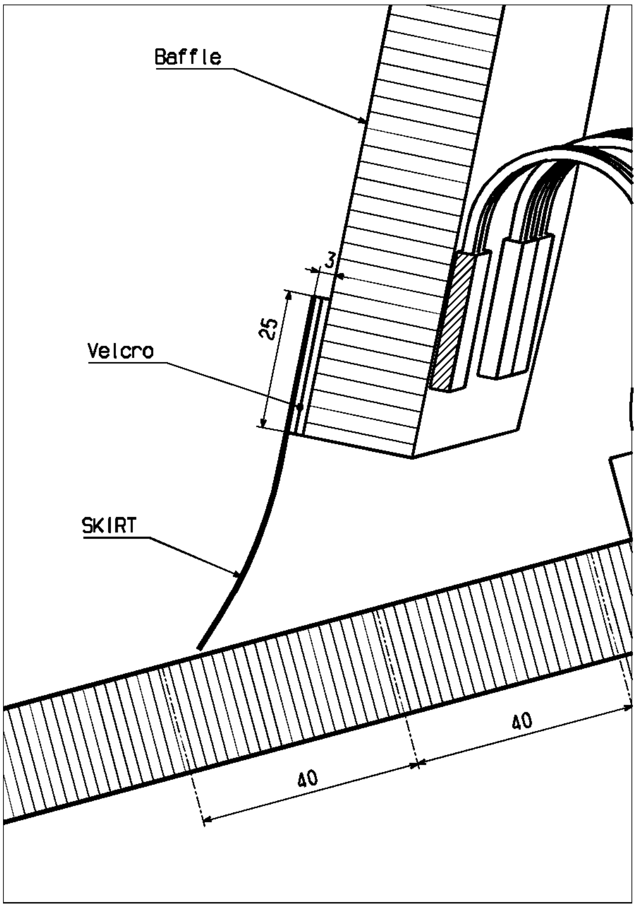

Figure 5.4-4 : slinding skirt design and manufacturing sample at CSAG

Main advantages and comments on the sliding skirt :

- Sliding on Groove 3 is possible in all 3 directions for the large expected displacements
- Installation is much more easier than the one of the ''attached on both sides'' concept (even with Velcro)
- Sliding is always on the shiny area of Groove 3 (no contact with the black painted zones of Groove 3)
- The stiffness of the Blanket when mounted in the configuration shown is very good (from manuf. sample)
- The mass is low, therefore it is not expected to have a problem of buckling or permanent deformation during vibration.

5.5 Cryo-structure & Baffle design

The detailed description of the Cryo-Structure and Baffle structure is performed in [RD17]. The main evolutions of their designs are described here after. Some pictures of the Qualification Model are presented at the end of the paragraph.

5.5.1 Main evolution of the Cryo-Structure

- Increase of the Goove 1 size : +5 mm on radius

  This modification comes from the need to have more comfortable margins regarding the 2 following critical aspects :

  Groove 1 shall not have a view factor with the sun

  => define the minimum diameter for the S.A.

  Groove 2, groove 3, Baffle and Telescope shall not have a view factor with the S.A.

  => define the maximum diameter for the S.A.

  The initial margins (of phase B) became to small regarding :

  the thermoelastic behavior of the Grooves (computed by CSAG with ASP thermal maps) : much more higher than required and expected, especially for Groove 1 : up to 8.4 mm in the out of plane direction (X PPLM). Note : this behavior is due to the high sensitivity of the groove aluminum large panel regarding thermal gradient in the panel thickness (deformation close to a bi-material beam effect).

  the manufacturing tolerance feasibility of this kind of very large Solar Array (S.A.) : uncertainty on the final real external diameter.

  The initial building of the grooves external dimensions was based on a shadowed cone of 12° coming from a Solar Array (S.A.) mini diameter of 4193 mm at X : 87.5 mm from the S/C coord. system.

  At this time, Planck was inside a SYLDA and the max allowed dimension for the S.A. was 4200 mm, thus the possible zone for the S.A. border was only 3.5 mm (on radius) without any margin.

  Consequently , to increase the margins, we took benefit of the new launcher configuration (with SPELTRA adaptor for Herschel) which allows to have a larger SA.

  The S.A. has now a 4220 ±2mm outer diameter (thus +13.5mm at radius w.r.t the initial diameter).

  The height of the +X edge remains at 87.5mm from the S/C coord system, the tolerance on this dimension is ±1mm.

This larger diameter of the S.A. implies a small increase of the Groove 1 diameter : +5 mm at radius , in order to keep the blanking of the Baffle with enough margin. The mass impact is rather low, about 0.3 kg regarding the initial configuration.

Main data for the study :

Groove border out-of-plane location at Operational T°	Groove 1 (mm)	Groove 2 (mm)	Groove 3 (mm)
C.S. manuf. / integration	±2	±2	±2
PPLM I/F / S/C	±0.5	±0.5	±0.5
Groove thermoelastic* *(X value) : w/o margin*	+8.4 *(+6.2)* 0 *(+2.2)*	+4.5 *(+3.1)* 0 *(+1.5)*	+1 *(+0.6)* -0.8 *(-0.5)*
Total	+10.9 -2.5	+7 -2.5	+3.5 -3.3

** the margin is close to 50% of the displacement range computed by CSAG (added on both sides of the Grooves)*

Groove border in-plane location at Operational T°	Groove 1 (mm)	Groove 2 (mm)	Groove 3 (mm)
C.S. manuf. / integration	±2.5 **	±2.5	±2.5
Location of SVM / SC	±0.15	±0.15	±0.15
Total	+2.7 -2.7	+2.7 -2.7	+2.7 -2.7

*** on the new definition of the Groove with +5mm on radius*

Baffle border location at Operational T°	''radialy'' (XZ plane) (mm)	Out-of-plane (X) (mm)
Baffle manuf. / integration	±3.5	±1.5
Tel / SVM location in-plane	±0.4	
SVM / S/C location in-plane	±0.15	
// C.S. (0.5 mm)	±0.6	
// SVM (0.5 mm)	±0.23	
C.S. / Tel shimming		+3 -0.5
C.S. out-of-plane tolerance		±1
SVM out-of-plane tolerance		±0.5
Total	±4.9	+6 –3.5

Note : the values taken into account for the study are +5 mm radialy and +10 mm out-of-plane (in order to have envelope values and to keep margins where possible).

Result of the study :

S.A. possible diameter at X= ±87.5 1 mm : **4208.5 mm < S.A. diameter< 4231.5 mm**

Note : this diameter is the upper edge of the S.A. panel (+X side)

Margins taken into account the specified S.A. tolerances (see drawing PLSA56GS001S : Planck S.A. Shadowing Capability) :

S.A. diameter = 4220 ±2 mm at X= ±87.5 mm

- Groove 1 to have a view factor with the sun : **4.75 mm**
- Baffle to have a view factor with the S.A. : **4.75 mm**

Note : the size of the 3 Grooves remains specified to CSAG at Operational Temperature regarding the former definition of the shadowed cone (with the S.A. =4193 mm), this only for convenience reason.

– The thermoelastic shrinking of the Aluminium panels of the Grooves is compensate at ambient temperature in order to reach the specified geometry at operational temperature.

The order of magnitude of the compensation is :

- Groove 3 : +7.5 mm (radialy, in the panel plane)
- Groove 2 : +7.3 mm (radialy, in the panel plane)
- Groove 1 : +6.5 mm (radialy, in the panel plane)

Note : the position of the Instruments interface holes do not take into account this compensation. The interface hole positions are specified at ambient and consequently move (mainly in the radial and out-of-plane directions) during the cool down. These displacement are taken into account at Instruments level via displacement requirements (expressed in the IIDA document).

5.5.2 Main evolution of the Baffle

– Optimisation of the Baffle edge geometry

The Baffle edge has evolved to a much more simple definition in order to release the manufacturing constraint. The status on the acceptability of this new design have been made on the basis of the Ticra RF analyses results.

The following figure shows a typical cross section of the new edge design : edge making a 90° angle with the Baffle walls.

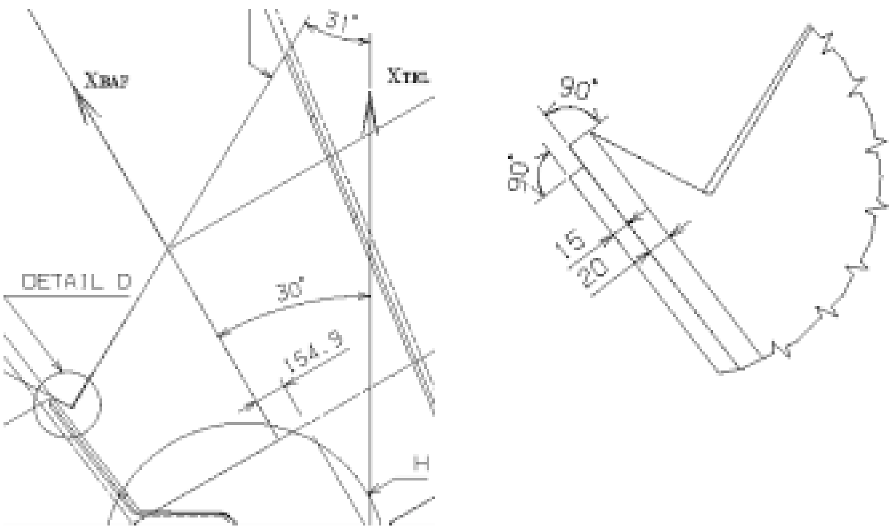

Figure 5.5-1 Baffle edge new design

– The thermoelastic shrinking of the Aluminium structure of the Baffle is compensate at ambient temperature in order to reach the specified geometry at operational temperature.

  The order of magnitude of the compensation is :

  - Upper edge : +3 mm perpendicular to the rim plane (close to X Baffle)
  - Radial, front (+Z) side : +2 mm
  - Radial, lateral (±Y) sides : +3 to +4 mm
  - Radial, back (+Z) side : +3 mm

5.6 Thermal design

5.6.1 Passive radiator

5.6.1.1 General design

As previously described in the mechanical and thermal architecture section, the passive thermal control design is based on :

- A 3 stage "V-Groove" radiative shield allowing to thermally uncouple efficiently SVM hot interface (300 K) from PPLM cold Instruments interfaces and optical environment (#50 K).

  The "V-Groove" rejection enhancement relies on low emissive and highly specular coatings, as well as controlled flatness and global geometry.
- An important (15 m²) and high emissive radiative surface implemented on 50K elements providing cold PPLM parts with sufficient heat rejection potential.
- Low conductive struts mechanically supporting the 50 K elements on the SVM.

Thermal homogeneity is moreover globally sought in order to optimise the radiating surface rejection and to limit hot spots around Instruments local heat inputs (use of thermal braids, high conductive materials …).

5.6.1.2 Cryo-structure design

5.6.1.2.1 Shields and baffle

Three faceted shields (Aluminium sandwich) compose the "V-Groove" system. Their proper definition and manufacturing are mandatory for an efficient heat rejection.

Unlike the two others, the shield 3 (coldest one) supports a high emissive coating including black painted open honeycomb.

The three shields edges (thickness at outer periphery) are painted black in order to enhance the shields power rejection ability.

The Shields sandwich skins are made of MIRO27 [EN AW 1085 H18 (Al 99.85)] coated with PVD [EN AW 1199 (Al 99.99%)]. This quite pure Aluminium presents the great advantage to be highly conductive at cold temperature. Moreover, its PVD coating ensures good thermo-optical properties (low emittance, high specularity).

Defaults and singularities (flatness, screws, holes…) of Shields surface have systematically been minimised in order to make the most of MIRO ideal thermo-optical properties.

- Screws are covered by Aluminium tape and chamfers have been chosen instead of steps.
- The pipes routing has been chosen so that it may yield the minimum radiative screening (pipes in radial direction when feasible), the mechanical blades are hidden behind the struts.
- The screens used to blind the shields "Wave Guides holes" have been designed in order to allow at best radial radiation rejection.
- "pipes and struts holes" are blinded by Aluminised Kapton foils (blinding enhanced by two Kapton layers on both sides of Shield1&2).

Shields facets are linked by three different interface designs, as described in Figure 5.6-1, Figure 5.6-2 and Figure 5.6-3.

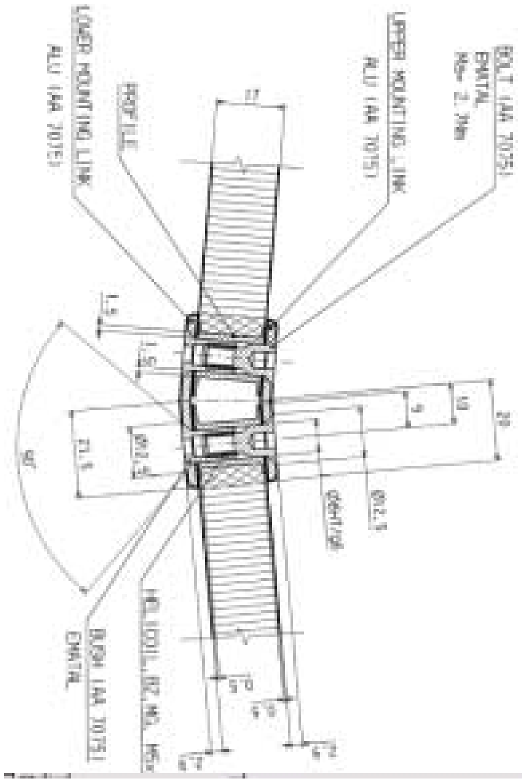

Figure 5.6-1 : Shields facets links : external - external

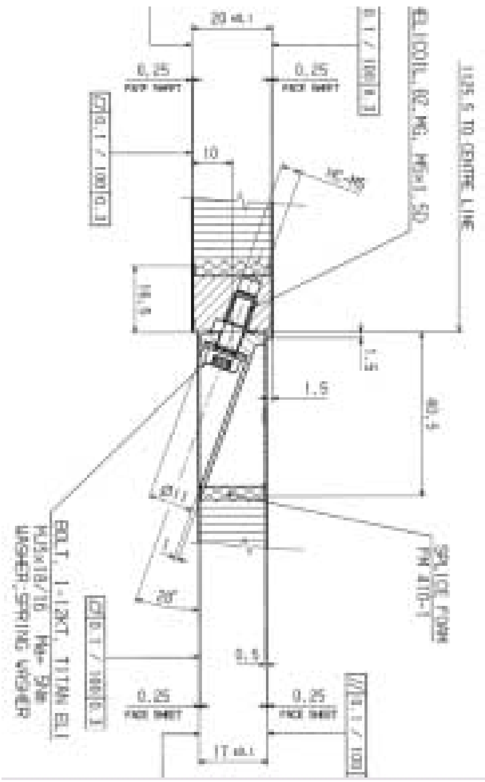

Figure 5.6-2 : Shields facets links : internal - external

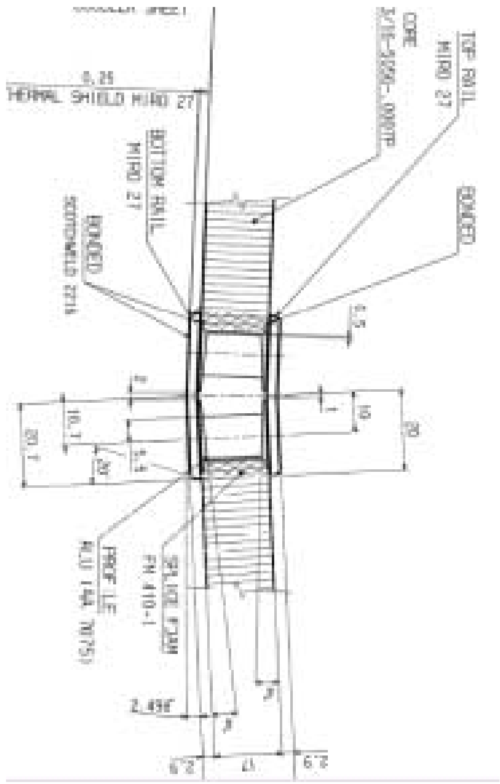

Figure 5.6-3 : Shields facets links : internal - internal

The links use additional Aluminium doubler (internal-internal & external-external) or facet-to-facet direct screwing (internal-external).

Unlike the internal-internal interface, based on glued contacts, the two other interfaces are based on dry contact surfaces. Dry contacts being in general very design sensitive, it has been necessary to comfort the associated thermal performance with dedicated measurements on representative samples at operational temperature.

The Baffle sandwich has also MIRO27 skins and supports an important part of the overall radiative area (about 70% of external baffle surface is equipped with black painted honeycomb).

5.6.1.2.2 Cryo struts

The cryo struts are made of GFRP for thermal insulation reasons. They are heat sinked to the shields by means of Aluminium blades and additional copper straps, as shown in Figure 5.6-4. Cryo struts inner volume is filled with low conductive ECCOSTOCK foam in order to prevent inner radiative couplings from degrading the insulating function of the struts.

Note that bracing struts between SVM and Shield 1 are also made of GFRP.

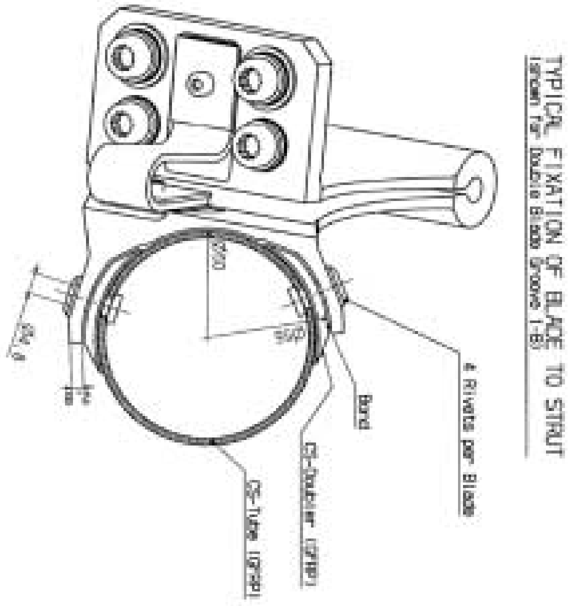

Figure 5.6-4 : Struts/Shields link

5.6.1.2.3 Telescope

Reflectors panels are made of CFRP/Aluminium Sandwich. Due to its large dimensions, primary reflector panel is covered by an important radiating area (part of which is black open honeycomb). Exception made of elements in view of the optical cavity, all telescope elements are black painted in order to improve heat rejection ability.

5.6.1.3 Groove 3 and baffle High emissivity coating

5.6.1.3.1 HEC description

After synthesis of :

- main constraints related to the use of paints,
  - availability,
  - applicability,
  - adhesion,
  - cleanability,
  - outgassing,
  - electrical resisitivity,
- available emissivity data,
  - specular reflectance at LEMTA,
  - direct measurements at LEEE,

PUK (MAP) appears to be the best candidate for Planck PLM High emissivity coating.

The associated emissivity performance requires the use of open honeycomb; this honeycomb has been sized at maximum allocated weight (in line with CSAG mechanical sizing) i.e maximum height (14.3mm height for 3/8" cells).

As described in Figure 5.6-5 and Figure 5.6-6, baffle and Shield 3 high emissive coatings combine areas covered with black open honeycomb or flat paint.

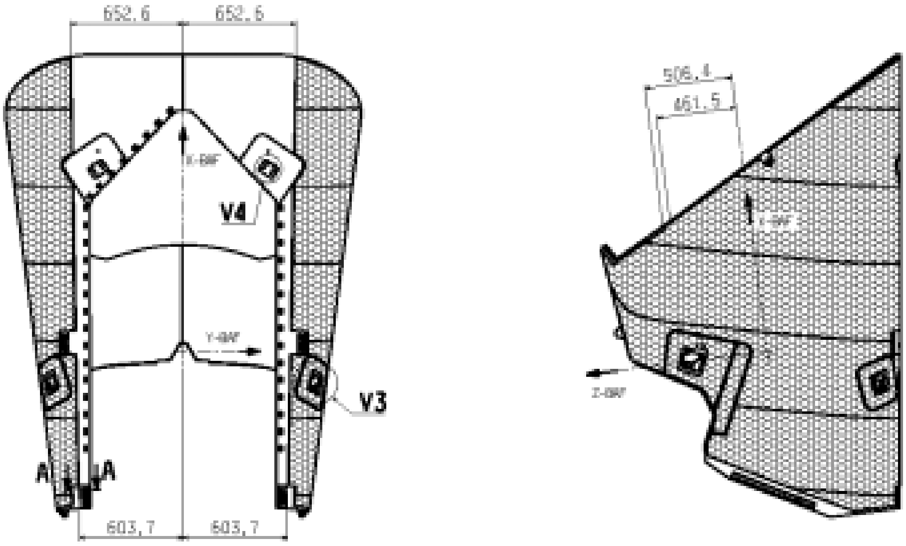

Figure 5.6-5 : Baffle open honeycomb coverage

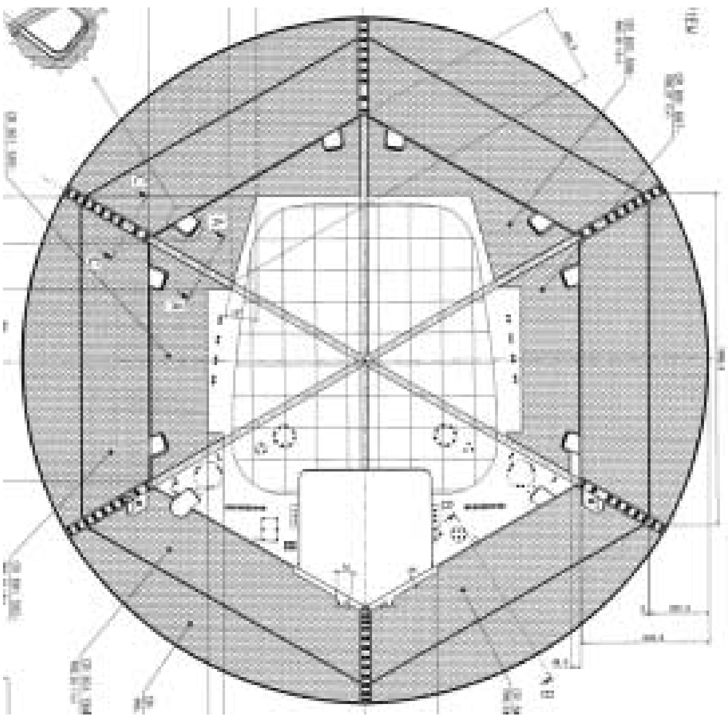

Figure 5.6-6 : Shield 3 open honeycomb coverage

Open honeycomb areas themselves are made of different patches with significant gaps between (not shown in drawings). Observations on hardware allowed to estimate the actual distribution between flat areas and open HC areas. For instance, Baffle open honeycomb can be considered as covering 90% of the theoretical surface, and represents 70% of the Baffle overall external surface. Observations also permitted to detect and take into account glue traces in the cells bottom (emissivity degradation).

5.6.1.3.2 HEC emitance characterisation

- LEEE measurements

  Emissivity is directly measured by using He cooled bolometer and synchronous detection.

  The used set-up is schematically presented in Figure 1-9.

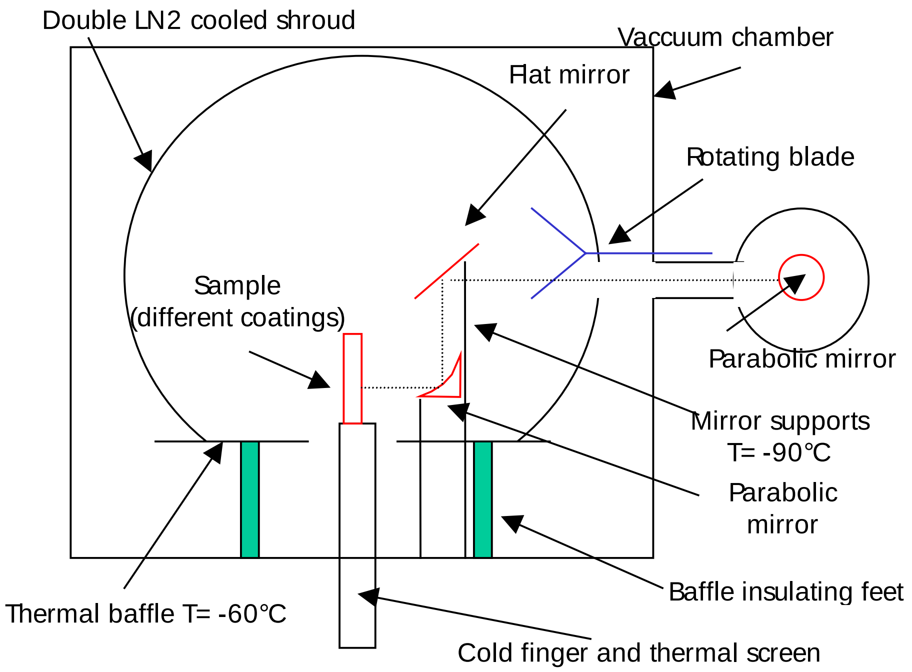

Figure 5.6-7 : LEEE emissivity measurement set-up

The method is based on relative measurements wrt blacbody emission (the blackbody being part of sample definition).

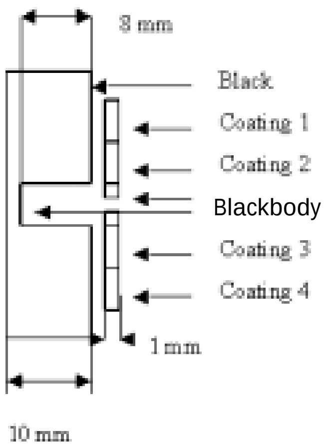

Figure 5.6-8 : LEEE sample

At the time this report is written, the blackbody performance is not as good as expected and only relative measurements between the different coatings composing the sample are possible. In order to estimate absolute values, the Z306 emissivity values are taken as reference. Parallell actions are in progress to improve the blackbody performance (new shape).

- LEMTA measurements

Normal Specular Reflectance measurements provide monochromatic data over the useful wavelength range. The processing of these data give optimistic emissivity values and must be handled cautiously.

Though these data were initially not intended to be directly used for emissivity determination, a few processing exercises have been performed in order to provide qualitative values to be compared to LEEE measurements.

Figure 5.6-9 shows directly derived emissivity "wrong" values (comparison with similar data got by ASED for Herschel):

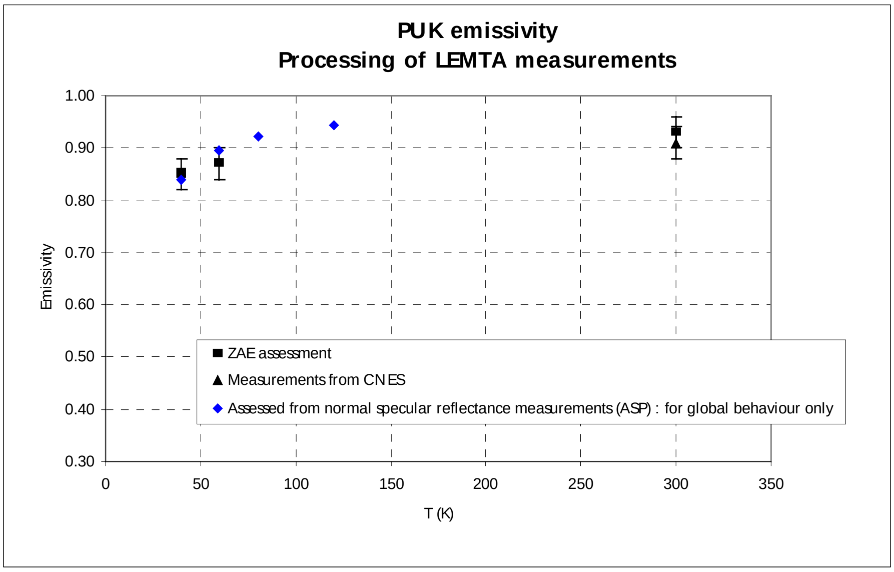

Figure 5.6-9 : PUK emissivity / LEMTA measurements processing

The obtained high emissivity values are very doubtful.

The same exercise, applied to Z306, is compared to ASP calorimetric measurements in Figure 5.6-10.

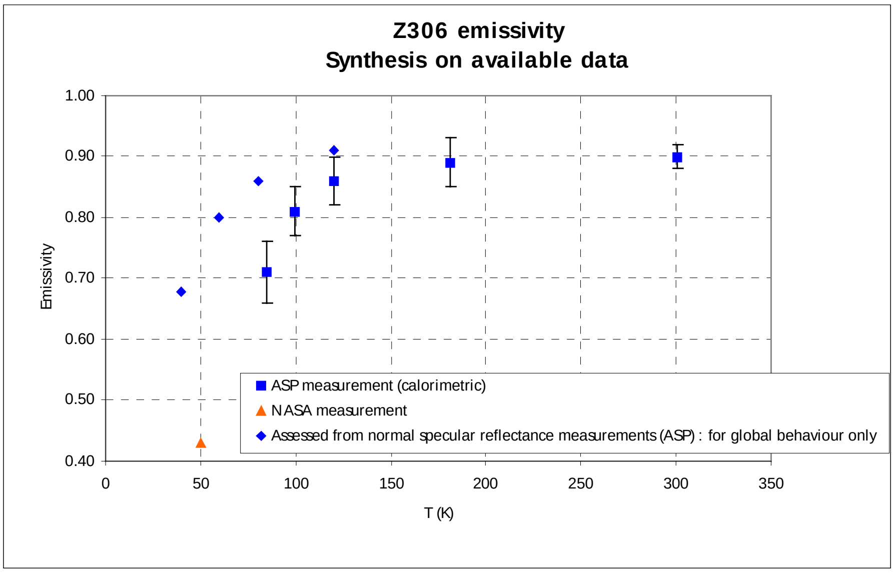

Figure 5.6-10 : Z306 emissivity

It is shown that a large correction has to be applied between Reflectance and Calorimetric measurements. If the same correction is applied to PUK measurements, Figure 5.6-11 shows that the obtained values are comparable to LEEE measurements.

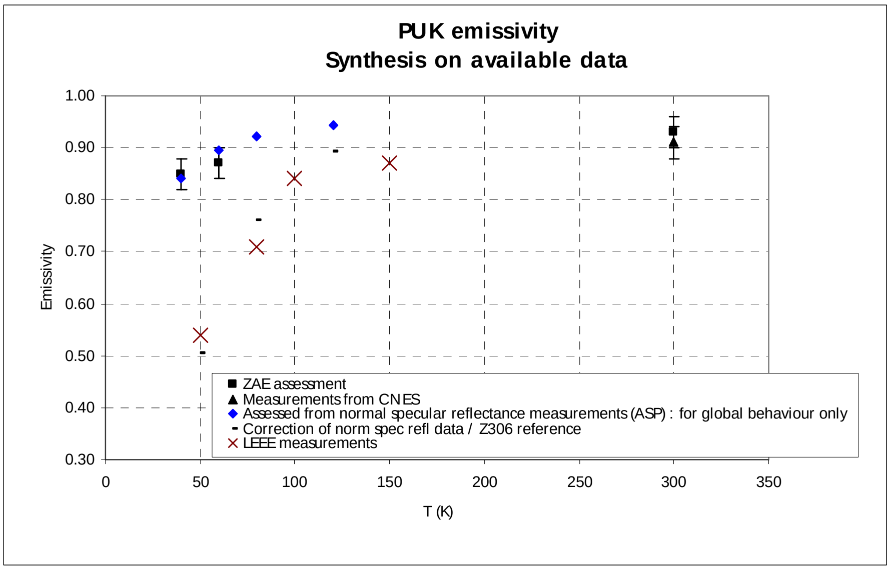

Figure 5.6-11 : PUK emissivity / Correction of reflectance measurements

Figure 5.6-12 shows the synthesis of all available data as well as the emissivity values used in TMM for performance assessment.

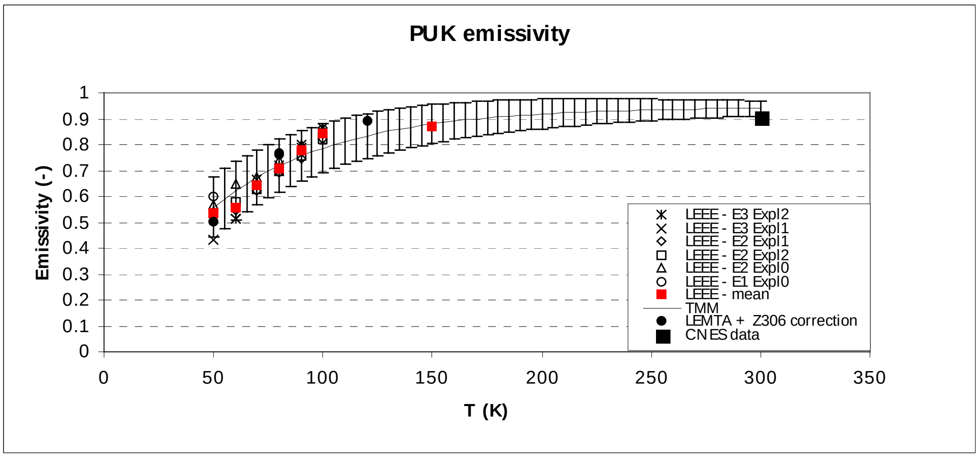

Figure 5.6-12 : PUK emissivity / Synthesis

One can note that the worst case value @50K is very low (#0.41).

Figure 5.6-13 shows the corresponding black open honeycomb emissivity values.

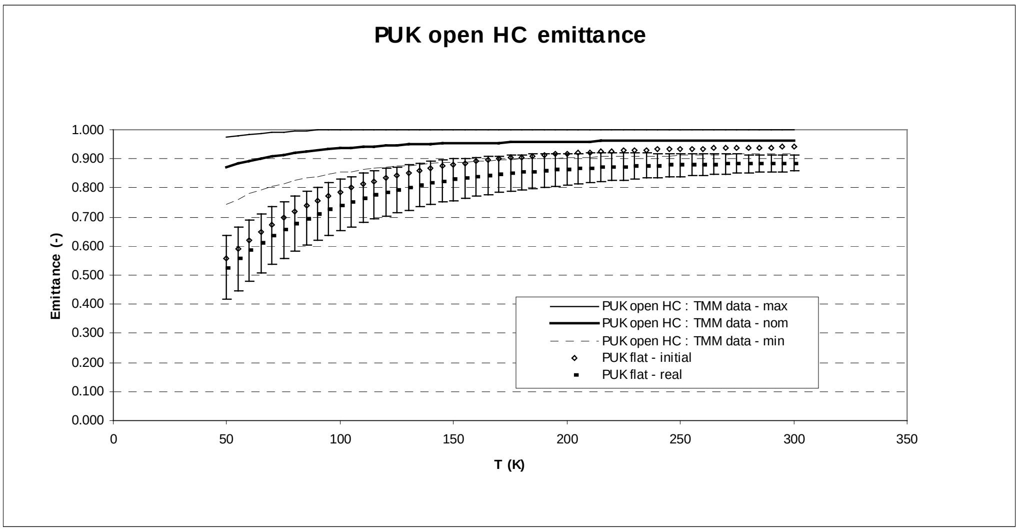

Figure 5.6-13 : Open HC emittance

Details about open HC emittance characterisation are reported in [RD**Erreur! Source du renvoi introuvable.**].

5.6.1.4 SLI shields

- Shields between the RAA WG and the Grooves

  These shields are attached by Velcro on the Lower Support Structure (LSS) flanges on one side (RAA interface) and on the Grooves on the other side (also with Velcro, Cryo-Structure interface).

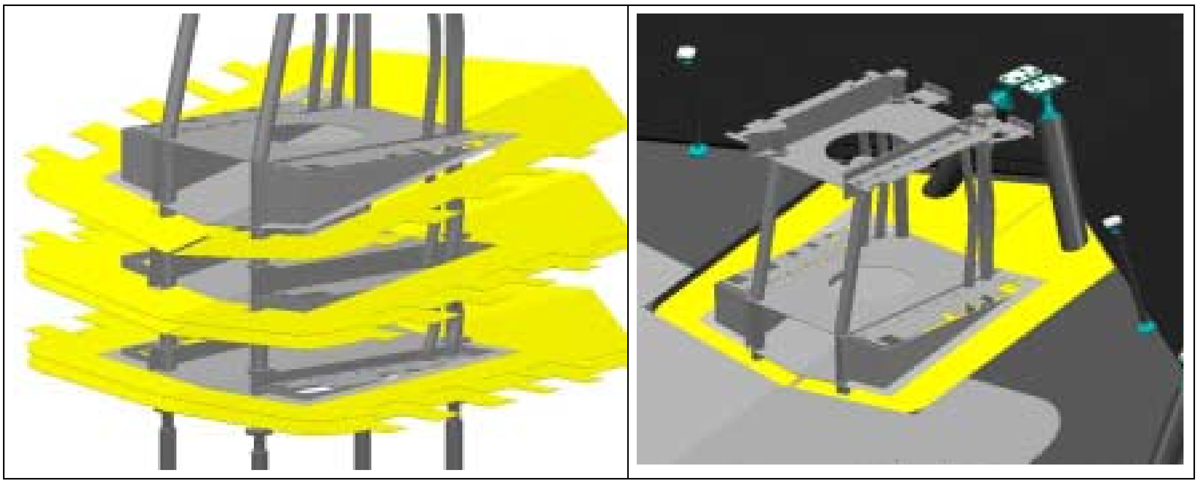

Figure 5.6-14 : shields between WG LSS and the Grooves

They are located on the lower and upper sides of Groove 1 and 2 in order to blank also the edge of the Grooves cuts-out.

The detailed composition of the shields is still in progress at the moment but the foreseen material is : SLI Kapton 125 µm (polyamide) with VDA coating on both faces (thickness < 0.1 µm). The choice for the Kapton foil thickness is driven by the required strength regarding mechanical and thermoelastic environments. The VDA coating answers to the low emissivity requirement on the Grooves.

Notes :

- The combination SLI + Velcro allows the differential thermoelastic displacements between the Grooves and the WG LSS. The order of magnitude of these displacements is :
    - From 3 to 5 mm in radial direction (shrinking of the Grooves towards the centre of the PPLM – X axis) => displacement on +Z at the LSS level
    - From 2 to 3 mm in the out-of-plane direction (flexure of the Grooves linked to thermal gradient in the panel thickness)
- There is no interference issue between these shields and the Wave Guides thermal braids (see Figure 5.6-15).

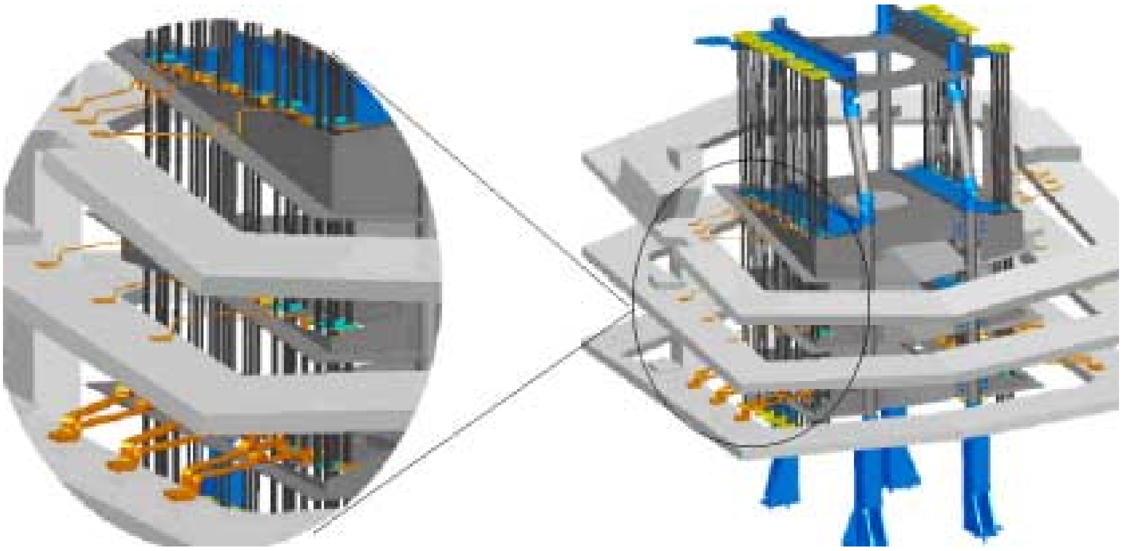

Figure 5.6-15 : Design of the WG thermal braids interfacing the Grooves

- Shields between the Cryo-Struts and the Grooves

These shields are only bonded onto the Grooves, on the central part panels. The small gap of 5 mm around each strut allows the crossing of the PPLM harness (sensors and reflectors heaters).

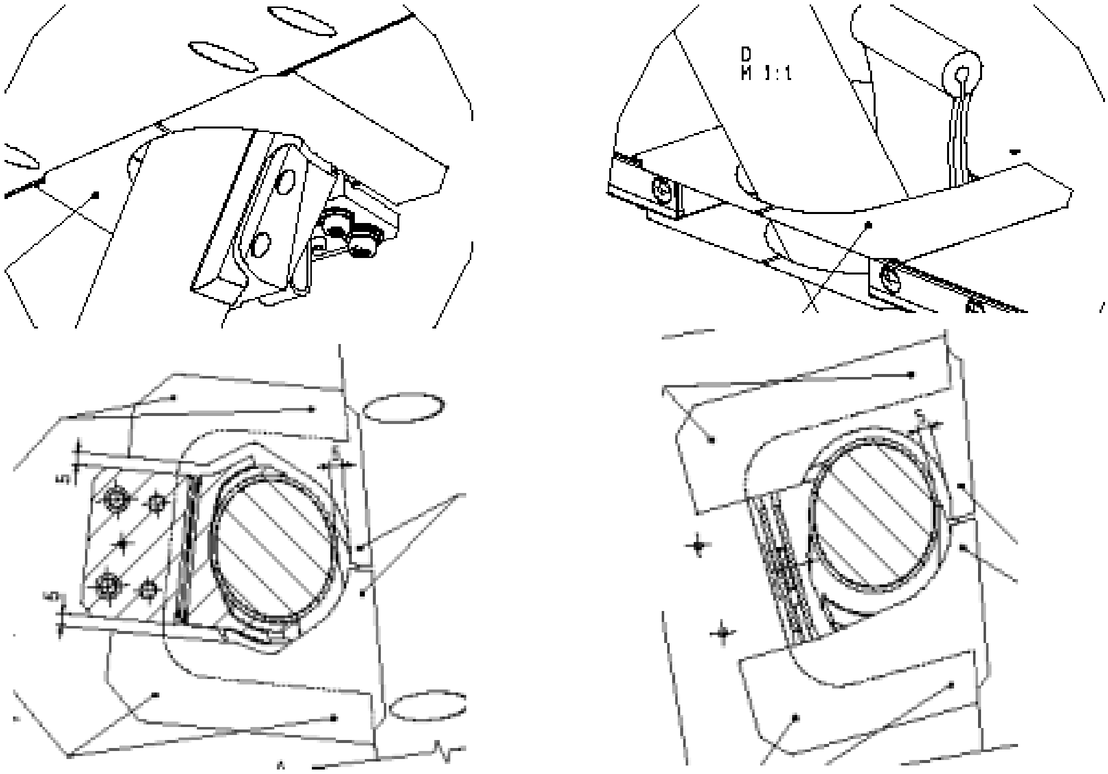

Figure 5.6-16 : shields between Cryo-Struts and the Grooves

As for the RAA shields, these shields are located on the lower and upper sides of Groove 1 and 2 and only on the lower side of Groove 3.

The detailed shields composition is : SLI Kapton 130 µm (polyamide) with VDA coating on external faces (thickness < 0.1 µm), bonded with Elecolit 325 (electrically conductive).

As for the RAA shields, the choice for the thickness of the Kapton foil is driven by required strength regarding mechanical environments. The VDA coating answers the low emissivity requirement on the Grooves.

Note that these foils are flexible enough to slide the Struts in, and stiff enough to keep their flat shape.

- Shields between the Sorption pipes (20K Cooler) and the Grooves

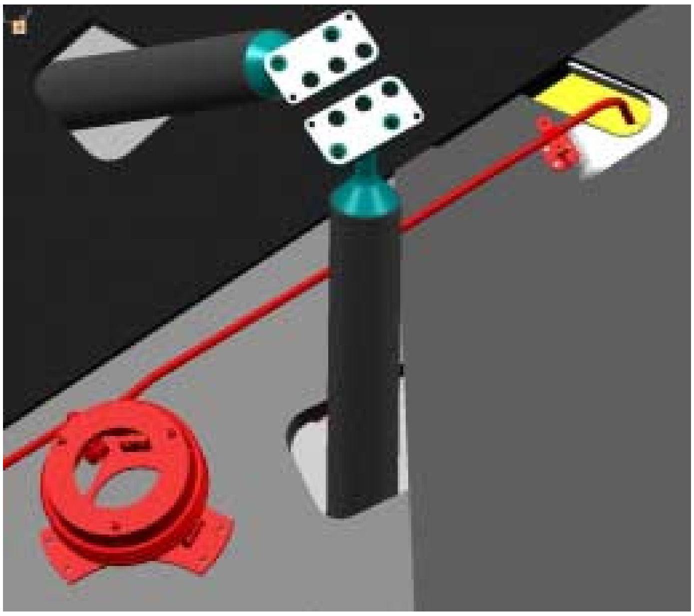

Figure 5.6-17 : shields between Sorption pipes and the Grooves (here : top view above Groove 3)

These shields are located on the lower and upper sides of Groove 1 and 2 in order to blank also the edge of the Grooves cuts-out.

The detailed composition of the shields is still in progress at the moment but the foreseen material is : SLI Kapton 125 µm (polyamide) with VDA coating on both faces (thickness < 0.1 µm)

They are attached only on the Grooves, with Velcro. They will have a thin razor cut to let cross the pipe.

The choice for the thickness of the Kapton foil is driven by required strength regarding mechanical and thermoelastic environments. The VDA coating answers to the low emissivity requirement on the Grooves.

- Shields between the HFI Bellow and the Grooves

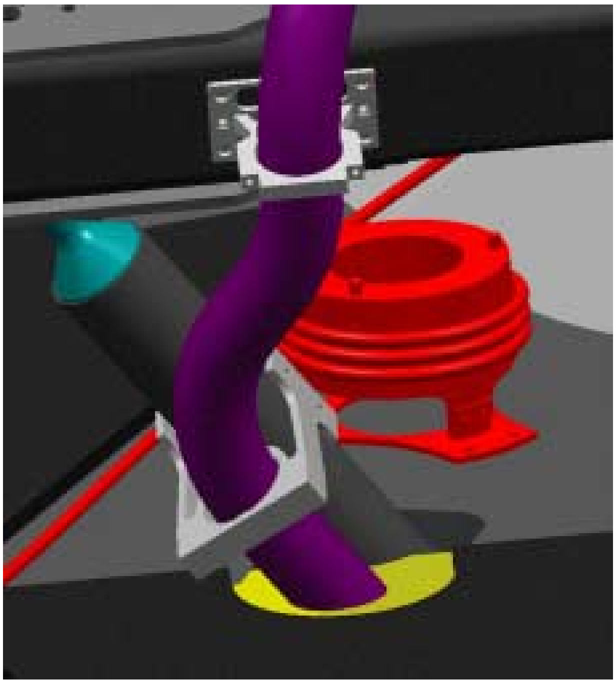

Figure 5.6-18 : shields between the HFI Bellow and the Grooves (here : top view above Groove 3)

These shields are located on the lower and upper sides of Groove 1 and 2 in order to blank also the edge of the Grooves cuts-out.

The detailed composition of the shields is still in progress at the moment but the foreseen material is : SLI Kapton 125 µm (polyamide) with VDA coating on both faces (thickness < 0.1 µm)

The shields are attached on the Grooves and also on the Bellow itself (TBC), with Velcro.

The choice for the thickness of the Kapton foil is driven by required strength regarding mechanical and thermoelastic environments. The VDA coating answers to the low emissivity requirement on the Grooves.

5.6.1.5 Thermal braids

Temperature homogeneïty between different Cryo-structure and Telescope elements is improved by use of Copper thermal braids.

Thermal braids thermally link :

- The Baffle lateral lower sides with Groove 3
- The Baffle rear lower sides with Groove 3
- The Baffle rear side with the Telescope main Panel (the PR Panel)
- The frame with PR and SR panels

Thermal braids assemblies are constituted from only one type of elementary braid. The number of elementary braids varies according to the required conductance. The different braids assembly characteristics are given here below :

Braids assemblies	Number of elementary braids	Average length (mm)
Baffle – Shield 3 (CSAG)	64	100
Baffle – Shield 3 (ASP)	120	350
Baffle – PR Panel	40	120
Frame – PR Panel	8	50
Frame – SR Panel	2	50

Table 5.6-1 : Braids assemblies description

The braids are either glued or screwed on each side according to dismountability needs.

Notes :

- All the thermal braids are symmetric on +Y and –Y (mirror w.r.t. the X,Z plane).
- The braids are either glued or screwed on each side according to dismountability needs.

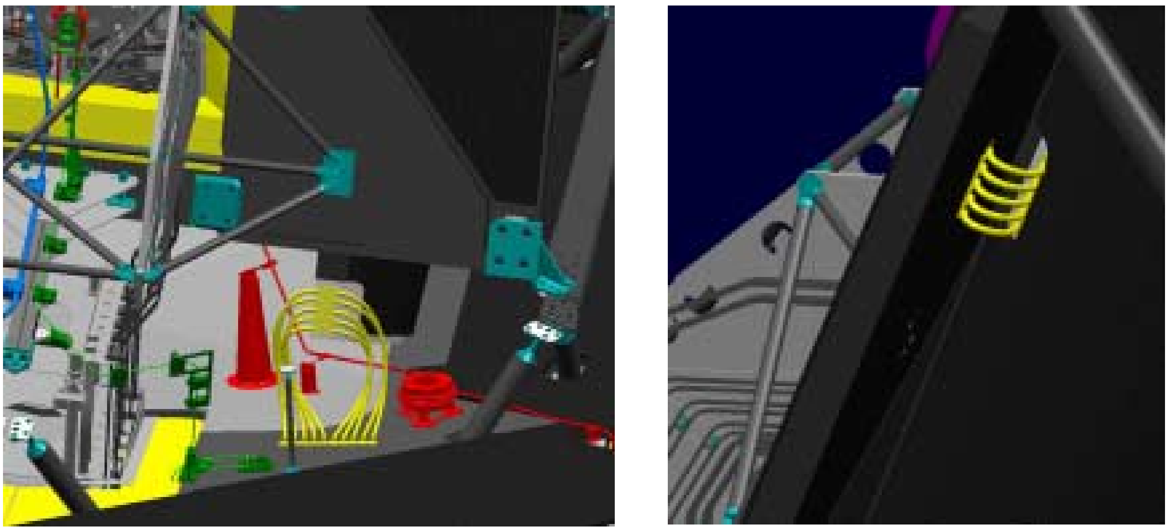

Figure 5.6-19 : Thermal braids at the rear side of the Baffle

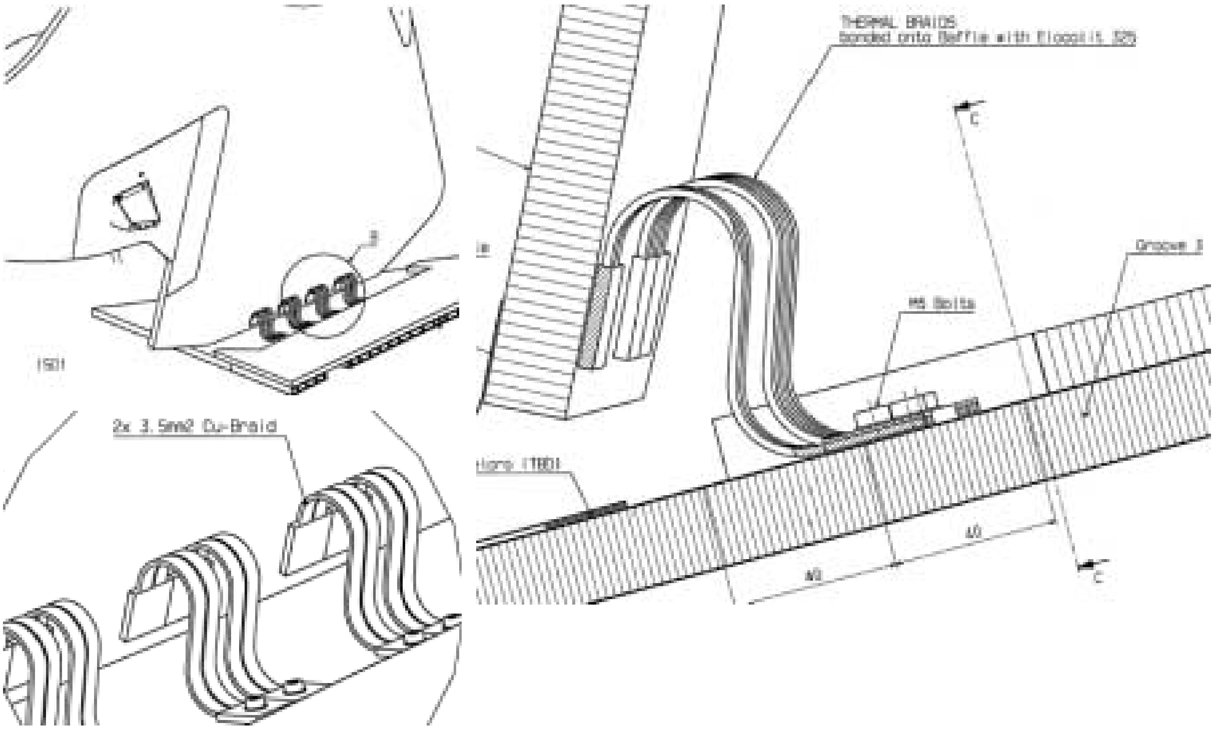

Figure 5.6-20 : Thermal braids on Baffle lateral sides

5.6.1.6 Design of the heat exchanger/grooves interfaces

The Sorption Cooler shield 3 coldest interface is a major parameter for the whole cooling chain proper functioning. The PPLM has therefore to ensure specified max temperatures at the Sorption Cooler exchangers interfaces. The temperatures being specified at the “exchanger side”, the thermal contact between the exchangers and the shields is under ASP responsibility.

In order to reduce the heat flow passing through the most critical I/F (coldest), and hence to limit the gradient occurring within this I/F, the shield 3 exchanger has been split into three different “sub-exchangers”.

Each Precooler is attached to the structure by used of titanium ELI screws (titanium specific for cryogenic temperature : Extra Low Interstitial). Spring washers are added in order to keep sufficient contact pressure and hence thermal conductance.

The used washers are made of CuBe2 with a conical shape (Belleville type) with a thickness of 0.4 mm, they are put together in parallel in order to have ‘’n’’ time the stiffness of 1 individual washer. The number of washers is defined to loose at maximum 20% of the screw pre-tension at ambient temperature. This number can reach from 1 to 10 pieces per screw depending on the temperature, the tightened material and the thickness.

A flat stainless steel washer is placed between the spring washers and the precooler (or braid end fitting) in order to avoid any damage of the tightened material.

The characteristics of the SC heat exchangers interfaces are listed in Table 5.6-2.

Sorption Cooler exchangers characteristics	Unit	Groove 1 (warmest)	Groove 2 (interm.)	Groove 3 (coldest)
Nb. of exchangers	-	1	1	3
Length	mm	350	350	196
Width	mm	35	35	35
Material	-	Copper	Copper	Copper
Nb. of screws per unit	-	2 x 16 M4	2 x 16 M4	2 x 9 M4
Op. temperature	K	150	100	50

Table 5.6-2 / Sorption Cooler exchangers

A detailed analytical study of “SC exchanger – Shield 3” coupling has been performed in order to provide solid assumptions for global analyses. This study involved dedicated local model detailing heat transfer, through inserts, from the copper exchanger to the shield.

5.6.2 Active thermal control hardware

The PPLM active thermal control (excepted the cryo-cooler system) is composed of decontamination heating lines and temperature sensors. All the electrical interfaces are detailed described in [RD18].

5.6.2.1 Reflectors decontamination heating lines

5.6.2.1.1 Overview

Heating lines	Line definition	Type	Max delivered power (W)
Primary Reflector	PR_N1	N	60
	PR_N2	N	60
	PR_R	R	60
Secondary Reflector	SR_N	N	60
	SR_R	R	60
Focal Plane Unit -HFI	FPUHFI_N	N	60
	FPUHFI_R	R	60
Focal Plane Unit -HFI	FPULFI_N	N	60
	FPULFI_R	R	60
Total nominal line	5		
Total redundant line	4		

Table 5.6-3 : Decontamination heating lines

5.6.2.1.2 Hardware description

- Heaters
  - PR heater type 1 :

    Geometry : as defined in DRW 2540-4100-30A01B of Planck reflector ICD reference PLA-ASED-RP-004 Issue 3.1

    Resistance : 492.3 Ω

    Resistance tolerance : ≤5%
  - PR heater type 2 :

    Geometry : as defined in DRW 2540-4100-30A02B of Planck reflector ICD reference PLA-ASED-RP-004 Issue 3.1

    Resistance : 391.6 Ω

    Resistance tolerance : ≤5%
  - SR heater :

    Geometry : as defined in DRW 2540-4200-30A01B of Planck reflector ICD reference PLA-ASED-RP-004 Issue 3.1

    Resistance : 534.1 Ω

    Resistance tolerance : ≤5%
- Harness and connectors
  - Harness between the heater mats and the ISMs (50K stage) :

    Twisted pair of copper wires AWG 28 with kapton insulation and polyimide lacquer according to ESA / SCC 390 10 1910 B
  - Harness between the ISMs (50K stage) and the PPLM subplatfom connector:

    Twisted pair of brass wires AWG 24 with PTFE insulation according to specification ESA / SCC 3901 and ASP specification 878468 Issue 01.00 and as defined in Figure 5.6-21.
  - Connector type on the PPLM subplatform, at the PPLM/SVM interface:

    1 x 340100201B DAMA15P NMB to connect the PR and SR nominal lines

    1 x 340100201B DAMA15P NMB to connect the PR and SR redundant lines
  - Contact type at the PPLM/SVM interface : ESA/SCC 3401 005 01B

Thermo-electrical optimisation (see [RD3]) lead to the use of AWG24 Brass wires for heating lines. See Figure 5.6-21 for cable description.

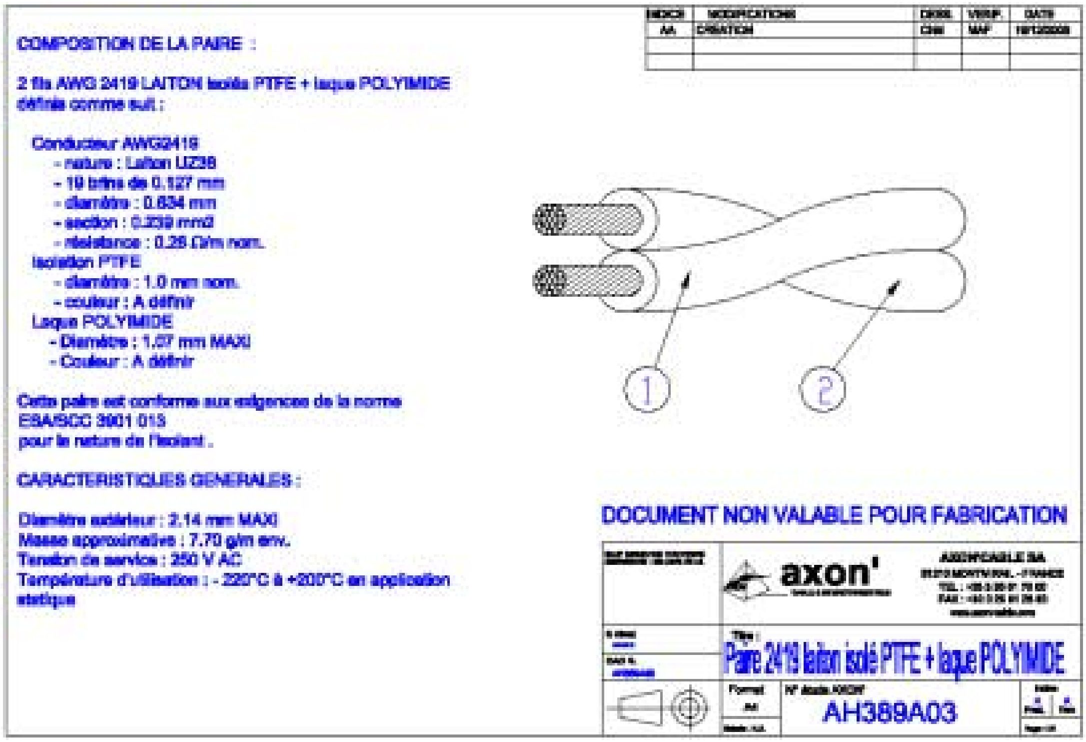

Figure 5.6-21 : Definition of the 50 K – 293K heater cable (AWG 24 brass cable)

5.6.2.2 Temperature Sensors

5.6.2.2.1 Overview

Operational Temperature sensors	Nominal / Redundant	Number
Shield 1	N	3
	R	3
Shield 2	N	2
	R	2
Shield 3	N	5
	R	5
Baffle	N	4
	R	4
PR Panel	N	4
	R	4
Reflectors	N	4
	R	4
Total nominal	22	
Total redundant	22	

Table 5.6-4 : Operational temperature sensors

Decontamination Temperature sensors	Number
Primary reflector	3
Secondary reflector	3
FPU LFI	3
FPU HFI	3
Total	12

Table 5.6-5 : Decontamination temperature sensors

5.6.2.2.2 Hardware description

- Sensors
  - Sensor type : Rosemount 118 MF 2000 2 wires
  - Potting : Stycast 2850 FT
- Harness and connectors
  - Fixation its support : bonded with Stycast 1266
  - Cable : Twisted pair of brass wires AWG 28 with PTFE insulation and polyimide lacquer, according to specification ESA / SCC 3901 and ASP specification 878468 Issue 01.00 and as defined in Figure 5.6-22.
  - Connection between the sensor and the cable : Cable joint 324369
  - Connector type on the PPLM subplatform, at the PPLM/SVM interface:

    1 x 340100201B DEMA 9S NMB to connect the PR nominal sensors

    1 x 340100201B DEMA 9S NMB to connect the PR redundant sensors

    1 x 340100201B DEMA 9S NMB to connect the SR nominal sensors

    1 x 340100201B DEMA 9S NMB to connect the SR redundant sensors

    1 x 340100201B DEMA 15S NMB to connect the FPU decontamination loop nominal sensors

    1 x 340100201B DEMA 15S NMB to connect the FPU decontamination loop redundant sensors

    1 x 340100201B DDMA 50S NMB to connect the PPLM structure nominal sensors

    1 x 340100201B DDMA 50S NMB to connect the PPLM structure redundant sensors

  Contact type at the PPLM/SVM interface : ESA/SCC 3401 005 04B

Note that sensors are acquired through 2-wire acquisition. See Figure 5.6-22 for AWG28 Brass wires description.

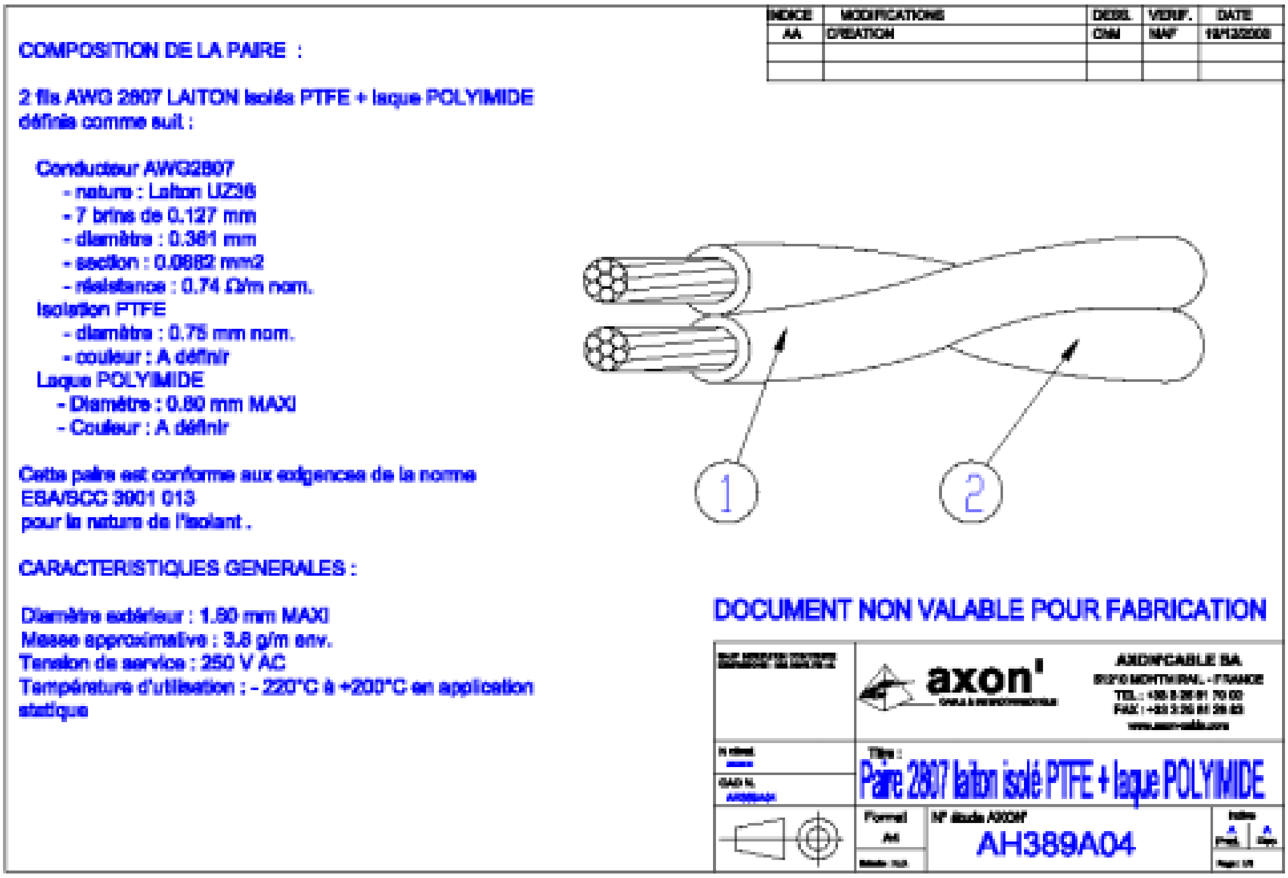

Figure 5.6-22: Definition of the 50 K – 293K temperature sensor cable (AWG 28 brass cable)

5.7 Instruments accommodation

5.7.1 General accommodation

The general accommodation of the Instruments with their interfaces on the PPLM Structural side (over the PPLM Subplatform, X > 966.5 mm) are presented here after.

The proposed design takes into account the requirements and constraints described in the HFI and LFI IIDB documents.

The Instruments units inside of the Planck SVM are shown here after for information, their accommodation is dealt directly with the System team in charge of the SVM.

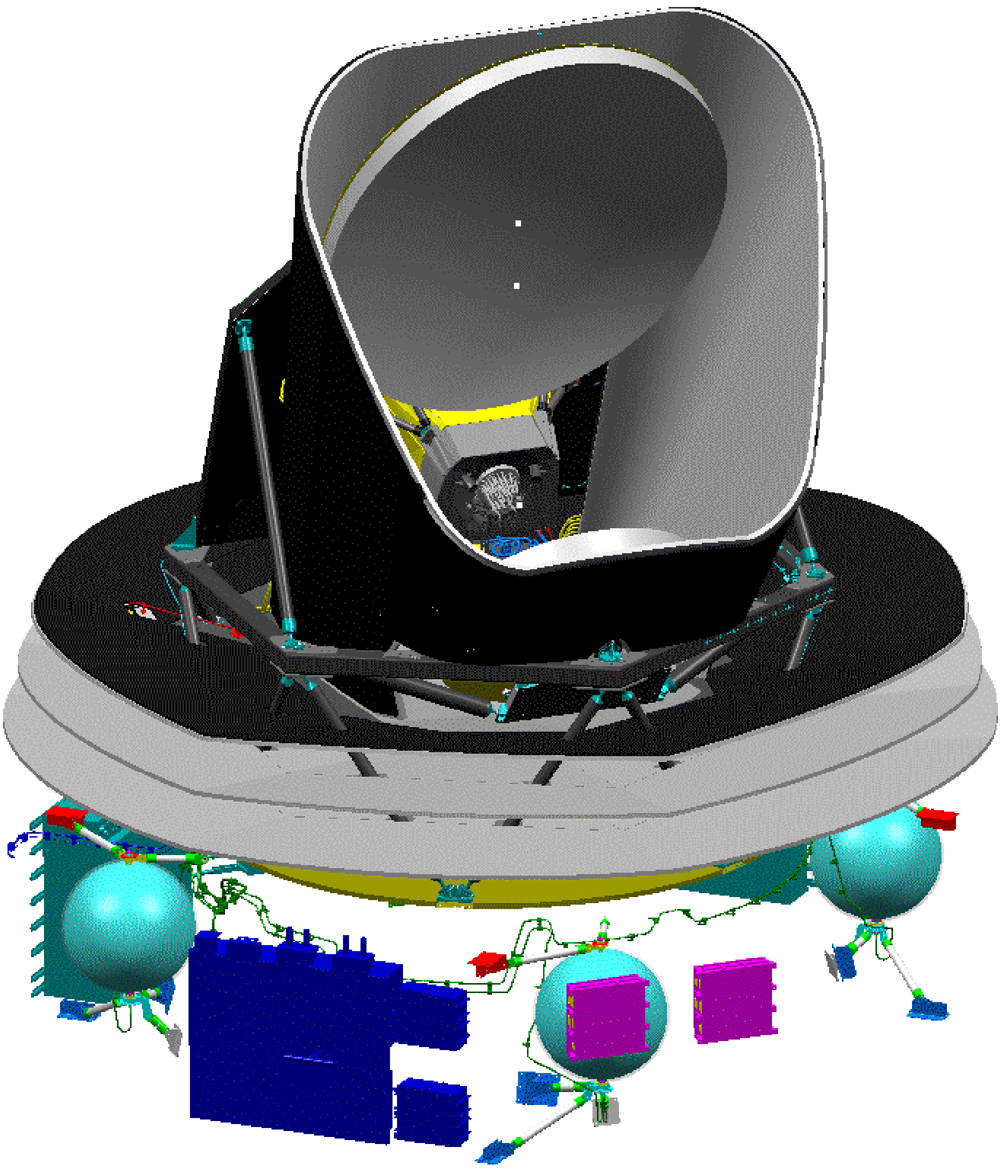

Figure 5.7-1 : Instruments general implementation (front side)

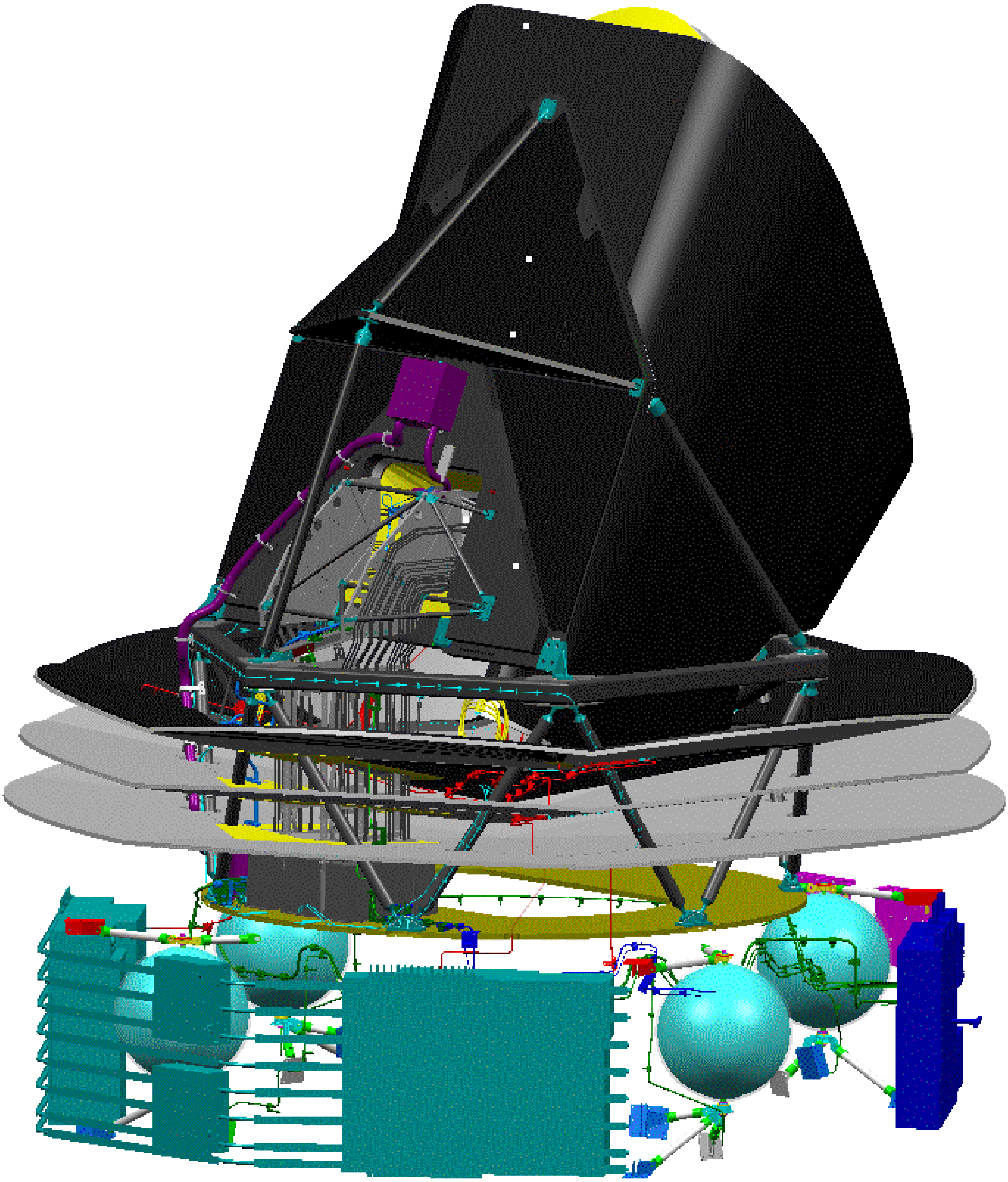

Figure 5.7-2 : Instrument general implementation (rear side)

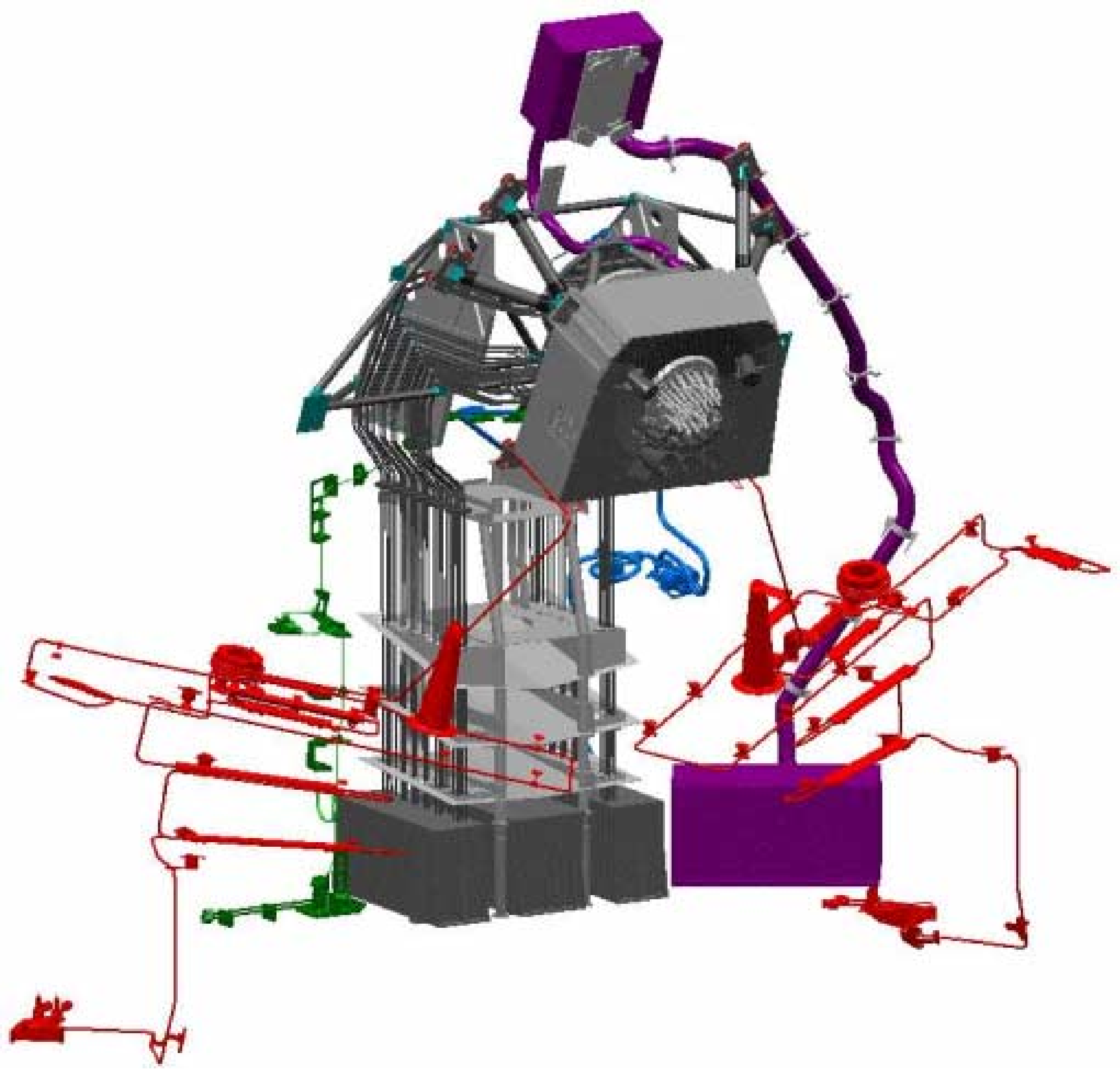

Figure 5.7-3 : PPLM Instruments without structure –general view (front side)

Color code : RAA assembly : grey, Sorption cooler : red, HFI Bellow/PAU/J-FET : purple, Dilution Cooler : blue, 4K cooler : green

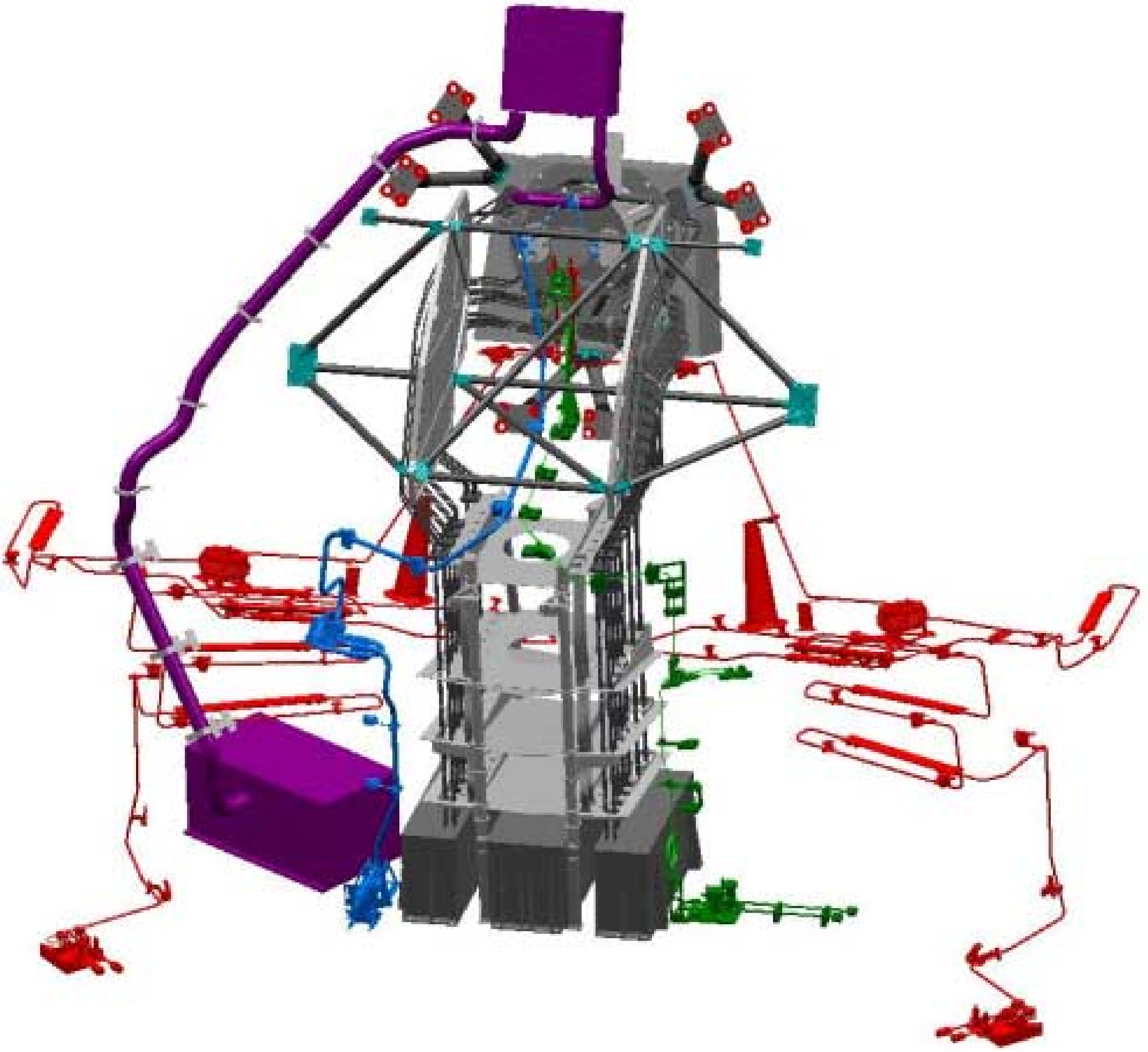

Figure 5.7-4 : PPLM Instruments without structure –general view (rear side)

Color code : RAA assembly : grey, Sorption cooler : red, HFI Bellow/PAU/J-FET : purple, Dilution Cooler : blue, 4K cooler : green

5.7.2 Radiometer Array Assembly (RAA)

5.7.2.1 general accommodation

The complete assembly of the RAA is a ''monobloc'' structure, it includes the :

- FPU interfacing :
    - the PR Panel with the 3 bipods

  - the PR Panel through the RF shield
- Wave Guides (WG) supported by the Upper and Lower Structures
- Upper Structure interfacing the PR Panel
- Lower Structure interfacing :
  - the Telescope Frame
  - the Grooves through the 3 SLI shields and the thermal straps
  - the SVM on the upper side of the Subplatform
- BEU (lateral trays & DAE box) interfacing the SVM (Subplatform)

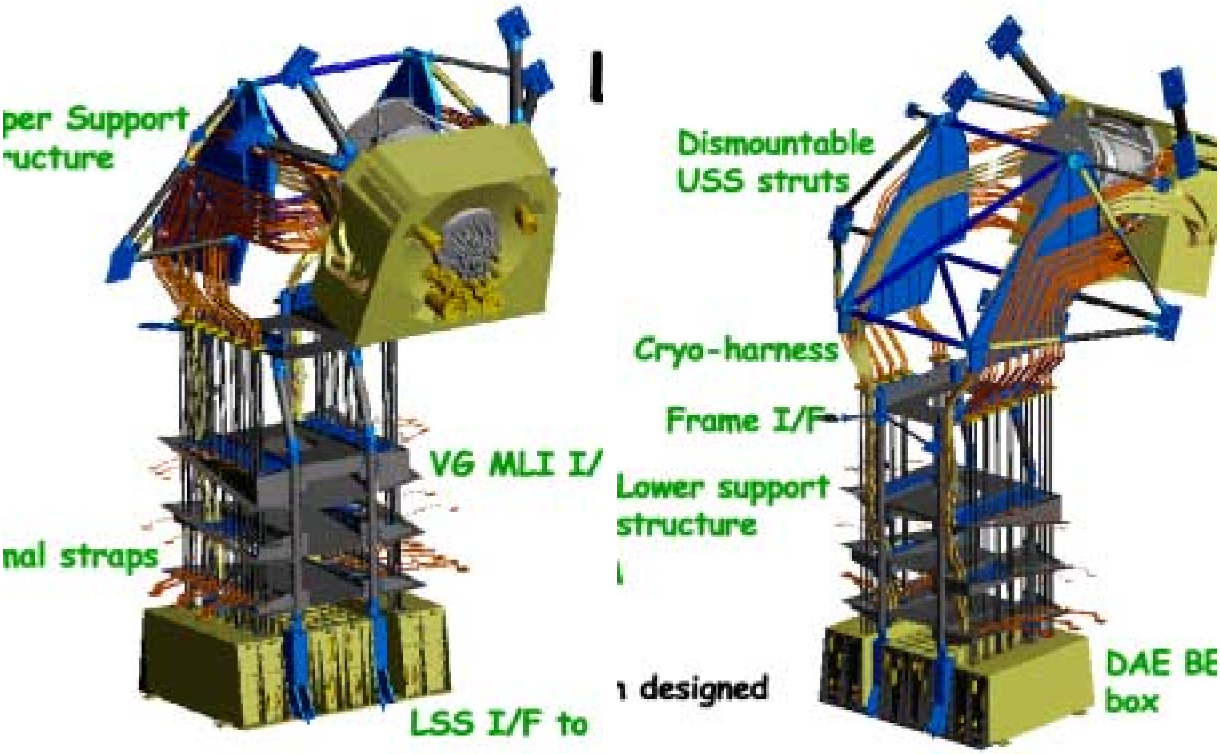

Figure 5.7-5 : Overview of the complete RAA

- Shimming of the RAA

  The main driver of the shimming definition for the PPLM is the FPU adjustment range of

  ± **3 mm** along Zrdp axis

  The FPU/PR Panel shim plates needed thickness will be known after the measurement of :

  - the Telescope performance alone
  - the FPU measurement alone

  Note : these shim plates will be machined before integration. They are washer like, in order to avoid any additional thermoelastic load on the 4 inserts of one foot.

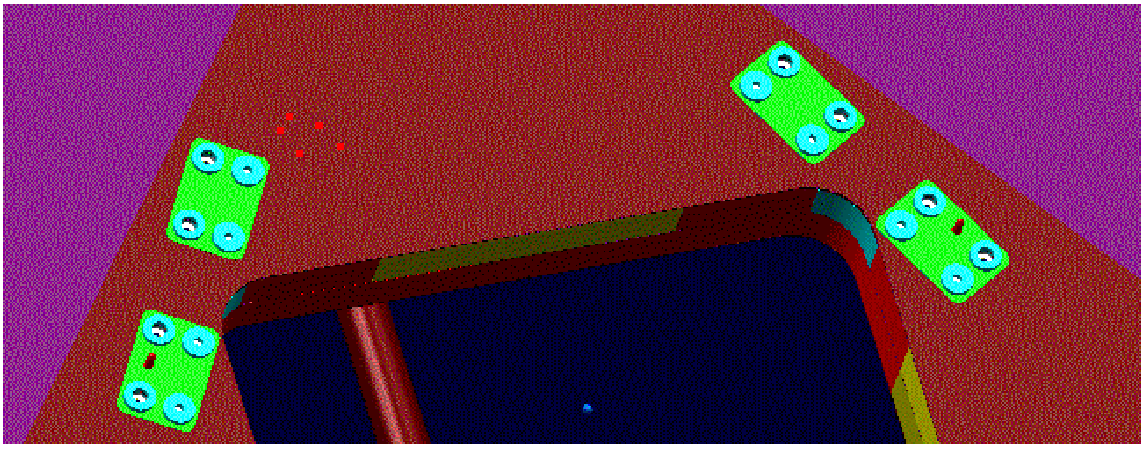

Figure 5.7-6 : FPU shim plates (in light blue)

Then, the BEU shim plate results of the :

- RAA position with the adjusted FPU
- real position of the BEU w.r.t. the FPU (RAA tolerance)
- The real location of the FPU interface w.r.t the SVM interface

It has to be noted that in the worst case of BEU proximity with the SVM (FPU Shim 8 mm + RAA at max length), the minimum thickness of 2 mm for the BEU shim plate can be kept by increasing the thickness of the **Telescope/Cryo-Structure shimming : up to 2 mm more** than the nominal range for flatness compensation.

The WG Upper Support Structure shall also be able to be fitted in translation on Zrdp in order to move with the Wave Guides, thus to have shim plates to :

- follow the FPU adjustment (±3 mm)
- compensate the tolerance on location of the rear face of the PR Panel (±1 mm)

The WG Lower Support Structure always keeps its interface with the SVM at the same level than the interface of the BEU (practicaly, the Lower Structure will be mounted on the same shim plate that the one of the BEU)

A shimming is also need on the upper side, at the Telescope Frame interface.

The central box of the BEU (DAE) is not expected to be shimmed since the offset between itself and the lateral trays is allowed by the BEU/DAE harness. This is important to **save up to 2.5 kg** in the thickest case for the shim (9.3 mm).

RAA Shimming	Nominal (mm)	Min (mm)	Max (mm)
FPU / PR Panel	5	2	8
BEU (lateral trays) / SVM. *	5	2	9.3
BEU (DAE box) / SVM	No shimming	/	/

WG Upper Support Stre / PR Panel	6	2	10
WG Lower Support Stre / Tel. Frame	4.5	2	7
WG Lower Support Stre / SVM	5	2	9.3
WG Lower Support Stre / Groove	No shimming	/	/
Telescope / C.S. (partially for RAA)	2	2	5

**thermal filler thickness (Sigraflex or other) to be included in these values*

5.7.2.2 Upper area implementation

The LFI FPU is mounted to the PR Panel with three bipods which are part of the FPU. This panel is tilted at an angle of 21.3° to be parallel to the FPU. It allows to have the 3 bipods with the same length leading to symmetric cool down properties for the FPU assembly.

The **lower bipod is dismountable** in order to allow the integration of the PR Panel (with the Telescope Lower Beam - and its associated Lower Beam connected to the frame - removed).

The FPU is fixed on the PR Panel with 24 M8 screw. Bushes have been placed on 2 points per foot in order to ensure the general stability of the FPU at this interface after the cool down. The 2 pins system have been kept as the FPU mechanical reference frame and also to be used as centering/accosting system during the integration phase.

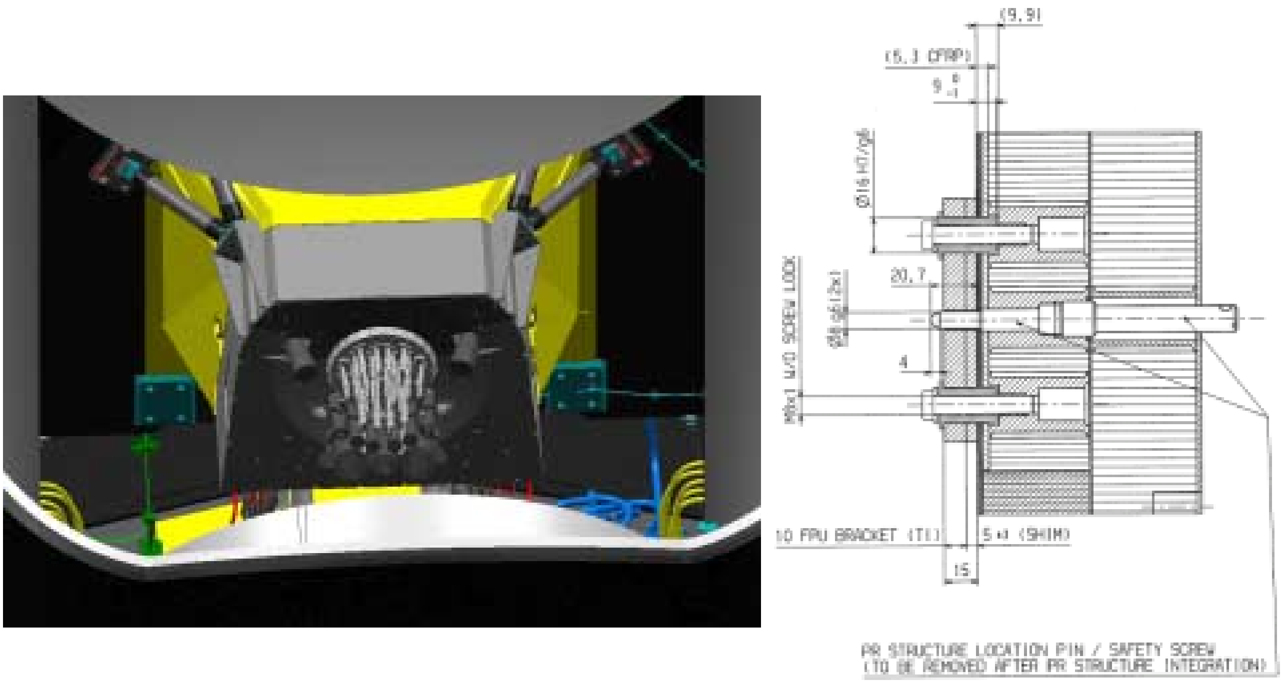

Figure 5.7-7 : FPU area in its environment (with PR and shield)

5.7.2.3 Main evolutions of the RAA

– Removing of the 100 GHz Wave Guides

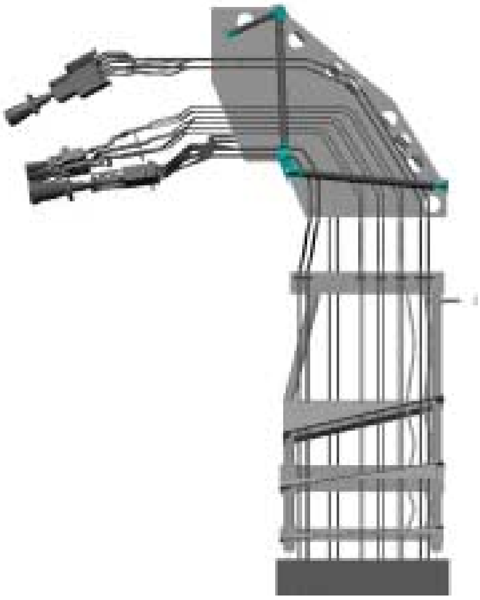

Apart from the mass and power impact, the removing of these wave guides have resolved the issue of the proximity between the Primary Reflector and the top side of the RAA at the Main Frame level.

Nevertheless the proximity remains with the 2 heighest struts of the FPU bipods : 14 mm in the nominal position for the PR and for the FPU.

Figure 5.7-8 : WG and their Support Structures (side view)

– Modification of the BEU in 3 units and Lower Structure new I/F on the SVM

For mass reason, and after the removing of the 100 GHz WG, the initial BEU in one box have been splited in 3 :

- The lateral trays which contains the BEMs and shall follow the FPU to not constrain the WG
- The central electronic box (with DAE) which is link to the others with the BEU ''internal'' harness

Consequently the WG LSS have modified with elongated ''legs'' in order to be attached on the SVM (and no more on the BEU upper side)

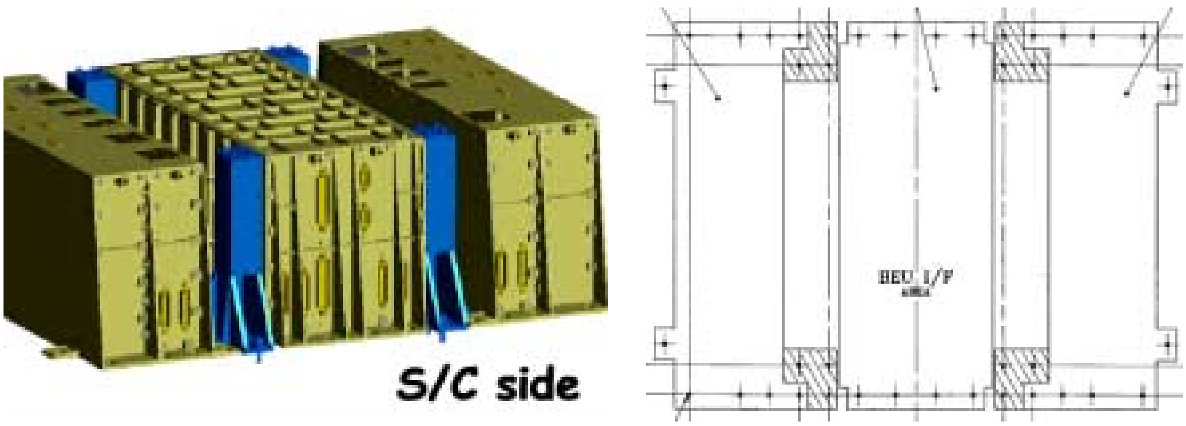

Figure 5.7-9 : BEU in 3 units, LSS elongated feet and I/F on the SVM

– Modification of the WG Upper Support Structure truss

The initial truss have been modified in order to be less sensitive to thermoelastic and then minimise the stress induced in the waves guides. Moreover the new design offers the possibility to dismount all the constituting struts and then to be compatible with any sequence of integration at S/C level.

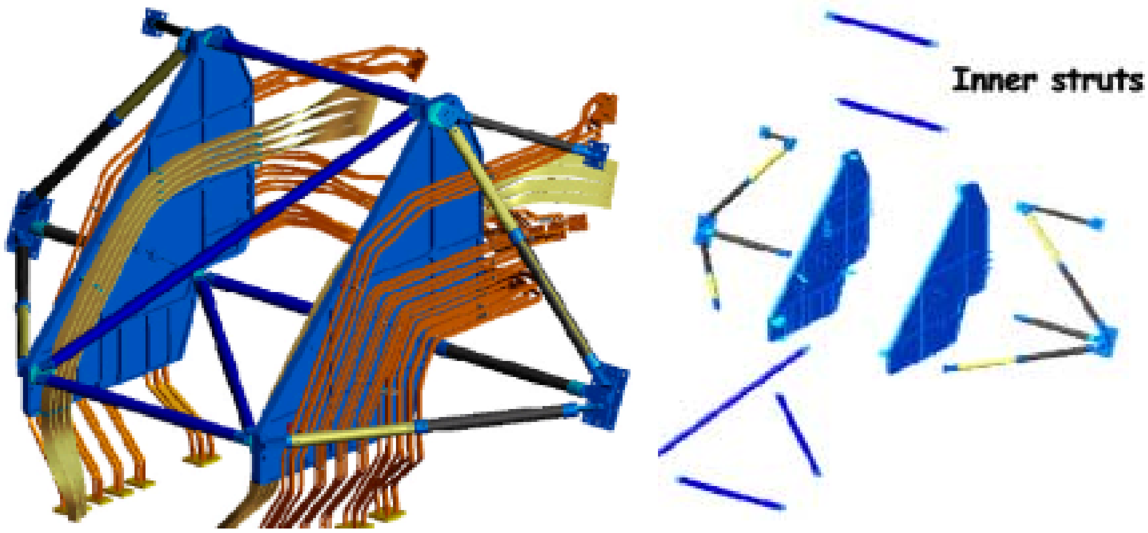

Figure 5.7-10 : Upper Support Structure and its dismountability

– Modification of the WG Lower Support Structure interfacing the Telescope Frame

Elongated holes (oriented in Z direction) have been added on the brackets of the LSS in order for it to be able to follow the WG (for the FPU/RAA adjustment need).

This upper area of the LSS remains equipped of flexible blades in order to limit at maximum the thermoelastic loads induced in the Telescope Structure.

The link between the 2 blades and the LSS structural tubes is now realised with a 3 struts system in ''V'' which permits an in-plane thermoelastic discoupling of the LSS w.r.t the Telescope Frame.

Figure 5.7-11 : Lower Support Structure interface part attaching the Tel. Frame

5.7.3 FPU alignment

FPU alignment status has been presented during the LFI IHDR dated on 24-25 march 2004. The following maximum thermoelastic unstability along Zrdp, induced by the cool down is modelled :

- -2.25 mm at the feed horn aperture
- -1.15 mm at the HFI/LFI interface

These values will be decreased respectively to – 1.75 mm at the feed horn aperture and – 0.65mm after the alignment of the FPU at telescope level if the telescope focal surface alignment is assumed worst case. It could be less if the current alignment budget of the telescope is confirmed.

Rough preliminary analyses have shown that the corresponding impact on the telescope WFE performance is around 10 µm rms for HFI horns and 40 µm rms for the LFI horns (TBC by more detailed analyses) which is not compatible with the current telescope budget (at least for HFI horns).

Two potential solutions have been identified by Laben to offset HFI FPU by 1.15 mm in the + Z direction to compensate the effect :

- modification the position of the HFI/LFI IF flange : This will lead to design modification of the IF and 4K load misalignment but WG design will not be affected
- Increase the shimming capability at the FPU/telescope. Such a solution could be easily implemented if we can assumed that the BEU position is not modified accordingly (i.e, if the WG can support the additional stress induced by the 1.15 mm additional bending).

These solutions have to be discussed more in detailed.

5.7.4 PAU / Bellow 50K / J-FET / Bellow 18K

5.7.4.1 general accommodation

The Bellow 50K is now routed :

- outside the Frame, for integration reason regarding the delivered assembly (PAU/Bellow/JFET as a single part)
- along and attached on one of the Cryo-strut for strength reason (much more stable and stiff than the Grooves)

The JFET is now oriented with the connector sides vertically (X), this configuration is the best regarding the length of the Bellows and the mountability of the connectors (with the Bellow 18K).

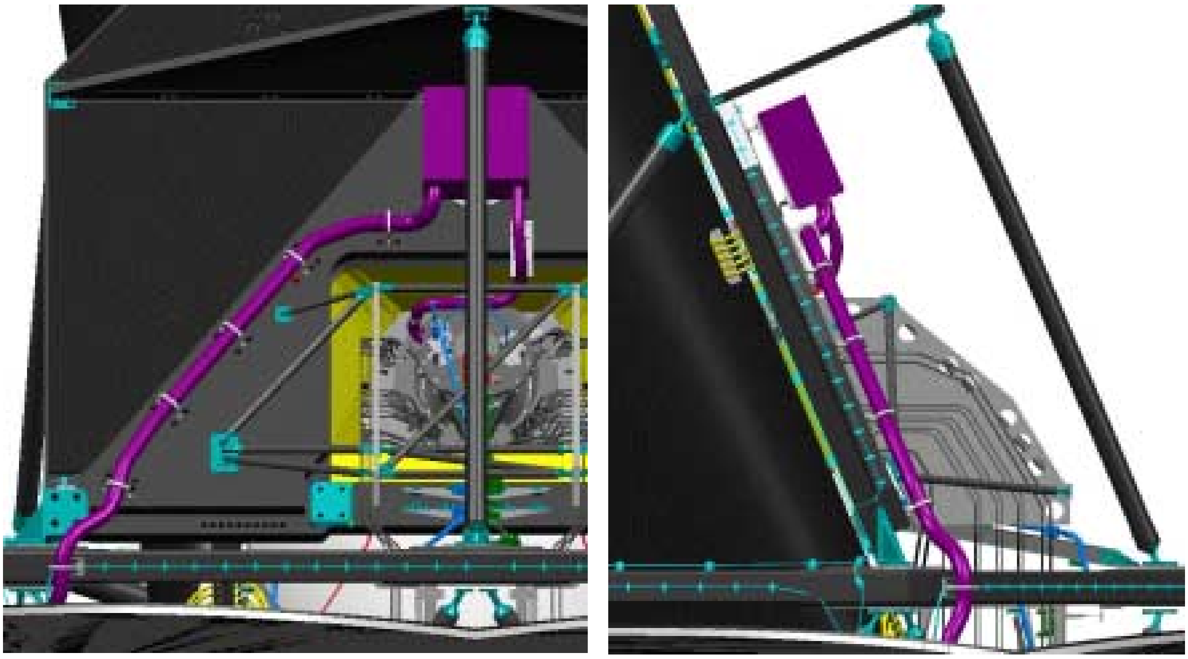

Figure 5.7-12 : Bellow 50K / JFET / Bellow 18K on Telescope

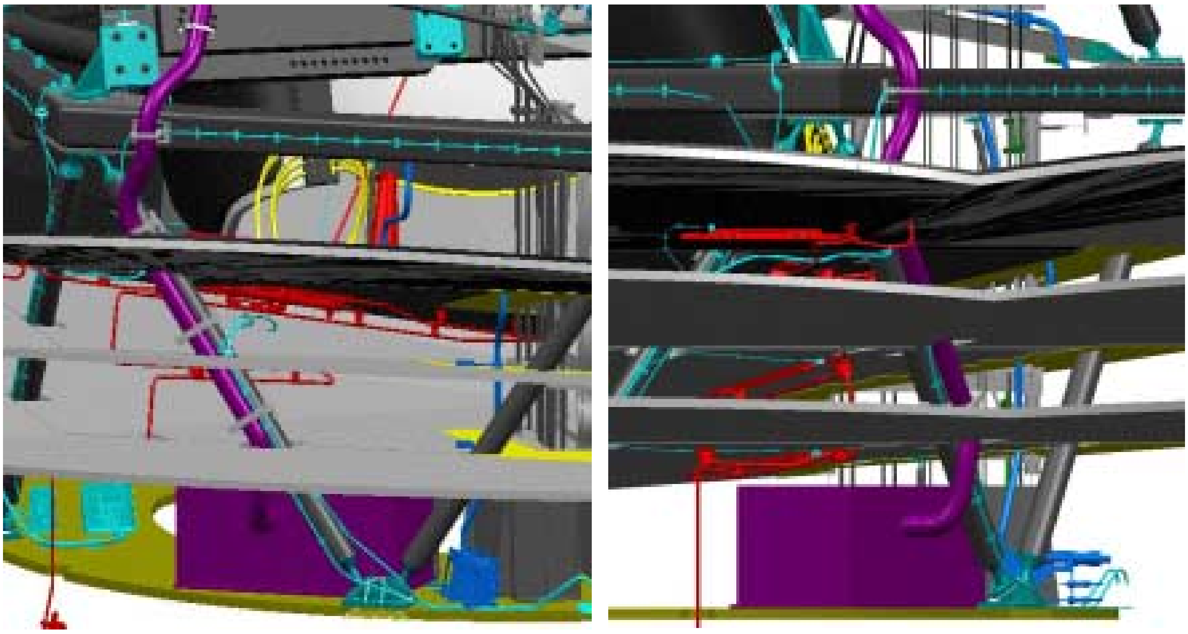

Figure 5.7-13 : Bellow 50K / PAU on Cryo-Structure

5.7.4.2 Bellows length

The following lengths are extracted from the current working CAD model given either by the Instruments themselves either build by ASP with the agreement of the Instruments.

Then, the values given here after are for information and have not to be confronted to a specific length requirement.

- PAU – JFET (Bellow 50K) : 2 290 mm
- JFET – 1st point on the 18K plate : 372 mm

Note : the total lenth of the Bellow 18K is 670 mm

5.7.5 SORPTION COOLER (20K)

5.7.5.1 general accommodation

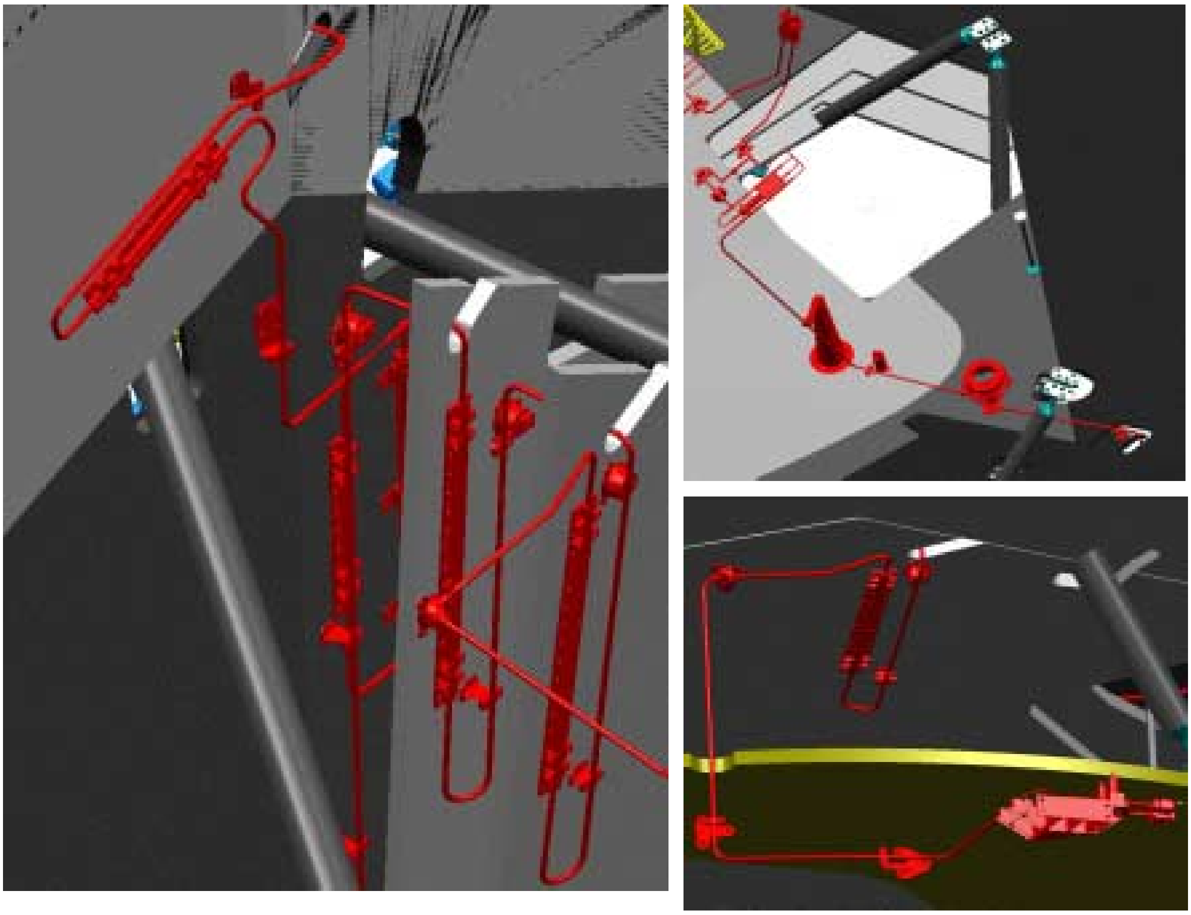

Figure 5.7-14 : Sorption Cooler pipes mounted on Cryo-Structure (-Y side)

5.7.5.2 Sorption pipes length

The following lengths are extracted from the current working CAD model given either by the Instruments themselves either build by ASP with the agreement of the Instruments.

Then, the values given here after are for information and have not to be confronted to a specific length requirement.

- SCC – Precooler 1A (nominal one, -Y) : 1 290 mm

- Precooler 1A – Precooler 2A : 1 443 mm
- Precooler 2A – Precooler 3A : 2 875 mm
- Precooler 3A – Precooler 3B : length inside JPL internal volume
- Precooler 3B – Precooler 3C : 524 mm
- Precooler 3C – SCCE (entry) : 3 346 mm

5.7.6 4K Cooler

5.7.6.1 general accommodation

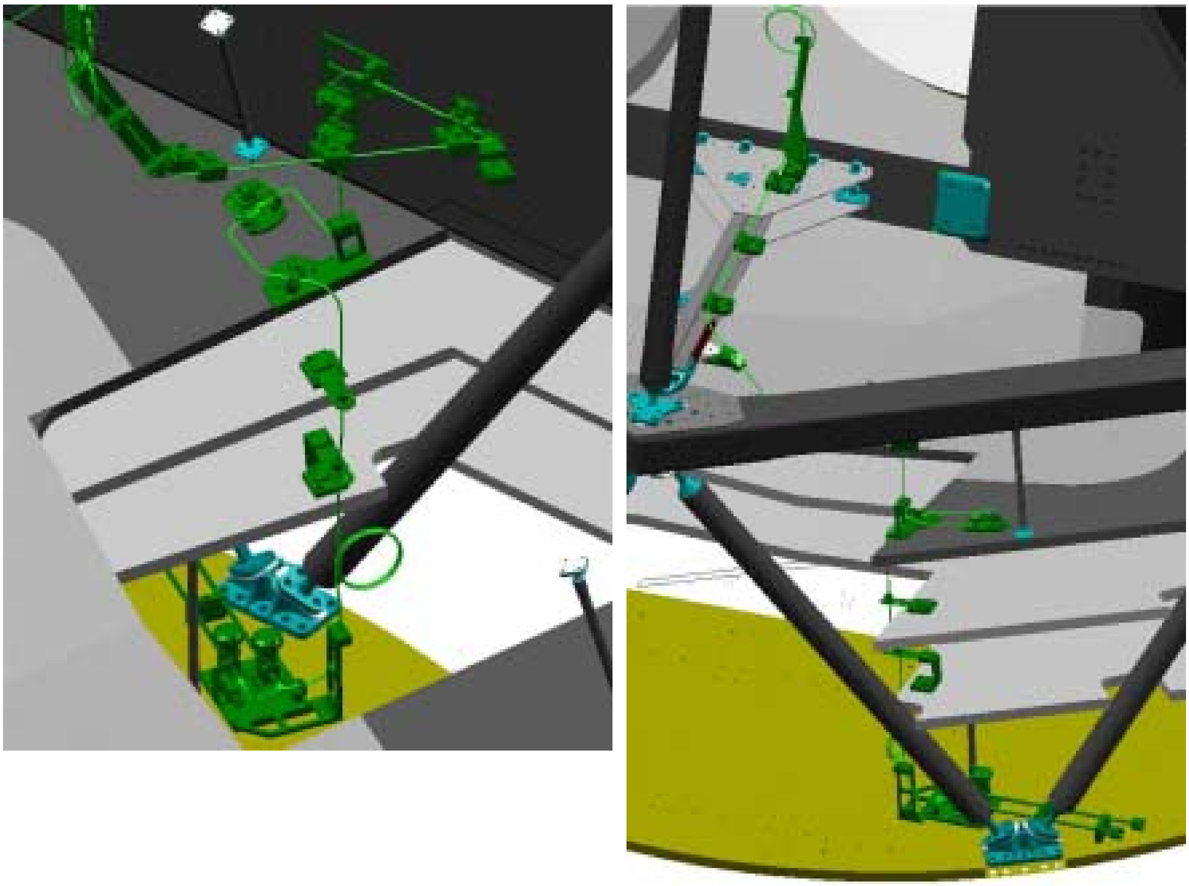

Figure 5.7-15 : 4K Cooler pipes mounted on Grooves and Telescope

5.7.6.2 4K pipes length

The following lengths are extracted from the current working CAD model given either by the Instruments themselves either build by ASP with the agreement of the Instruments.

Then, the values given here after are for information and have not to be confronted to a specific length requirement.

- 300K disconnection box – 50K precooler : 769 mm (without length on Subplatform)

- 50K precooler – FPU (18K plate) : 1 364 mm

5.7.7 Dilution Cooler (0.1K)

5.7.7.1 general accommodation

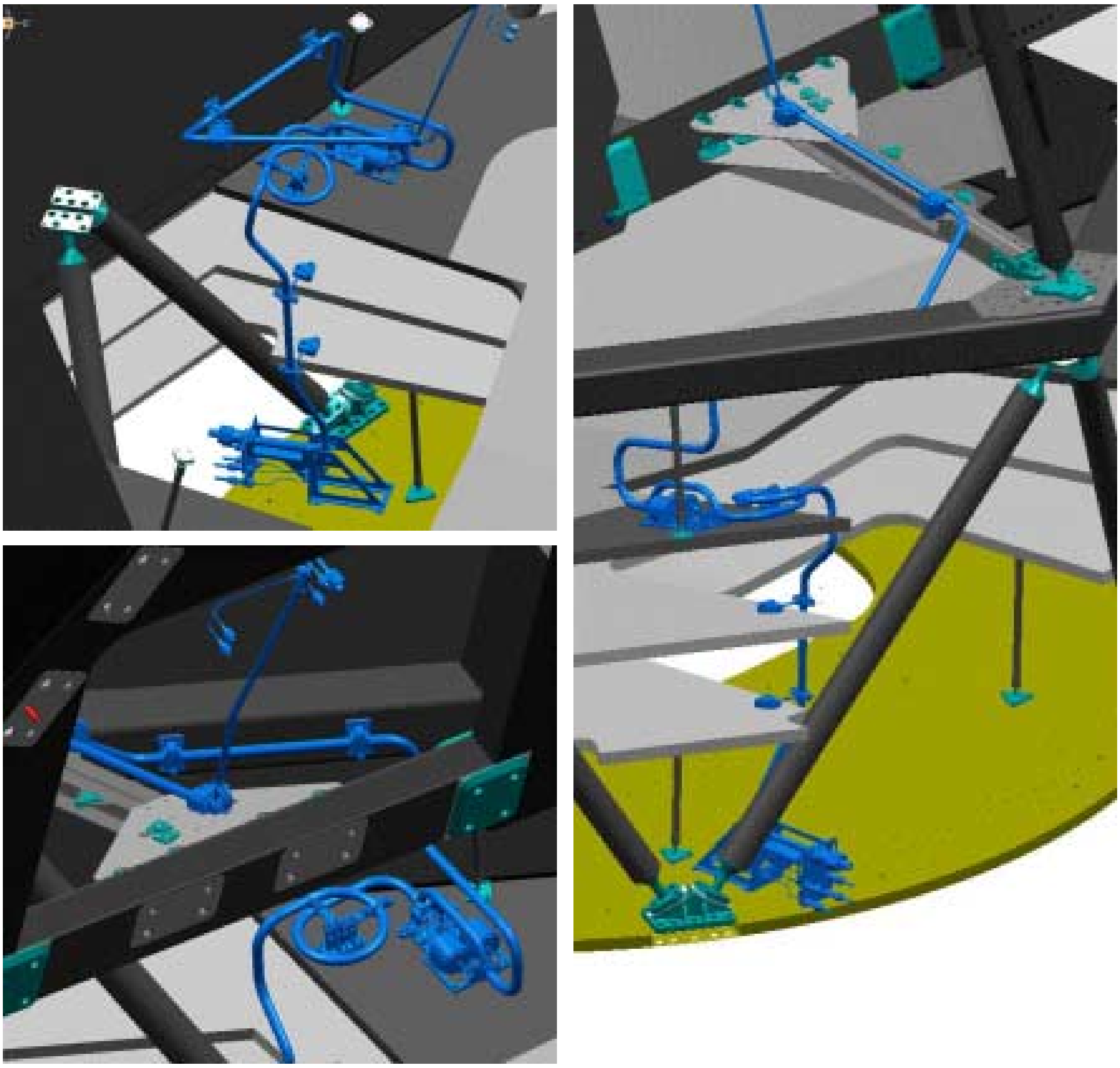

Figure 5.7-16 : 0.1K Cooler pipes mounted on Grooves and Telescope

5.7.7.2 Dilution pipes length

The following lengths are extracted from the current working CAD model given either by the Instruments themselves either build by ASP with the agreement of the Instruments.

Then, the values given here after are for information and have not to be confronted to a specific length requirement.

- 300K disconnection box – Groove 1 : 214 mm
- Groove 1 – Groove 2 : 159 mm
- Groove 2 – 50K precooler : 735 mm
- 50K precooler – FPU (18K plate) : 1 734 mm

6. INTEGRATION SEQUENCE

The detailed PPLM integration sequence is described in [RD19]. The mains steps are reviewed here after :

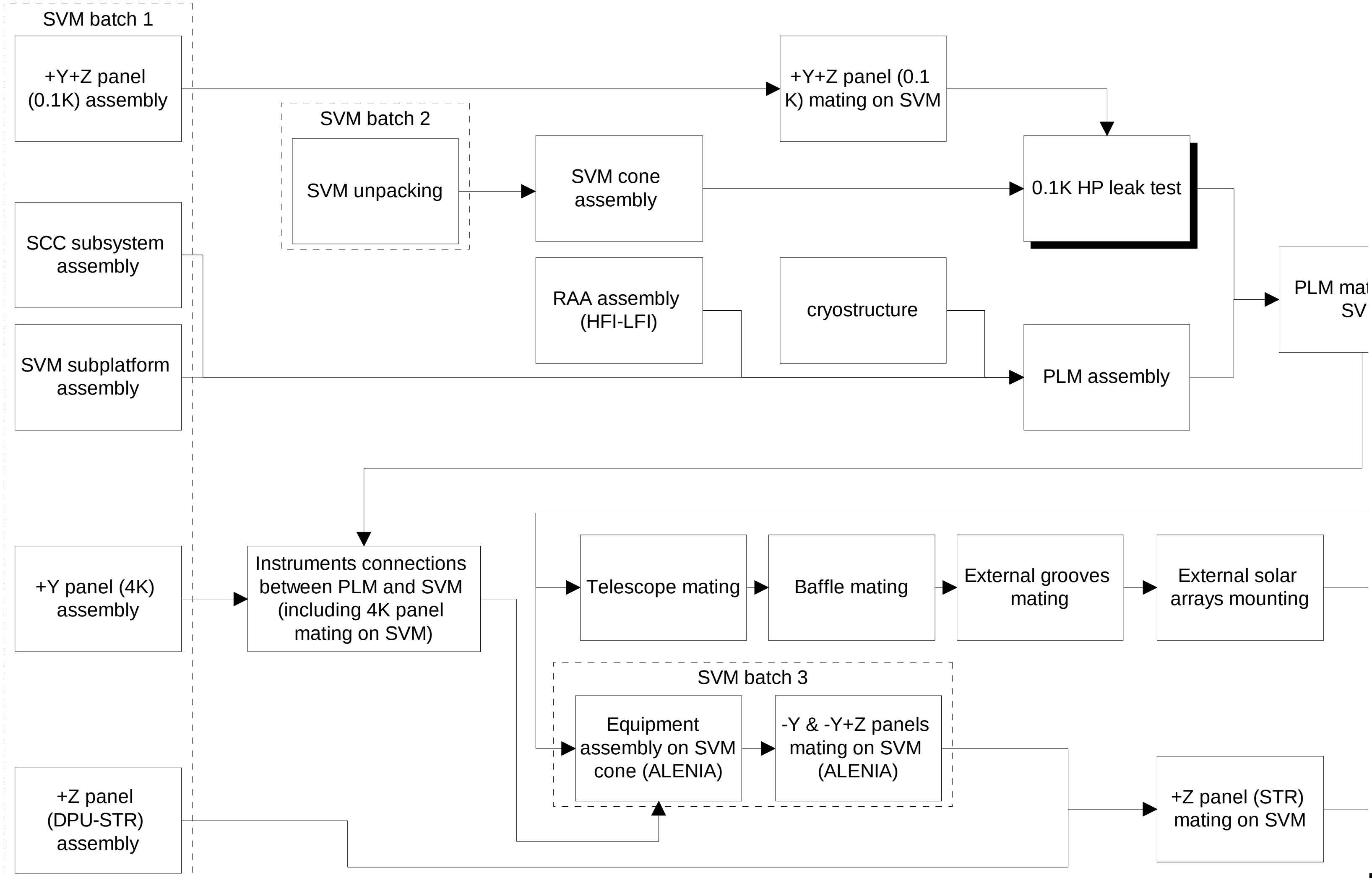

Figure 5.7-1 : Overall integration sequence of the FM

7. ANALYSES AND PERFORMANCES

The detailed description of the optical, RF, thermal and mechanical analyses are presented respectively in [RD1], [RD2], [RD3] and [RD4].

8. PERFORMANCES AND BUDGETS

This chapter presents the summary of the majors PPLM performances compared to specifications and goal when applicable.

8.1 Mass – CoG – Inertia

8.1.1 Introduction

The following paragraphs reviews the main PPLM MCI performance and the associated assumptions. The PPLM MCI budget is fully described in document H-P-3-ASPI-BT-0275.

8.1.2 Mass

The contingency definition for telescope and cryo-structure takes into account the critical aspect for each element and the progress level of the project.

This current contingency is :

– Telescope structure global value : 5.2%
– Cryo-structure global value : 6.4%
– PPLM system hardware : 30%, high value linked to the BEU shim plate thickness uncertainty.

The actual best estimate mass of the PPLM (without any Instrument and reflectors) maximum mass is : 269.9 kg for a requirement of 272 kg.

The margin in mass of 2.1 kg represents less than 1% of the max total mass.

Telescope Structure	Nominal mass	Max mass	Spec.	Δ max mass	Comments
Telescope structure	78.5	82.6	73.3	+9.3	Over weight compensated by the Cryo-structure mass.
Reflectors Adapter	1,3	1,4			To be placed in System Hardware
S/Total	79.8	**84.0**	73.3	+9.3	

Cryo-Structure	Nominal mass	Max. mass	Spec.	Δ max mass	Comments
Baffle	34.2	36.5	39.0	-2.5	
Cryo-structure	130.8	139.0	147,0	-8.0	

S/Total	165.0	**175.5**	186,0	-10.5	
System Hardware	Nominal mass	Max. mass	Spec.	∆ max mass	Comments
System Hardware	7.9	10.4	12.7	-2.3	∆ max mass = -0.9 with the Reflectors adaprtors
S/Total	7.9	**10.4**	12.7	-2.3	
TOTAL	**252.7**	**269.9**	**272**	**-2.1**	

8.1.3 Center of mass and inertia

The PPLM CoG and inertia budget are based on the nominal masses of :

- the PPLM Structure (telescope structure, cryo-structure and baffle, PPLM system hardware)
- PR and SR (with the associated ISMs)
- The Instruments located on PLM side (above the Subplatform, on X >966.5 in S/C coord. system) – For more detail see document H-P-3-ASPI-BT-0275.

The assumptions on which are based the CoG and inertia performance are the following :

S/S	**Nominal Mass (Kg)**
Telescope Structure	79,8
Cryo-Structure	165
PPLM System Hardware	7,9
PPLM Structure S/Total	**252,7**
Reflectors	42,3
HFI +LFI	115,2
Sorption	19,7
PPLM Instrument & Reflectors S/Total	**177,3**
TOTAL	**430,0**

<u>Position of the CoG</u>

The CoG coordinates in the satellite (S/C) reference frame are presented in the following table. They are computed with the nominal masses without units inside the SVM. The uncertainties are linked to the different uncertainties at S/S level.

	Nominal CoG location in the S/C reference frame (mm)	Uncertainty (mm)
X_{COG}	**1913.6**	±41
Y_{COG}	**-20.7**	±5.5
Z_{COG}	**-112.9**	±13.5

Main inertia

The main inertia are expressed in the satellite (S/C) reference frame at the CoG of the PPLM, computed at nominal mass, without units inside the SVM :

	nominal Main Inertia at PPLM CoG, in S/C reference frame (kg.m²)
Ixx	**374.9**
Iyy	**445.1**
Izz	**413.3**
Pxy	5.8
Iyz	6.3
Izx	49.1

The uncertainty on these inertia are linked to the different uncertainties at S/S level. It is assumed at ±10%

8.2 Mechanical performances

Even if not specified at PPLM level (frequency requirement are directly derived into frequency requirement at telescope and cryo-structure level), the PPLM main mode are presented here after :

Frequency (Hz)	Mx [Kg]	My [Kg]	Mz [Kg]	Mode description
18.6	0.0	160.3	0.0	First Y lateral mode
25.7	3.5	0.0	217.3	First Z lateral mode
33.1	0.6	105.9	6.3	Second Y lateral mode
33.3	11.7	7.8	88.8	Second Z lateral mode
53.7	35.6	0.0	4.1	First longitudinal mode
64.9	69.6	0.0	1.5	Main longitudinal mode

Figure 8.2-1 : PPLM main modes

8.3 Thermal performances

8.3.1 PPLM modelling

8.3.1.1 Cryo-Structure and telescope

The PPLM structure modelling is based on :

- Detailed analytical studies

  These detailed studies aim at providing the global mathematical model with consolidated assumptions (open honeycomb performance, thermal coupling between shield 3 and Sorption Cooler exchanger …)

- Experimental data issued from intensive materials and coating characterisation

  Assumptions take into account data drawn from latest measurements, including HEC emittance, processed by ASP and compared to CSAG assessments

- CSAG CDR definition

  All geometrical parameters have been updated according to CDR engineering drawings

- Observations on CQM hardware

  Actual CQM coating detailed definition (open honeycomb covering) has been taken into account after observations on specimen

All modelling parameters are given with uncertainty through (min – nom – max) values in order to build (cold – nom – hot) global TMM cases.

8.3.1.2 Instruments interfaces

The global TMM takes into account nominal Instruments modelling (meaning as delivered by Instruments).

These nominal Instruments TMM will be used for cold and nominal operating cases definition. Since the corresponding interface heat loads should be inferior to the allocated ones, the hot case uses fixed extra power in order to reach allocated values.

If,

- ✓ $\varphi(T)$ is the I/F allocated load at temperature T,
- ✓ Q(T) is the I/F heat load resulting from the use of the Instrument model,
- ✓ T_c is the computed I/F temperature with the Instrument model,

the extra power δQ injected at I/F will be written : $\delta Q = \varphi(T_c) - Q(T_c)$.

The hence “modified” Instrument modelling therefore produces $Q'(T_c) = \varphi(T_c)$ at I/F.

Note that non-operating case takes into account nominal Instruments TMM in OFF mode i.e without any fluidic dissipation at PPLM interfaces.

8.3.2 Analysed configurations

Configurations are macroscopically presented here below.

- Operating mode

Operational cases	PPLM structure	Instruments I/F	SVM I/F	Operating Sorption Cooler
Nominal	*Nominal*	*Nominal*	*Nominal*	*Nominal*
Hot	*Hot*	*Allocations*	*Hot*	*Redundant*
Cold	*Cold*	*Nominal*	*Nominal*	*Nominal*

Table 8.3-1 : Operational cases definition

- Non-operating mode

Non-operational case	PPLM structure	Instruments I/F	SVM I/F
Safe cold	*Cold*	*OFF*	*Safe*

Table 8.3-2 : Non-operational case definition

8.3.3 Analyses results

8.3.3.1 Nominal operating

Figure 8.3-1 shows the PPLM nominal operating temperature cartography.

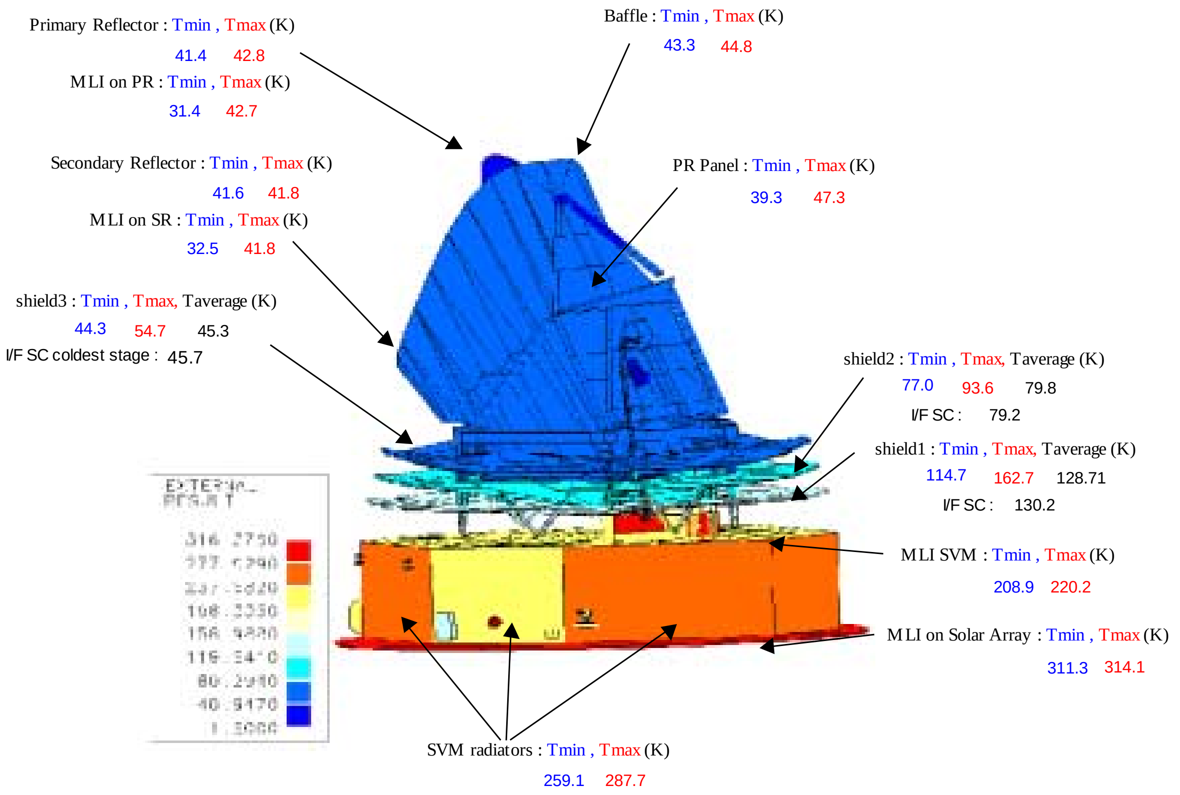

Figure 8.3-1 : Nominal PPLM temperature cartography

Table 8.3-3 presents a summary of PPLM / Instruments interfaces temperatures in nominal operating case.

PPLM interfaces temperatures		Computed temperatures **Nominal operating case** (K)
LFI WG	I/F with VG1	138.3 – 142.8
	I/F with VG2	79.9 - 83.1
	I/F with VG3	46.0 – 47.2
Sorption Cooler	I/F with VG1	136.5
	I/F with VG2	83.3
	I/F with VG3	49.8 / 47.5 / 45.7
4K Cooler coldest exchanger		45.8
0.1K Cooler coldest exchanger		46.2
JFET box		47.3
FPU interface		[41.9 - 44.9]
Primary Reflector		[41.4 – 42.8]
Secondary Reflector		[41.6 – 41.8]

Table 8.3-3 : PPLM / Instruments nominal interfaces temperatures

8.3.3.2 Hot operating

Figure 8.3-2 shows the PPLM "hot" temperature cartography.

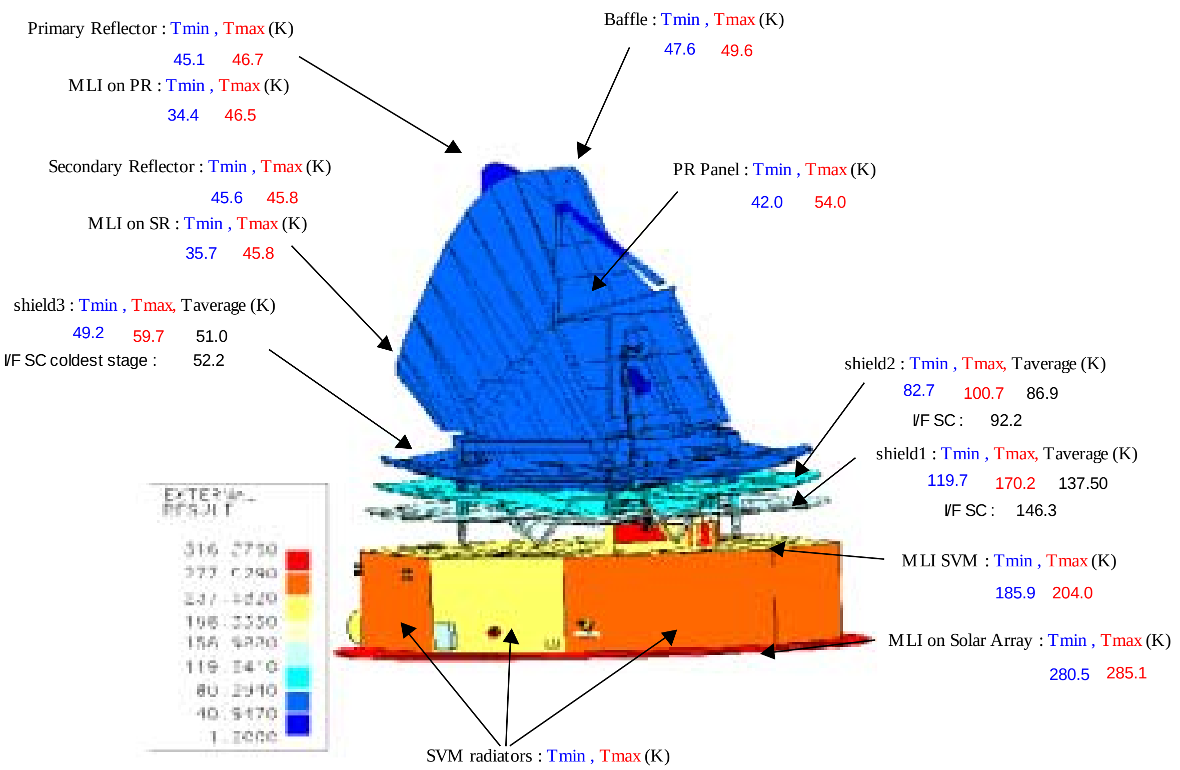

Figure 8.3-2 : "hot" PPLM temperature cartography

Table 8.3-4 presents a summary of PPLM / Instruments interfaces temperatures in worst hot case.

PPLM worst interfaces temperatures		Computed temperatures **hot case** (K)	Mathematical uncertainty (K)	Worst hot temperatures (K)	Max T (K)
LFI WG	I/F with VG1	155.6 – 156.8	+ 2	157.6 – 158.8	170
	I/F with VG2	89.1 – 91.1	+ 2	91.1 – 93.1	120
	I/F with VG3	54.1 – 55.0	+ 2	56.1 – 57.0	60
Sorption Cooler	I/F with VG1	146.3	+ 2	148.3	170
	I/F with VG2	92.2	+ 2	94.2	120
	I/F with VG3 (3C)	52.2	+ 2	54.2	60
4K Cooler coldest exchanger		53.1	+ 2	55.1	-
0.1K Cooler coldest exchanger		51.3	+ 2	53.1	-
JFET box		54	+ 2	56	60
FPU		[45.4 – 50.1]	+ 2	[47.4 – 52.1]	65
Primary Reflector		[45.1 – 46.7]	+ 2	[47.1 – 48.7]	50
Secondary Reflector		[45.6 – 45.8]	+ 2	[47.6 – 47.8]	50

Table 8.3-4 : PPLM / Instruments worst hot interfaces temperatures

Results show compliance with margin for all interfaces.

A comparison between :

- the allocated interface heat loads -including system margin- (orange),
- the heat loads computed with Instruments models (pale blue),
- the total injected interface loads -including fixed extra power- (dark blue),

is given in Figure 8.3-3. This comparison shows that the loads, on which the hot case is built, are conservative wrt allocations.

An additional case “Hot PLM”, as described in Table 8.3-5, has been studied for comparison with 50K goal only.

50K Goal	PPLM structure	Instruments I/F	SVM I/F	Operating Sorption Cooler
Hot PLM	*Hot*	*Nominal*	*Hot*	*Nominal*

Table 8.3-5 : “Hot PLM” case definition

The computed Sorption Cooler I/F 3C temperature is 48K, leading to 50K when including mathematical uncertainties. The 50K goal is then achieved with Instruments interfaces as currently modelled.

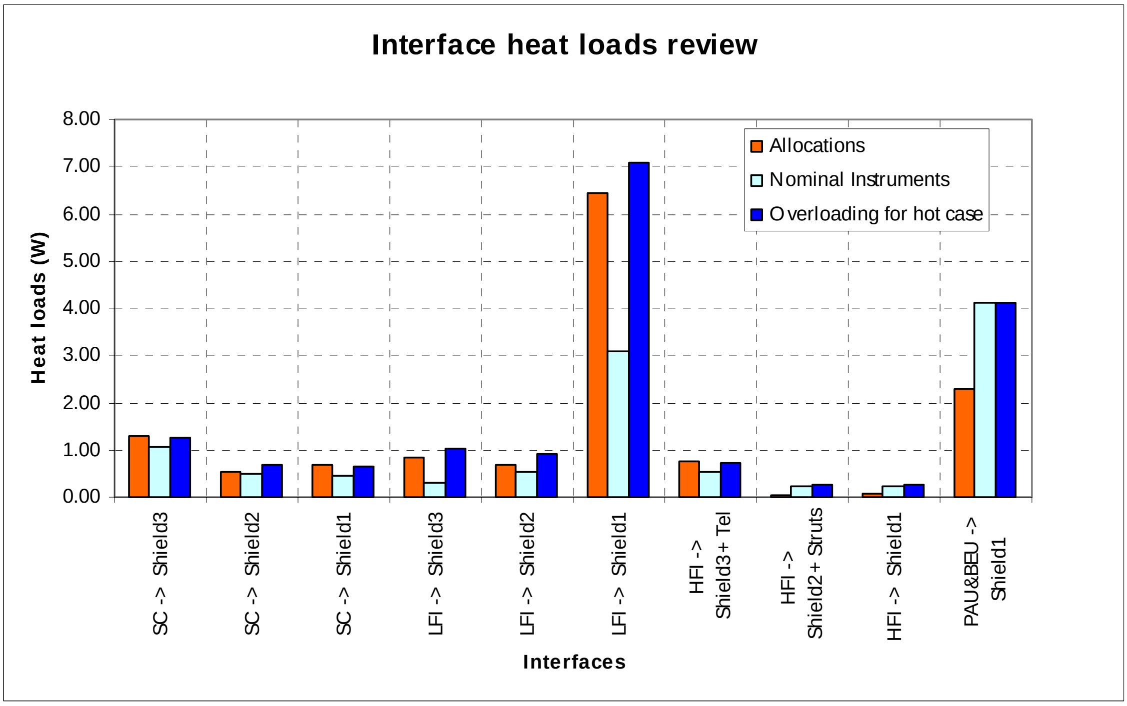

Figure 8.3-3 : Heat loads review

8.3.3.3 Cold operating

Table 8.3-6 presents a summary of PPLM / Instruments interfaces temperatures in worst cold operating case.

PPLM worst cold interfaces temperatures (operating)		Computed temperatures **cold operating case** (K)	Mathematical uncertainty (K)	Worst cold operating temperatures (K)	Min T (K)
LFI WG	I/F with VG1	136.5 – 140.7	- 2	134.5 – 138.7	-
	I/F with VG2	78.6 – 81.3	- 2	76.6 – 79.3	-
	I/F with VG3	44.5 – 45.7	- 2	42.5 – 43.7	-
Sorption Cooler	I/F with VG1	135.1	- 2	**133.1**	**150**
	I/F with VG2	81.7	- 2	**79.7**	**100**
	I/F with VG3	44.2	- 2	**42.2**	**45**
4K Cooler coldest exchanger		44.5	- 2	42.5	-
0.1K Cooler coldest exchanger		44.8	- 2	42.8	-
JFET box		45.4	- 2	43.4	40
FPU		[40.7 – 43.4]	- 2	[**38.7** – 41.4]	**40**
Primary Reflector		[40.1 – 41.5]	- 2	[38.1 – 39.5]	30
Secondary Reflector		[40.3 – 40.6]	- 2	[38.3 – 38.6]	30

Table 8.3-6 : PPLM / Instruments worst cold operating interfaces temperatures

Minor deviations have to be noted wrt cold operating conditions, mainly at Sorption Cooler interfaces.

8.3.3.4 Cold non-operating

Figure 8.3-4 shows the PPLM cold non-operating temperature cartography.

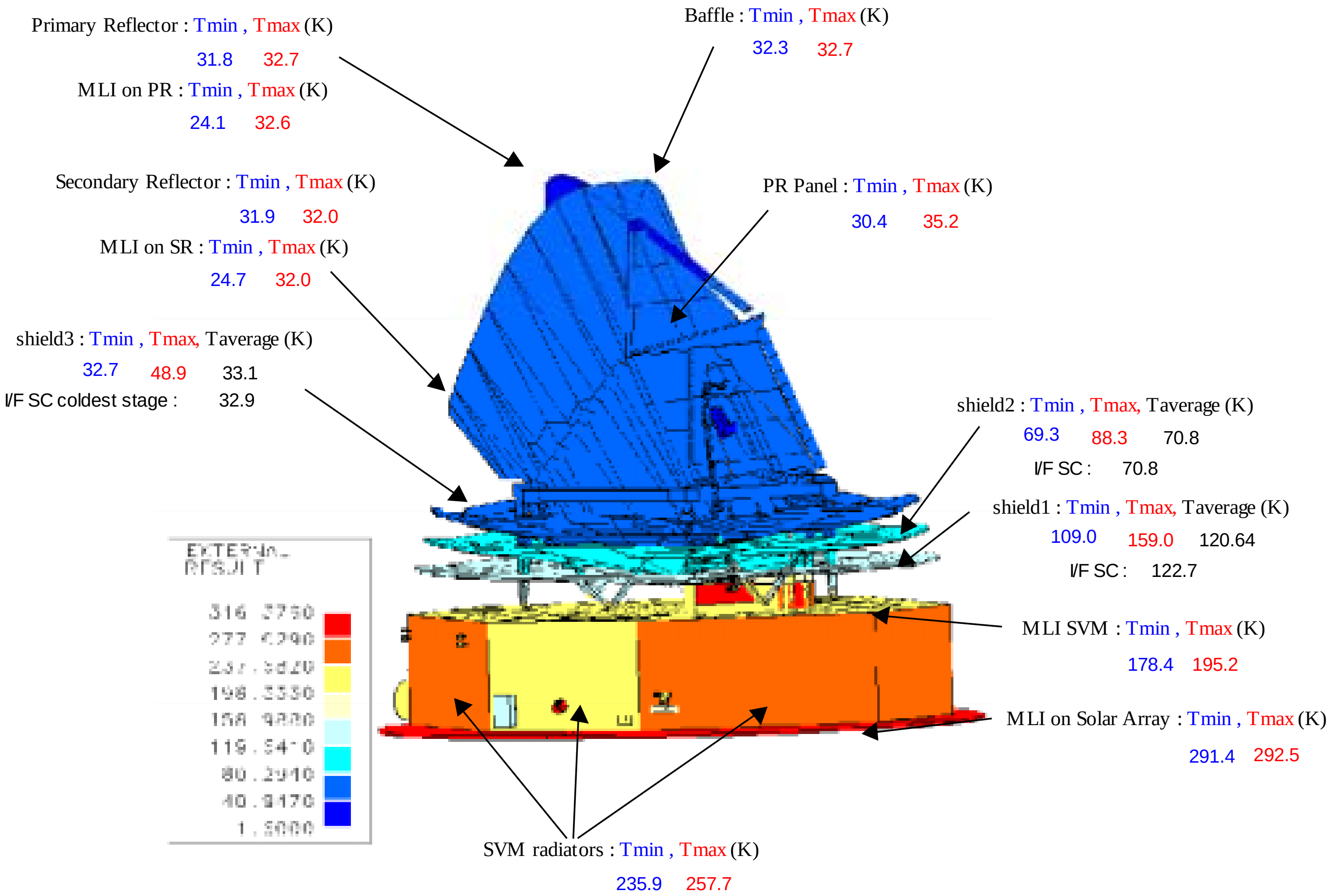

Figure 8.3-4 : Cold non operating PPLM temperature cartography

Table 8.3-7 presents a summary of PPLM / Instruments interfaces temperatures in worst non-operating cold case.

PPLM worst cold interfaces temperatures (non-operating)		Computed temperatures **Cold non operating case** (K)	Mathematical uncertainty (K)	Worst non-operating cold temperatures (K)	Min T (K)
LFI WG	I/F with VG1	130.1 – 134.1	- 2	128.1 – 132.1	-
	I/F with VG2	71.4 – 72.4	- 2	69.4 – 70.4	-
	I/F with VG3	33.8 – 34.1	- 2	31.8 – 32.1	-
Sorption Cooler	I/F with VG1	123	- 2	**121**	**150**
	I/F with VG2	71	- 2	**69**	**100**
	I/F with VG3	33	- 2	**31**	**40**
4K Cooler coldest exchanger		33	- 2	31	-
0.1K Cooler coldest exchanger		33	- 2	31	-
JFET box		32	- 2	30	30
FPU		32	- 2	30	-
Primary Reflector		32	- 2	30	30
Secondary Reflector		32	- 2	30	30

Table 8.3-7 : PPLM / Instruments worst non-operating cold interfaces temperatures

As for operating case, minor deviations have to noted at Sorption Cooler interfaces.

It is also to be noticed that Shield3 and Telescope predicted min average temperatures are close to 30K (lower materials&process qualification range), the coldest parts belonging to PR panel and reaching 28K.

8.4 Telescope optical performances

8.4.1 WFE performance

The total WFE degradation (2 σ budget) is presented in the following table and compared to the WFE specification. The performance is reached for all the frequencies.

horn	Budget (2σ)	specification	Horn	Budget (2σ)	specification
LFI_30_27	47,6	119,0	H_100_1	47,0	72,0
LFI_30_28	49,9	119,0	H_100_2	50,1	72,0
LFI_44_24	47,6	92,0	H_100_3	49,0	72,0
LFI_44_25	51,9	92,0	H_100_4	48,7	72,0
LFI_44_26	56,0	92,0	H_143_1	46,7	60,0
LFI_70_18	47,0	92,0	H_143_2	46,8	60,0

LFI_70_19	46,7	92,0
LFI_70_20	46,7	92,0
LFI_70_21	45,4	92,0
LFI_70_22	44,8	92,0
LFI_70_23	43,2	92,0
H_143_3	46,5	60,0
H_143_4	46,1	60,0
H_143_5	46,5	60,0
H_143_6	47,5	60,0
H_143_7	46,4	60,0
H_143_8	46,0	60,0
H_217_1	43,2	57,0
H_217_2	42,8	57,0
H_217_3	42,6	57,0
H_217_4	42,1	57,0
H_217_5	43,3	57,0
H_217_6	42,7	57,0
H_217_7	41,2	57,0
H_217_8	41,9	57,0
H_353_1	38,7	50,0
H_353_2	38,2	50,0
H_353_3	37,5	50,0
H_353_4	37,6	50,0
H_353_5	37,2	50,0
H_353_6	36,7	50,0
H_353_7	37,2	50,0
H_353_8	37,2	50,0
HFI 545-1	38,2	48,0
HFI 545-2	37,6	48,0
HFI 545-3	37,2	48,0
HFI 545-4	37,1	48,0
HFI 857-1	38,4	**42,0**
HFI 857-2	38,3	**42,0**
HFI 857-3	38,4	**42,0**
HFI 857-4	38,5	**42,0**

Figure 8.4-1 : 2 σ Telescope WFE budget (µm rms)

This budget assumed that the FPU alignment performance is consistent with allocation defined in [RD8]. Analyses are in progress on instrument level to refine the current FPU stability performance. The telescope budget will be updated accordingly when data will be delivered.

The 1 σ budget is also presented to be compared to the goal performance :

horn	budget	specification	Horn	budget	specification
LFI_30_27	34,7	80,0	H_100_1	35,0	48,0
LFI_30_28	37,1	80,0	H_100_2	37,8	48,0
LFI_44_24	35,1	61,0	H_100_3	36,7	48,0
LFI_44_25	38,5	61,0	H_100_4	36,4	48,0
LFI_44_26	42,6	61,0	H_143_1	35,7	40,0
LFI_70_18	35,9	61,0	H_143_2	35,8	40,0
LFI_70_19	35,7	61,0	H_143_3	35,6	40,0
LFI_70_20	35,7	61,0	H_143_4	35,1	40,0
LFI_70_21	34,4	61,0	H_143_5	35,4	40,0
LFI_70_22	33,8	61,0	H_143_6	36,4	40,0
LFI_70_23	32,1	61,0	H_143_7	35,4	40,0
			H_143_8	35,0	40,0
			H_217_1	33,4	38,0
			H_217_2	33,0	38,0
			H_217_3	32,8	38,0
			H_217_4	32,3	38,0
			H_217_5	33,5	38,0
			H_217_6	32,9	38,0
			H_217_7	31,6	38,0
			H_217_8	32,1	38,0
			H_353_1	30,6	33,0
			H_353_2	30,2	33,0
			H_353_3	29,6	33,0
			H_353_4	29,8	33,0
			H_353_5	29,3	33,0
			H_353_6	28,8	33,0
			H_353_7	29,2	33,0
			H_353_8	29,1	33,0
			HFI 545-1	30,1	32,0
			HFI 545-2	29,6	32,0
			HFI 545-3	29,3	32,0
			HFI 545-4	29,0	32,0
			HFI 857-1	30,6	**28,0**
			HFI 857-2	30,5	**28,0**

HFI 857-3	30,6	**28,0**
HFI 857-4	30,6	**28,0**

Figure 8.4-2 : 1 σ Telescope WFE budget (μm rms)

For the 857 Ghz HFI horn, the goal is not reached 30.6 μm rms to be compared to 28 μm rms) but it could be if the reflector performance would be within their goal.

8.4.2 LOS alignment

8.4.2.1 End of Life LoS direction with regards to P-PLM interface frame

Contributor	**LoS deviation (arcmin)**
Telescope	1.4
Cryostructure	0.6
FPU	0.86
Total	<1.8 arcmin
Alignment need	51

The alignment need is met with confortable margins. This is because the stability is mostly driven by image quality need rather than LOS direction.

8.4.2.2 PPLM around LoS knowledge

Contributor	**Around LoS knowledge (arcmin)**
Horn orientation knowledge	+/-0.33
Telescope around LOS knowledge	+/-0.3
Theodolite accuracy	0.17
Total (RSS)	+/-0.48
Need	<+/-2 arcmin

The around-LoS knowledge requirement is fulfilled with margins.

8.4.2.3 PPLM LoS stability between 2 calibrations

No thermal evolution will occurs between 2 calibrations since the PPLM is permanently shadowing by the Sa and the grooves. Consequently, no short term unstability will be induced.

8.4.3 Emissivity performance

Contributor		**Stage**	**Total emissivity %**
Reflectors		BoL	1
		EoL (goal)	5(2)
System contamination	Molecular	EoL	<10-2
	particulate	EoL	0.8
	contingency	EoL	0.2
Total		**EoL(goal)**	**6(3)**

The required 6% are just met, considering a system contigency of 0.2. The reflectors are the main contributors

8.5 PPLM RF performance

8.5.1 Telescope main lobe performance

The total gain degradation (2 σ budget) is presented in the following table and compared to the gain specification. The performance is reached for all the frequencies with a important margin.

detector n°	Total Deterministe dB	Total Random dB	Total Budget dB	Specifications dB
LFI_70_18	0,0172	0,0228	0,0399	0,5
LFI_70_19	0,0195	0,0245	0,0439	0,5
LFI_70_20	0,0207	0,0257	0,0463	0,5
LFI_70_21	0,0217	0,0257	0,0474	0,5
LFI_70_22	0,0119	0,0244	0,0363	0,5
LFI_70_23	0,0200	0,0227	0,0426	0,5
LFI_44_24	0,0236	0,0280	0,0516	0,5
LFI_44_25	0,0192	0,0370	0,0562	0,5
LFI_44_26	0,0222	0,0369	0,0591	0,5
LFI_30_27	0,0130	0,0149	0,0279	0,5
LFI_30_28	0,0136	0,0149	0,0285	0,5
HFI_100_1	0,0255	0,0370	0,0625	0,5
HFI_100_2	0,0392	0,0352	0,0744	0,5
HFI_100_3	0,0344	0,0350	0,0694	0,5
HFI_100_4	0,0202	0,0370	0,0572	0,5
HFI_143_1	0,0256	0,0450	0,0706	0,5
HFI_143_2	0,0269	0,0361	0,0631	0,5
HFI_143_3	0,0335	0,0308	0,0643	0,5
HFI_143_4	0,0173	0,0450	0,0623	0,5
HFI_143_5	0,0349	0,0522	0,0870	0,5
HFI_143_6	0,0536	0,0502	0,1038	0,5
HFI_143_7	0,0595	0,0496	0,1090	0,5
HFI_143_8	0,0494	0,0550	0,1043	0,5
HFI_217_1	0,0289	0,0471	0,0760	1
HFI_217_2	0,0285	0,0356	0,0641	1
HFI_217_3	0,0274	0,0359	0,0632	1
HFI_217_4	0,0422	0,0444	0,0866	1
HFI_217_5	0,0532	0,0419	0,0951	1
HFI_217_6	0,0299	0,0287	0,0586	1
HFI_217_7	0,0349	0,0291	0,0640	1
HFI_217_8	0,0594	0,0453	0,1048	1
HFI_353_1	0,1971	0,1849	0,3820	1
HFI_353_2	0,1352	0,1131	0,2482	1
HFI_353_3	0,0853	0,0779	0,1632	1
HFI_353_4	0,0613	0,0685	0,1299	1
HFI_353_5	0,0672	0,0655	0,1327	1
HFI_353_6	0,0952	0,0838	0,1790	1
HFI_353_7	0,1437	0,1259	0,2696	1
HFI_353_8	0,1953	0,1860	0,3813	1
HFI_545_1	0,3462	0,3610	0,7072	1,4
HFI_545_2	0,2366	0,2726	0,5092	1,4
HFI_545_3	0,2468	0,2892	0,5361	1,4
HFI_545_4	0,3307	0,3610	0,6917	1,4
HFI_857_1	0,2570	0,4292	0,6863	2,5
HFI_857_2	0,1335	0,3625	0,4959	2,5
HFI_857_3	0,1605	0,3774	0,5379	2,5
HFI_857_4	0,2967	0,4550	0,7517	2,5

Figure 8.5-1 Complete Budget (2σ)

8.5.2 Elipticity degradation

For the ellipticity performance, no additionnal analysis have been performed since the PDR. Discussion on the method to be aplied to compute this performance is still open.

8.5.3 Rejection toward Sun, Earth and moon direction

The following table synthesizes all contributors to the rejection modification. The nominal performance is the one of the Planck spacecraft with ideal reflector, the baffle extension and the gaussian feed model. This nominal performance is degraded by different contributor. The only contributor of importance is the dust contamination at the highest frequency. The far out side lobe are then dominated by the dust effect. In the following table the total rejection is obtained as the maximum of the different rejection computd alone (ie total rejection = max (rejection with no dust , rejection from dust model).

30 GHz

	Rejection with no dust (dB)	Rejection from dust model	Rejection from grating lobes	Rejection from primary diffusion	Total rejection (dB)	Rejection requirement (dB)	Rejection goal (dB)	Margin / requirement (dB)	Margin / goal (dB)
Moon	-83	NA	NA	NA	-83	-71	NA	12	NA
Earth	-100	NA	NA	NA	-100	-78	NA	22	NA
Sun	-136	NA	NA	NA	-136	-91	NA	45	NA

100 GHz

	Rejection with no dust (dB)	Rejection from dust model	Rejection from grating lobes	Rejection from primary diffusion	Total rejection (dB)	Rejection requirement (dB)	Rejection goal (dB)	Margin / requirement (dB)	Margin / goal (dB)
Moon	-107	-103	NA	NA	-103	-71.5	-73	32	30
Earth	-125	-99	NA	NA	-99	-78.5	-86	21	13
Sun	-183	-98	NA	NA	-98	-91.5	-99	6	-1

353 GHz

	Rejection with no dust (dB)	Rejection from dust model	Rejection from grating lobes	Rejection from primary diffusion	Total rejection (dB)	Rejection requirement (dB)	Rejection goal (dB)	Margin / requirement (dB)	Margin / goal (dB)
Moon	-150	-103	NA	NA	-103	-72	-81	31	22
Earth	-170	-99	NA	NA	-99	-79	-95	20	4
Sun	-234	-97	NA	NA	-97	-92	-108	5	-11

857 GHz

	Rejection with no dust (dB)	Rejection from dust model	Rejection from grating lobes	Rejection from primary diffusion	Total rejection (dB)	Rejection requirement (dB)	Rejection goal (dB)	Margin / requirement (dB)	Margin / goal (dB)
Moon	-170	-109	NA	NA	-109	-78	-95	31	14
Earth	-187	-111	NA	NA	-111	-85	-109	26	2
Sun	-259	-116	NA	NA	-116	-98	-122	18	-6

Table 8.5-1 : Final performance rejection comparison wrt to the requirements and the goals.

As a conclusion, positive margin are obtained at all frequencies wrt the requirement whereas small negative margin is observed for the Sun for the comparison with the goals.

8.5.4 Space craft self emission

The PDR budget has been updated taking into account the last TICRA computation for the RF coupling. PDR temperature fluctuations inputs have been maintained since covering the ones issued from the TCS CDR. The spacecraft self emission budget is presented in the following table.

	ASD Requirement (W/Hz^1/2)	ASD Performance (W/Hz^1/2)
30 GHz	3,40E-18	8,54E-19
100 GH (HFI)	2,10E-18	4.20E-19
353 GHz	1,80E-18	4.48E-19
857 GHz	2,20E-17	/

Figure 8.5.4-1 : Spacecraft self emission budget

The requirement is fulfil for each specified frequency. Note that as far as there's no RF power exchanged between the detector and the spacecraft surfaces at 857 GHz, there's no self spacecraft emission level from a numerical point of view.

9. CONCLUSIONS – OPEN AND CRITICAL AREAS – ASSOCIATED WORK PLAN

A global overview of the PPLM design and performances has been presented in the CDR design report and optical, RF, thermal and mechanical reports.. All these analyses confirm and detail the design & performances of the PPLM :

- The test of the QM cryo-structure and the telescope are in progress as well as the FM manufacturing.
- The detailed definition of some specific component such as the shields of the optical cavity is not fully completed but the associated development schedule is compatible with the global QM one.
- Instrument interface design is completed. However; for most of them, formal agreement (final drawings) is still needed (see detailed status presented in [RD16]). Analyses are still in progress on HFI side to confirm the design the 4K and 0.1K pipes wrt mechanical environment. Again, the LFI upper structure interface onto the PR panel would need to be reinforced (M5 insert instead of M4). Conservative approach for the FM is recommended.
- 60 K thermal performances is fulfill as well as the 50K goal when nominal performances of the instruments are assumed. The computation are performed with a PPLM model including measured material and IF thermal conductivity's.. Selection of the PUK for the high emissivity coating has been confirmed by the last LEE results. They have provided a comparison between the 3 candidates even if the absolute measurement accuracy is still not satisfactory. Work is in progress to improve the situation (black body performance)
- The WFE budgets fulfill the specification whereas the goal is not reached at 857 GHz. Note that the performance is computed assuming that the FPU is compliant with its alignment specification. This is not in line with the preliminary results presented at the LFI IHDR. Solutions to recover the situation has been proposed by Laben. They are currently in analysis at ASP and have to be discussed in priority.
- RF main lobe budget, spacecraft emission and rejection are also compliant to the specification. On the other hand rejection goal toward the sun direction at 100GHz, 353 GHz and 857GHz is not reached.

END OF DOCUMENT